Invariant natural killer (iNKT) cells and their potential in the context of immune tolerance and tumor control

Dissertation
der Mathematisch-Naturwissenschaftlichen Fakultät
der Eberhard-Karls-Universität Tübingen
zur Erlangung des Grades eines
Doktors der Naturwissenschaften
(Dr. rer. nat.)

vorgelegt von
Emmanuelle Moraes Ribeiro, M.Sc.
aus Itacoatiara, Brasilien

Tübingen
2023

Gedruckt mit Genehmigung der Mathematisch-Naturwissenschaftlichen Fakultät der Eberhard-Karls-Universität Tübingen.

Tag der mündlichen Qualifikation:	08.09.2023
Dekan:	Prof. Dr. Thilo Stehle
1. Berichterstatter:	Prof. Dr. Dominik Schneidawind
2. Berichterstatter:	Prof. Dr. Matthias Schwab

Abstract

Invariant natural killer (iNKT) cells are a small T-cell subset that express an invariant T-cell receptor (TCR) and show potent immunoregulatory and cytolytic properties. Importantly, iNKT cells have been associated with a decreased incidence of graft-versus-host disease (GvHD), which represents an important cause of therapy failure after allogeneic hematopoietic stem cell transplantation (allo-HSCT). In murine models, iNKT cells modulate immune tolerance through the expansion of regulatory T cells (Treg). Here, the first goal of this work was to identify the mechanism used by human iNKT cells to prevent GvHD using a human *in vitro* setting. Further, a comprehensive analysis of the potential of CD19-CAR-iNKT cells as an off-the-shelf immunotherapeutic strategy alone and in combination with the PD-1 inhibitor nivolumab to further increase functionality was performed. Human *ex vivo* expanded third-party iNKT cells were analyzed in the context of mixed lymphocyte reactions (MLR) using artificial antigen presenting cells (aAPCs) and/or dendritic cells (DCs) as stimulators and T cells in an allogeneic setting. T-cell activation and proliferation was only decreased by iNKT cells in MLR with DCs used as stimulators instead of aAPCs. Further, transwell assays demonstrated that this effect happens in a cell contact dependent manner. Analyses using blood DCs of healthy donors and patients revealed that iNKT cells induce preferential apoptosis of conventional DCs (cDCs), which are important promoters of T-cell activation and proliferation and express high levels of CD1d. iNKT cells were genetically modified to express a third-generation chimeric antigen receptor (CAR) against CD19 and showed robust cytotoxicity against CD19+ cell lines and patient blasts. Importantly, CD19-CAR-iNKT cells retained their CD1d restriction and could induce both CD19 and CD1d-mediated cytotoxicity. Although PD-1 checkpoint inhibition could not improve short-term cytotoxicity of CD19-CAR-iNKT cells, cytokine release and proliferation capacity were significantly increased in nivolumab-treated samples. Moreover, repetitive antigen encounters also had a negative effect on the functionality of CD19-CAR-iNKT cells, especially after three stimulation rounds. Nevertheless, this effect could be partially reversed upon checkpoint inhibition. Importantly, CD19-CAR-iNKT cells maintained their inhibitory properties and could prevent T-cell activation and proliferation even under checkpoint inhibition. Thus, this work demonstrates the potential of iNKT cells and CD19-CAR-iNKT cells in the context of immune tolerance and for tumor control. iNKT cells promote immune tolerance through selective apoptosis induction of cDCs, while sparing plasmacytoid DCs (pDCs). Meanwhile, genetically modified iNKT cells are able to promote efficient tumor control of CD19+ malignancies. Further, checkpoint inhibition may increase their functionality without exacerbating the risk of GvHD after allo-HSCT making them an ideal cytotherapeutic to treat relapse in this clinical setting.

Zusammenfassung

Invariante natürliche Killer-T-Zellen (iNKT-Zellen) gehören zu einer kleinen Untergruppe von T-Lymphozyten, die einen invarianten T-Zell-Rezeptor (TZR) exprimieren und robuste immunregulatorische und zytotoxische Funktionen aufweisen. Zudem werden iNKT-Zellen mit einer niedrigeren Inzidenz der Transplantat-gegen-Wirt-Erkrankung (*graft-versus-host disease,* GvHD) assoziiert, die für die Erfolgsaussichten nach einer allogenen Stammzelltransplantation (allo-SZT) bedeutsam ist. In Mausmodellen wurde gezeigt, dass iNKT-Zellen durch die Expansion von regulatorischen T-Zellen (Treg) inhibitorische Effekte gegenüber alloreaktiven T-Zellen ausüben. Das Ziel dieser Arbeit war, den Mechanismus, durch den humane iNKT-Zellen immunologische Toleranz verursachen, in einem *in vitro* System zu untersuchen. Des Weiteren wird das Potential genetisch modifizierter iNKT-Zellen als Immuntherapeutikum alleine oder in Kombination mit PD-1-Checkpoint-Inhibition zur Verbesserung der Funktionalität dieser Zellen analysiert. Humane *ex vivo* expandierte iNKT-Zellen wurden im Rahmen von gemischten Lymphozyten-Reaktion (*mixed lymphocyte reactions*, MLR) untersucht, wobei die T-Zell-Aktivierung und -Proliferation durch künstliche Antigen-präsentierenden Zellen (*artificial antigen presenting cells*, aAPCs) oder dendritische Zellen (*dendritic cells*, DC) stimuliert wurden. Es konnte gezeigt werden, dass T-Zell-Aktivierung und -Proliferation nur durch iNKT-Zellen gehemmt werden, wenn T-Zellen durch DCs und nicht durch aAPCs stimuliert werden. Ferner zeigten Transwell-Untersuchungen, dass dieser Effekt in einer Zell-Kontakt-abhängigen Weise stattfindet. Untersuchungen mit Blut-DCs von gesunden Spendern und Patienten deckten die präferentielle Apoptose von konventionellen DCs (*conventional dendritic cells*, cDCs) durch iNKT-Zellen auf, die interessanterweise die höchste CD1d-Expression aufweisen und wichtige T-Zell-Stimulatoren sind. Weiterhin wurden iNKT-Zellen genetisch modifiziert, um einen chimären Antigen-Rezeptor (CAR) gegen das CD19-Antigen zu exprimieren. Diese Zellen zeigten robuste Zytotoxizität gegen CD19+ Zelllinien und Patienten-Blasten. Zudem behielten CD19-CAR-iNKT-Zellen ihre CD1d-Abhängigkeit und konnten sowohl über CD19 als auch CD1d zytotoxisch wirken. Obwohl PD-1-Checkpoint Inhibition keine Auswirkung auf die kurzfristige Zytotoxizität von CD19-CAR-iNKT-Zellen hatte, wurden signifikant erhöhte Mengen von Zytokinen und eine verbesserte Proliferation von Nivolumab-behandelten CD19-CAR-iNKT-Zellen festgestellt. Des

Weiteren konnte sowohl die zytotoxische Wirkung als auch Zytokin-Freisetzung nach drei Stimulationsrunden mithilfe von Checkpoint-Inhibition partiell verbessert werden. Auch unter Checkpoint-Inhibition behielten CD19-CAR-iNKT-Zellen ihre inhibitorischen Eigenschaften und konnten die T-Zell-Aktivierung und -Proliferation weiter effizient verhindern. Diese Ergebnisse weisen auf das Potential von iNKT- und CD19-CAR-iNKT-Zellen im Rahmen der immunologischen Toleranz und für die Tumorkontrolle hin. iNKT-Zellen sind in der Lage allogene Immunreaktionen zu verhindern, während sie durch genetische Modifikation Krebszellen effizient beseitigen. Ferner konnte Checkpoint-Inhibition ihre Funktion verbessern, ohne das GvHD-Risiko zu erhöhen. Diese Daten weisen darauf hin, dass iNKT-Zellen ein ideales Immuntherapeutikum darstellen, welches seine Anwendung bei Rezidiven nach allo-SZT finden könnte.

List of contents

List of tables

List of figures

List of abbreviations

Abbreviation	Full form
α-GalCer	α-galactosylceramide
µL	microliter
µm	micrometer
2-ME	2-mercaptoethanol
7-AAD	7-aminoactinomycin D
AA	amino acid
AF	alexa fluor
aGvHD	acute graft-versus-host disease
AICD	activation-induced cell death
ALL	acute lymphoid leukemia
Allo-HSCT	allogeneic hematological stem cell transplantation
AML	acute myeloid leukemia
ANOVA	analysis of variance
APC	antigen presenting cells
APC	allophycocyanin
ATCC	American type culture collection
ATG	anti-thymocyte globulin
ATP	adenosine triphosphate
Auto-HSCT	autologous hematological stem cell transplantation
Axi-cel	Axicabtagene ciloleucel
BL	Burkitt lymphoma
BM	bone marrow
BV	brilliant violet
CAR	chimeric antigen receptor
CCL5	chemokine (C-C motif) ligand 5
CD	cluster of differentiation
cDC	conventional dendritic cell
CFSE	carboxyfluorescein succinimidyl ester
cGvHD	chronic graft-versus-host disease
CLL	chronic lymphoid leukemia
cm	centimeter

CML	chronic myeloid leukemia
CO_2	carbon dioxide
CB	cord blood
CR	complete remission
CTLA-4	cytotoxic T-lymphocyte-associated protein 4
Ctrl	control
CTV	CellTrace^{TM} Violet
Cy	cyanine
CyA	cyclosporin A
DAMP	damage-associated molecular pattern
DC	dendritic cell
DLI	donor leucocyte infusion
DMSO	dimethyl sulfoxide
DN	double negative
DNA	deoxyribonucleic acid
DP	double positive
DPBS	Dulbecco's phosphate-buffered saline
ds	double stranded
e.g.	*Latin: exempli gratia*; English: for example
E:T	effector to target
ECP	extracorporeal photopheresis
EDTA	ethylenediaminetetraacetic acid
EHAA	Eagle Hank's amino acids
EOMES	eomesodermin
FACS	fluorescence-activated cell sorting
FBS	fetal bovine serum
FcR	Fc receptor
FITC	fluorescein isothiocyanate
FMO	fluorescence minus one
FoxP3	forkhead box P3
FSC	forward scatter
FSC-A	forward scatter-area
GI	gastrointestinal
GM-CSF	granulocyte-macrophage colony-stimulating factor

GPFS	GvHD and progression-free survival
Granz A	granzyme A
Granz B	granzyme B
GvHD	graft-versus-host disease
GvL	graft versus leukemia
Gy	gray
HEK	human embryonic kidney
HEPES	4-(2-hydroxyethyl)-1-piperazineethanesulfonic acid
HLA	human leucocyte antigen
HNSCC	head and neck squamous cell carcinoma
HPLC	high performance liquid chromatography
HSCT	hematological stem cell transplantation
I.U.	international unit
IC	intracellular
ICS	intracellular staining
IFN	interferon
iGb3	isoglobotriosylceramide
IL	interleukin
IMDM	Iscove's modified Dulbecco's medium
Inc.	incorporation
iNKT cell	invariant natural killer T cell
iTCR	invariant T-cell receptor
JAK	Janus kinase
kg	kilogram
$KHCO_3$	potassium bicarbonate
KIR	killer-cell immunoglobulin-like receptor
KLRG1	killer cell lectin-like receptor subfamily G member 1
L	liter
LAG-3	lymphocyte-activation gene 3
LB	lysogeny broth
LPS	lipopolysaccharide
LS	lysogeny broth
MACS	magnetic-activated cell sorting
MEM	minimum essential medium

MFI	median fluorescence index
mg	milligram
MHC	major histocompatibility complex
miHA	minor histocompatibility antigen
MIP	macrophage inflammatory protein
mL	milliliter
MLR	mixed lymphocyte reaction
mm	millimeter
MMF	mycophenolate mofetil
Mo-DC	monocyte-derived dendritic cell
MTX	methotrexate
NEAM	non-essential amino acids
ng	nanogram
NH_4Cl	ammonium chloride
NIH	National Institutes of Health
NK cell	natural killer cell
NKR	natural killer receptor
NKT cell	natural killer T cell
nM	nanomolar
ns	not significant
OS	overall survival
P/S	penicillin/streptomycin
PB	peripheral blood
PBMC	peripheral blood mononuclear cell
PD-1	programmed cell death protein 1
pDC	plasmacytoid dendritic cell
PDGF	platelet-derived growth factor
PD-L1	programmed death-ligand 1
PD-L2	programmed death-ligand 2
PE	R-phycoerythrin
PerCP	peridinin-chlorophyll-protein
pg	picogram
PI	propidium iodide
rh	recombinant human

RORγt	RAR-related orphan receptor gamma T
RNA	ribonucleic acid
RPM	rotation per minute
RPMI	Roswell park memorial institute
RT	room temperature
scFv	single chain variable fragments
SD	standard deviation
SEM	standard error of the mean
SSC	side scatter
SSC-A	side scatter-area
SSC-W	side scatter-width
T_{cm}	central memory T cells
TCR	T-cell receptor
T_{FH}	follicular helper T cell
TGF	transforming growth factor
Th	T helper
TIGIT	T-cell immunoreceptor with Ig and ITIM domains
TIM-3	T-cell immunoglobulin and mucin-domain containing-3
Tisa-cel	Tisagenlecleucel
TLR	toll-like receptor
TM	transmembrane
TNF	tumor necrosis factor
TOX	thymocyte selection-associated HMG BOX
TRAIL	TNF-related apoptosis-inducing ligand
Treg	regulatory T cell
TW	transwell
T-bet	T-box expressed in T cells
UT	untransduced
UV	ultraviolet
VD	viability dye
VH	variable heavy
VL	variable light
WT	wild type

1 Introduction

1.1 Allogeneic hematopoietic stem cell transplantation (allo-HSCT)

Hematopoietic stem cell transplantation (HSCT) revolutionized the treatment of malignant and non-malignant diseases in the 20th century and settled the pathway for cell and immunotherapeutic approaches in medicine. Since then, it has been used for the treatment of several cancers (e.g., multiple myeloma, lymphomas, and acute myeloid leukemia), autoimmune diseases and other blood diseases such as aplastic anemia and thalassemia [1, 2]. For many of these diseases, it represents the only curative option. Worldwide, it is estimated that about 90.000 transplantations take place each year [3]. In Germany, 51,250 procedures were documented between 1998 and 2021, mostly for the treatment of acute myeloid leukemia [4].

HSCT is a generic term comprising different techniques with the final goal of restoring the patient's hematological system after it has been compromised by disease and/or treatment. Autologous HSCT (auto-HSCT) is performed with stem cells obtained from the patient's peripheral blood (PB) or bone marrow (BM), while allogeneic grafts are composed of stem cells derived from BM, cord blood (CB) or PB from matched/mismatched healthy donors, who can be related to the patient or not [1, 2, 5]. In this sense, the terms "matched" and "mismatched" refer to the human leucocyte antigens (HLA) typing. HLA proteins are surface proteins encoded by the HLA system located in the major histocompatibility complex (MHC) and exert an important role on immunological responses in allo-HSCT [6]. The HLA molecules HLA-A, HLA-B and HLA-C, which bind to CD8+ T cells and HLA-DP, HLA-DQ and HLA-DR, which bind to CD4+ T cells are the molecules of higher significance in this context [7]. Differences in the HLA identity of patient and donor is an important risk factor for the occurrence of graft-versus-host disease (GvHD), which represents one of the major complications of allo-HSCT [1, 2, 8, 9].

A huge progress in the field has been observed in the last decades, however several drawbacks are yet to be overcome. The biggest challenge for malignancies, for instance, is the achievement of a complete cure without the development of GvHD after allo-HSCT [10, 11]. Considering the role that T cells play for the development of GvHD, anti-T-cell approaches have been adopted in allo-HSCT. For example, drugs to suppress T-cell function as calcineurin inhibitors and antiproliferative agents such as methotrexate (MTX) have become standard in the prophylaxis of GvHD [12-14]. Further, strategies to deplete T cells from grafts have also achieved relevance in this context. However, these methods have also been shown to correlate positively with higher relapse rate due to the impairment of the graft-versus-leukemia effect (GvL), which is promoted by T cells in the graft against remaining tumor cells and contributes to disease control [15]. Thus, the development of new strategies to apply the potential of T cells for tumor control while avoiding GvHD and restoring the immune system after allo-HSCT is urgently needed.

1.2 GvHD

GvHD is a reaction caused by immunologically competent T cells present in the graft, which become activated upon encountering foreign antigens presented by host cells. Upon activation, alloreactive T cells proliferate and induce cell-mediated tissue damage in the host. Up to 50% of the patients will eventually develop acute GvHD (aGvHD) after allo-HSCT, while 30-70% will develop chronic GvHD (cGvHD) [16, 17]. It is a serious complication and drastically impacts the outcome of allo-HSCT [11].

1.2.1 Pathogenesis

GvHD is a highly complex event, but can be briefly summarized in three phases. Phase I starts with the conditioning process, which patients undergo prior to transplantation. Conditioning regimens, usually chemotherapy alone or in combination with T-cell-depleting antibodies or radiotherapy, are meant to suppress the host’s defenses to avoid graft rejection and to reduce the number of cancerous cells [18]. This process, however, induces tissue damage and consequently, the release of proinflammatory cytokines, such as interleukin (IL) 6, tumor necrosis factor alpha (TNF-α) and IL-1, which in turn, activate host antigen presenting cells (APC) [19, 20]. In a second phase, mature APC induce activation and proliferation of mature alloreactive donor T cells through the presentation of foreign antigens [8]. Third, a cellular and further humoral response takes place. Directed by chemokines, both T helper (Th) 1 and Th2 T and natural killer (NK) cells migrate to tissues and promote, for instance, liver, gastrointestinal (GI) and skin damage through the release of effector molecules such as interferon gamma (IFN-γ) and IL-2 and direct target cell lysis, especially through the Fas/FasL and perforin/granzyme pathways [21-24]. Skin and GI damage may further provoke a characteristic cytokine storm through activation of toll-like receptors (TLR), maximizing tissue injury (**Fig.1**) [23].

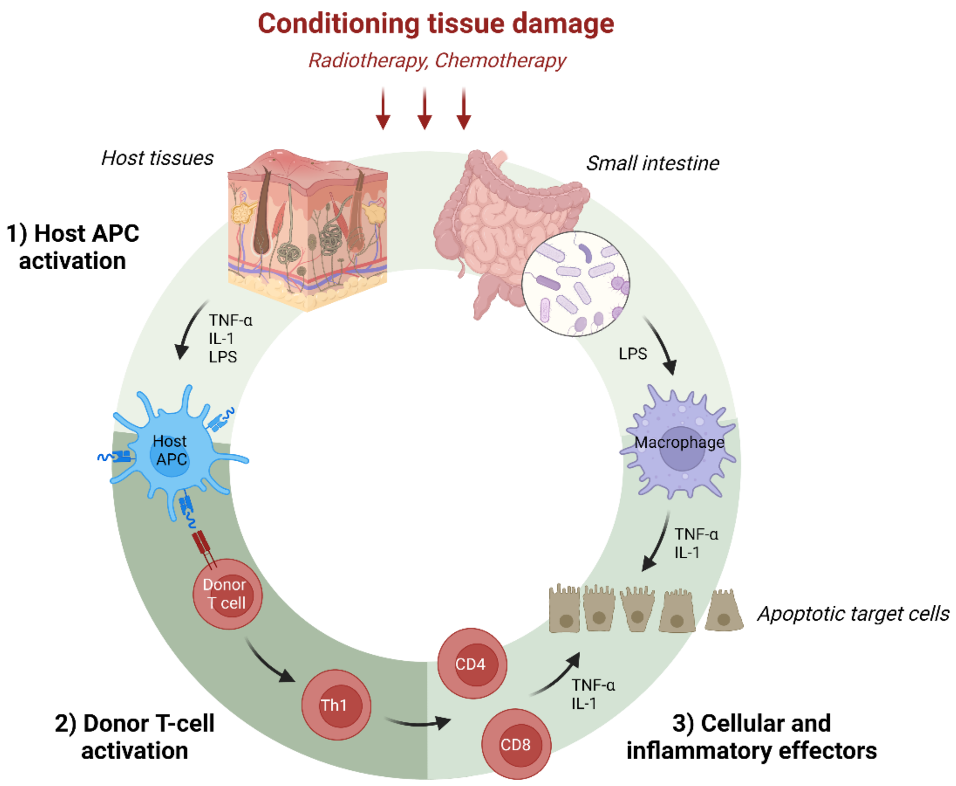

Figure 1: GvHD pathogenesis

Despite being a highly complex process, GvHD pathogenesis can be divided into three main events. Patients usually undergo a conditioning process to reduce cancer burden and suppress host defense mechanisms. At one hand, the conditioning process induces tissue damage with the subsequent release of pro-inflammatory factors such as TNF-α and IL-1, which in turn induce the activation of host APCs **(1)**. Upon contact with activated APCs, mostly Th1, but also Th2 donor T cells become activated **(2)** and induce damage on host cells through cellular and soluble factors **(3)**. On the other side, conditioning also induces damage of the small intestines and consequently of the microbiota. This event provokes the release of lipopolysaccharide (LPS) and thus, induces further damage through macrophage-induced cellular and inflammatory responses. Figure generated with Biorender®. Adapted from Ferrara [8].

At the molecular level, this process involves the recognition of protein fragments presented by the MHC, located on chromosome 6, by alloreactive T cells. In a mismatched setting, this process depends on the recognition of major antigens of the HLA systems (e.g., HLA-A, HLA-DR), while in a matched setting, an allogeneic reaction is started by the recognition of their less immunogenic counterparts, the minor histocompatibility antigens (miHA). Approximately 40% of all allogeneic reactions are caused by T-cell recognition in the context of miHAs [8]. MiHAs are small polymorphic peptides containing 9-12 amino acids (AA), which are recognized by alloreactive T cells in the context of HLA (**Fig. 2**). Polymorphism of AA, gene deletions and intracellular mechanisms might induce single or multiple AA disparities, which are often sufficient to induce immunogenicity [25, 26]. Some miHAs may have different effects on the allogeneic reactions. For instance, the miHAs HY and HA-3 are known to induce both GvHD and GvL, while the miHAs HA-1 and HA-2 have a stronger effect on GvL than on GvHD [8].

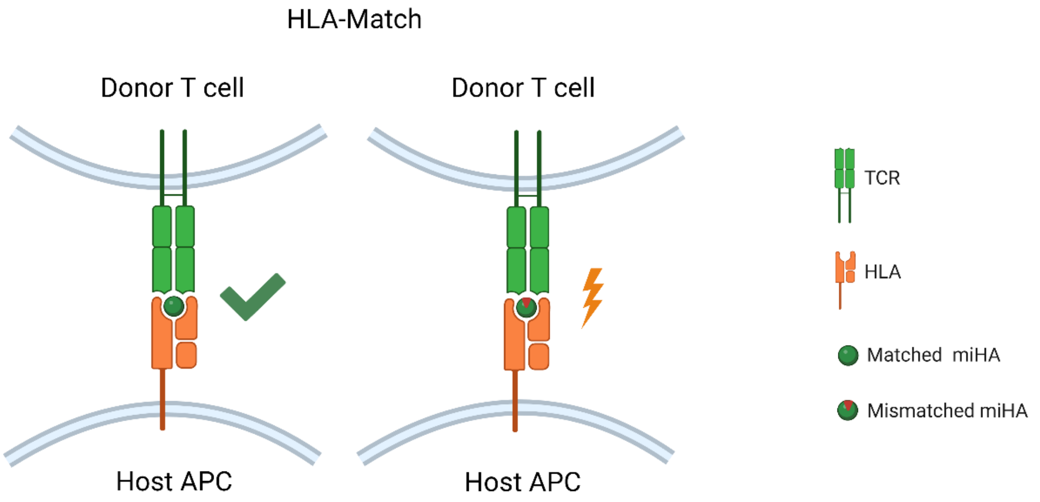

Figure 2: Recognition of HLA molecules and miHAs by T cells

Allogeneic reactions in a mismatched setting are initiated by major allo-antigens. Meanwhile, allo-reactions in a matched setting are mostly promoted by the recognition of minor histocompatibility antigens (miHA). These are small peptides (9-12 AA), with single or multiples disparities, which are often enough to induce an allogeneic reaction. Figure generated with Biorender®. Adapted from Koyama and Hill [27].

These events might contribute to both acute and chronic GvHD, however, cGvHD has shown to rely on more complex processes. Similar to the pathogenesis of aGvHD, a

three-phase mechanism for cGvHD based on mouse models has been purposed [28]. Nevertheless, these data seem to be supported by few studies in human settings.
The first phase is characterized by early inflammation events and tissue damage. It starts right after the HCT as a reaction to tissue damage, which leads to the migration of Th1 and Th17 cells to affected sites. Further tissue damage also promotes the release of damage-associated molecular patterns (DAMPs), such as DNA, RNA and adenosine triphosphate (ATP). These molecules activate different TLRs and consequently, the expression of IFN-α, TNF-α and IL-6 [29, 30]. The ATP-dependent formation of the inflammasome NLRP3 leads to the expression of IL-1β. Altogether, IFN-α, TNF-α, IL-6 and IL-1β induce T-cell differentiation into Th1 and Th17, which through the action of chemokines, migrate to tissues and promote further damage [30-33]. The second phase is identified by a chronic inflammation and immune dysregulation. It has been shown that thymic dysfunction caused by aGvHD might contribute to the development of cGVHD resulting in a defective negative selection and subsequent generation of allo-reactive donor T cells [34-36]. Allo-reactive CD4+ T cells seem to play an important role for the induction of a chronic inflammatory state [37, 38]. Another hallmark of this phase is the production of auto-antibodies by dysregulated B cells, such as anti-H-Y, anti-platelet-derived growth factor alpha (PDGF-α) and anti-double stranded DNA (dsDNA), giving cGvHD its autoimmune characteristics [39-41]. At last, autoantibodies induce monocyte and macrophage activation, while promoting tissue damage and consequent release of transforming growth factor beta (TGF-β). TGF-β stimulates collagen production through the stimulation of fibroblasts and establishes an aberrant tissue repair process that culminates in organ fibrosis and dysfunction [42, 43].

1.2.2 Clinical aspects and treatment

GvHD is mainly classified according to its onset before or after 100 days post-transplantation into aGvHD and cGVHD, respectively. In 2005, the National Institutes of Health (NIH, USA) considered this classification insufficient and established a new classification based on clinical features rather than on the onset time. In this sense, new categories, such as late-onset aGvHD and overlap syndrome have been proposed [44]. However, the classification into acute and chronic forms is still widely accepted.

GvHD is classified into aGvHD when clinical signs start within 100 days post-transplantation. In aGvHD, the most susceptible organs are the skin (81% of the cases), GI (54%) and liver (50%). The skin is usually the organ most often involved and shows a maculopapular rash as a common clinical feature, together with eventual blisters, and ulcers in more severe cases [45]. GI involvement shows a more variable picture, with symptoms varying from nausea in mild cases to severe diarrhea (>2 L per day). Hepatic involvement has an even more variable picture and can be hardly distinguished from other hepatic pathologies. Depending on the clinical severity, this form of GvHD can be further classified into four grades: I (mild), II (moderate), III (severe) and IV (very severe) [8]. The grade of severity according to this classification has been shown to have an important correlation with overall survival [46, 47].

Several strategies have been used or studied for the treatment of aGvHD but none of them has been shown to be highly efficient and safe for standard use. Steroids (e.g., methylprednisolone) are considered the gold standard of GvHD therapy, alone or in combination with other agents. However, studies have shown that steroids induce rather low response rates in high-grade GvHD and also compromise beneficial GvL effects [45, 48]. Alternatively, the use of anti-thymocyte globulin (ATG) has been extensively studied in cases of steroid-refractory GvHD. However, due to highly diverse data, no consensus regarding its efficacy and safety in the context of GvHD has been achieved [49-51].

To a lesser extent, other strategies have also been used to treat GvHD. Extracorporeal photopheresis (ECP) has shown promising results for the treatment of steroid-refractory GvHD [52, 53]. Blood of the patient is collected by apheresis, treated with a DNA-intercalating agent (e.g., 8-methoxypsoralen), exposed to ultraviolet (UV) light and infused back into the patient. TNF-α-blockers represent another alternative since TNF-α blockade prevents the activation of host DCs and consequently the following steps of GvHD pathogenesis. Despite the high incidence of infections in clinical studies, TNF-α blockers have been shown to induce 55% complete responses, especially in cases of GvHD with gut involvement [54]. Most recently, the efficacy and safety of ruxolitinib, a selective Janus kinase (JAK1 and JAK2) inhibitor, was analyzed in a multicenter, randomized, open-label, phase III trial for the treatment of steroid-refractory GvHD. The overall response and durable overall response rates were higher in the group treated with ruxolitinib than in the control group (62% vs. 39% and 40% vs. 22%) [55]. Further targets are CD52 [56], IL-2-receptor [57] and others.

In German-speaking countries, steroids are the first-line therapy combined with calcineurin inhibitors and supportive measures (pain control, antibiotics, etc.). The second line of treatment is more heterogeneous, but mycophenolate mofetil (MMF) and ECP were shown to be more commonly used. The algorithm showing the treatment for aGvHD recommended by the German, Swiss and Austrian guidelines is depicted in figure 3 [58].

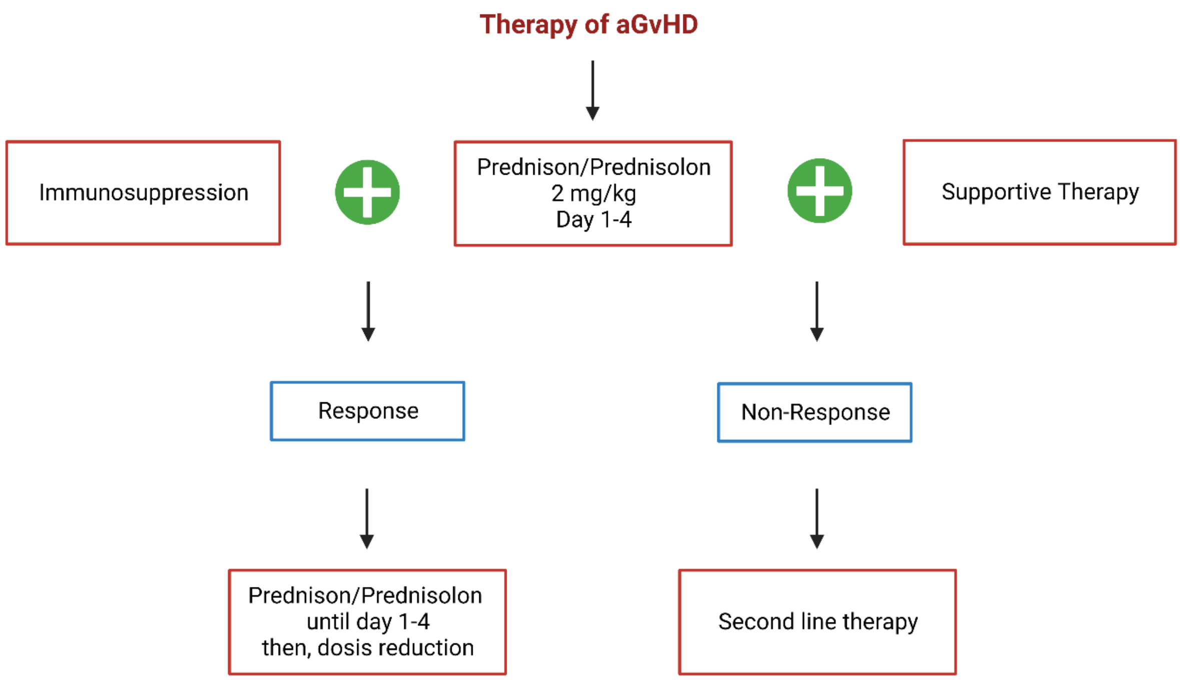

Figure 3: Algorithm for the treatment of aGvHD in Germany, Austria and Switzerland
The therapy of aGvHD depends on the severity of the manifestations. The first line of therapy consists of steroids and supportive therapy. In case of response, steroids (1-2 mg/kg) are continued until day 7 post-manifestation, with subsequent dose reduction. Figure generated with Biorender®. Adapted from the German, Swiss and Austrian guidelines for aGvHD [59].

The clinical manifestation of GvHD after 100 days post-transplantation is usually classified as cGvHD, which can result from a progressive aGvHD process, interrupted or quiescent (after resolved aGvHD) and *de novo* [8]. Thus, therapies focusing on the treatment of aGvHD could also, to some extent, indirectly prevent its chronic form. Although the manifestation of cGvHD correlates with lower relapse rates, cGvHD represents a major non-relapse-related cause of death after HSCT [60]. Regarding its clinical manifestations, cGvHD affects several organs with a clinical picture that resembles the ones of several autoimmune diseases, such as pulmonary restriction or obstruction, joint stiffness and cicatricial conjunctivitis, among others.

Steroids are also the agents of choice for cGvHD and are used topically or systemically depending on the severity of the disease [16, 61]. In more severe cases, cyclosporin A (CyA) or tacrolimus might also be recommended additions to steroid therapy, as shown in figure 4. Further targets have been tested for the treatment of cGvHD based on its complex pathogenesis, most of them focusing on the neutralization of B-cell function [62-64]. Moreover, beneficial effects could also be achieved by the expansion of conventional Treg and invariant natural killer T cells (iNKT cells) [65-67].

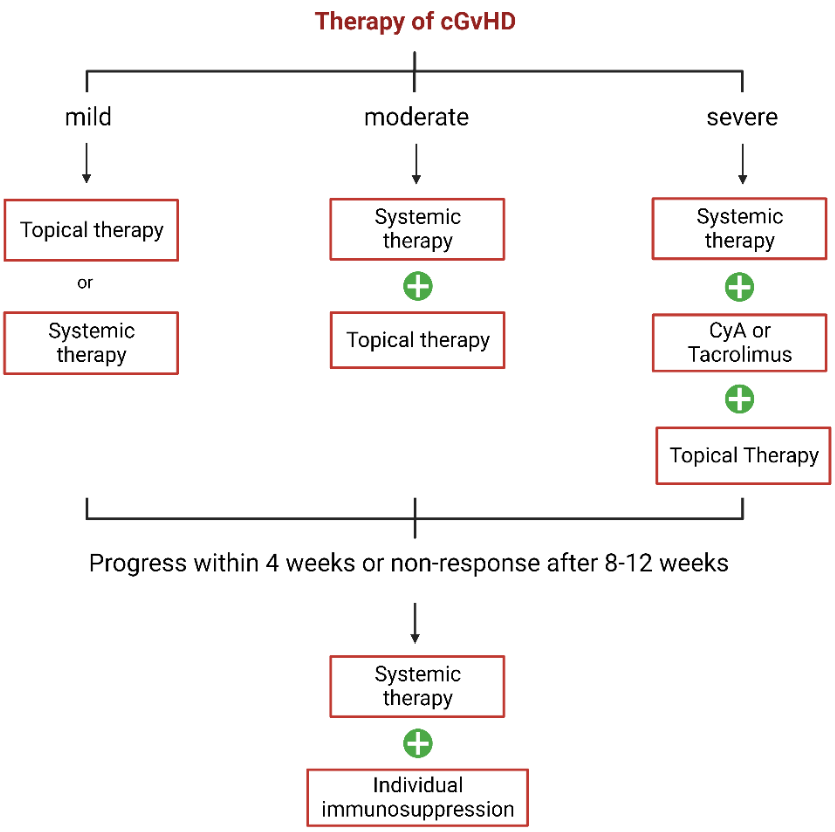

Figure 4: Algorithm for the treatment of cGvHD in Germany, Austria and Switzerland

The therapy of choice for cGvHD depends on the severity of the manifestations. Mild cases are usually treated with topical steroids or low doses of systemic steroids. For moderate cases, a combination of systemic steroids in combination with topical therapy is recommended, while for more severe cases, the addition of CyA or tacrolimus is suggested. Further manifestations must be treated with systemic steroids in combination with individual immunosuppression. Figure generated with Biorender®. Adapted from the German, Swiss and Austrian guidelines for cGvHD [68].

1.2.3 Prevention

The regimen to prevent aGvHD is chosen based on factors such as remission of the disease, age of the patient and HLA compatibility. Calcineurin inhibitors such as CyA or tacrolimus in combination with MTX or MMF are the standard agents most commonly used in Germany and Switzerland [59]. A randomized, open-label, multicenter phase III study showed that the addition of ATG-Fresenius (ATG-F) to the prophylaxis with CyA and MTX decreased the incidence of both aGvHD and cGvHD after matched unrelated transplantation, without increasing relapse rates and not affecting overall survival [69]. Based on this data, ATG-F has also been included in the German, Swiss and Austrian guidelines for the prevention of GvHD for high-risk patients who underwent matched related HSCT or those who underwent unrelated HSCT.

Nevertheless, the current approaches have been shown to be rather inefficient for both the prevention and treatment of GvHD after allo-HSCT. Therefore, alternative strategies are still needed.

1.3 Natural killer T cells (NKT cells)

NKT cells are a small T-lymphocyte subset characterized by the expression of a non- or less variable T-cell receptor (iTCR) [70]. Conversely to traditional T cells, which recognize peptides in the context of MHC molecules, NKT cells recognize glycolipids presented by the MHC class I-like molecule CD1d [71] (**Fig. 5**). Moreover, NKT cells might express common surface markers of NK (e.g., NK1.1 in mice and CD161 humans and CD56) and conventional T cells. These features allow NKT cells to be activated through both NK- and T-cell mechanisms [72, 73]. Upon activation, NKT cells release copious amounts of cytokines and effector molecules, such as IFN-γ, IL-4, TNF-α, granzyme and perforin [74-77]. This ability poses NKT cells in a “double-edge” position since they can play both a protective as well as a harmful role in immunological responses.

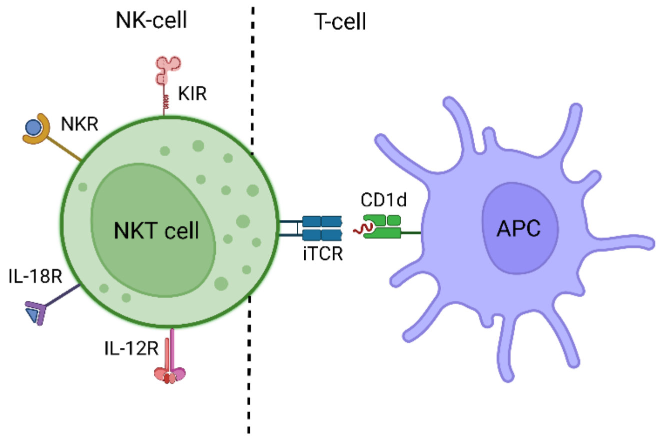

Figure 5: NKT cells and their NK- and T-cell markers

NKT cells bear an invariable TCR, which recognizes glycolipids, such as the α-galactosylceramide (α-GalCer), presented by the MHC-I-like molecule CD1d. Due to the expression of NK markers, NKT cells can also be activated through NK mechanisms, such as KIR, NKR, IL-18R and IL-12R. Both pathways lead to a fast and robust cytokine release. Figure generated with Biorender®. Adapted from Krijgsman et al. [78].

1.3.1 Development

NKT cells originate from CD4+CD8+ cortical thymocytes [79, 80]. Regarding early events of their development, NKT cells arise from rare and random Vα14Jα18 or Vα24JαQ rearrangements (in mice and humans, respectively), which once expressed, will induce a full commitment of these thymocytes to the NKT-cell lineage [81, 82]. Most studies concerning the NKT-cell development, however, focus on murine NKT cells, so little is known about this process in humans. In mice, NKT cells arise from a CD24highCD4+CD8+ precursor [79]. Their canonical TCR allows NKT cells for receiving positive survival signals from the RAR-related orphan receptor gamma T (RORγt) [80, 83]. Thus, they may continue in their developmental pathway, interacting with endogenous ligands such as iGb3, which is presented by CD1d-expressing cells in the thymic cortex [73, 84-86]. Later, CD24 and CD8 expression are downregulated in favor of a CD4 expression and eventually, CD4 expression is also downregulated for the generation of CD4-CD8- (DN) NKT cells [79]. In humans, however, CD4-CD8+ subsets can still be observed [87]. NKT cells also undergo several rounds of cell proliferation and achieve an effector memory phenotype before leaving the thymus [88]. Once NKT cells have left the thymus, they can be found at low frequencies in blood, lymph nodes and spleen, among others (<0.1% of total lymphocytes) and at higher frequency in the liver, kidney, and colon (approximately 1% of the total lymphocytes) [78].

1.3.2 Subpopulations and functions

Considering their TCR repertoire, NKT cells are classified into type I and type II NKT cells [89]. Type I NKT cells or invariant NKT cells (iNKT cells) recognize the glycosphingolipid α-GalCer or its analogs presented by the MHC-I-like molecule CD1d [90]. On the other hand, type II NKT cells have a more diversified TCR repertoire, also recognizing non-α-GalCer-analog molecules [91, 92].
Moreover, like conventional T cells, NKT cells can also be classified according to their cytokine-secretion pattern (Th-profile) upon activation, which is resumed in figure 6. In this context, iNKT cells can be classified into five groups. Like conventional T cells, Th1-like iNKT cells release IFN-γ and TNF-α, while Th2-like iNKT cells produce IL-4 and IL-13 upon stimulation [87, 93]. Other subsets such as Th17-like (characterized by the expression of IL-17, IL-21 and IL-22), Tfh-like (IL-21) and Treg-like (IL-10) have also been described [94-96]. Only Th1 and Th2-like type II NKT cells have been identified [97, 98].
Regarding their role in host defense, NKT cells have been shown to be efficient against bacteria, parasites and viruses [99-101]. The focus of this work, however, will be on the immunoregulatory and anti-tumor properties of iNKT cells.

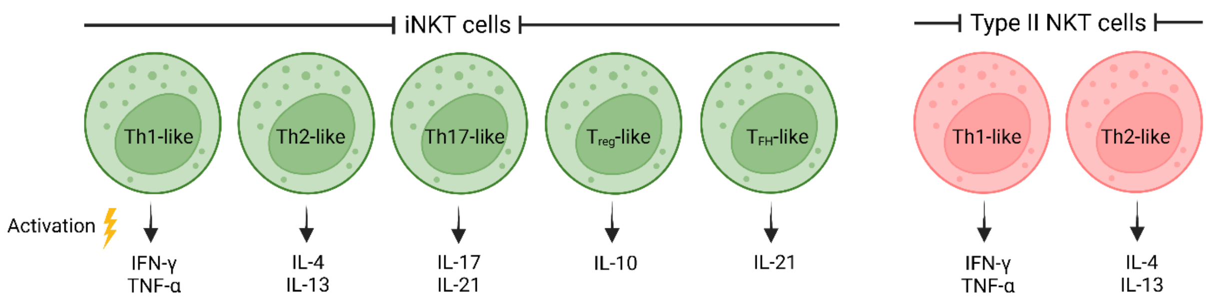

Figure 6: Classification of NKT cells according to their cytokine profile upon activation
NKT cells can be classified according to the cytokines they release upon activation (Th-profile). Five functional subsets of iNKT cells have been identified: Th1, Th2, Th17, Treg and Tfh-like NKT cells. So

far, only Th1-like and Th2-like type II NKT cells have been documented. Figure generated with Biorender®. Adapted from Krijgsman et al. [78].

For their ability to release cytokines fast and in large amounts, NKT cells are considered important immunoregulators. Depending on their functional subset, NKT cells can drive several cell types of both innate and adaptive immunity into an inflammatory state or tolerance. These features are summarized in figure 7. NKT cells can, for instance, induce DC activation through their iTCR with CD1d in a CD40/CD40L-dependent manner, leading to IL-12 production by DCs and subsequent IFN-γ expression by Th1-like NKT cells [99, 102].

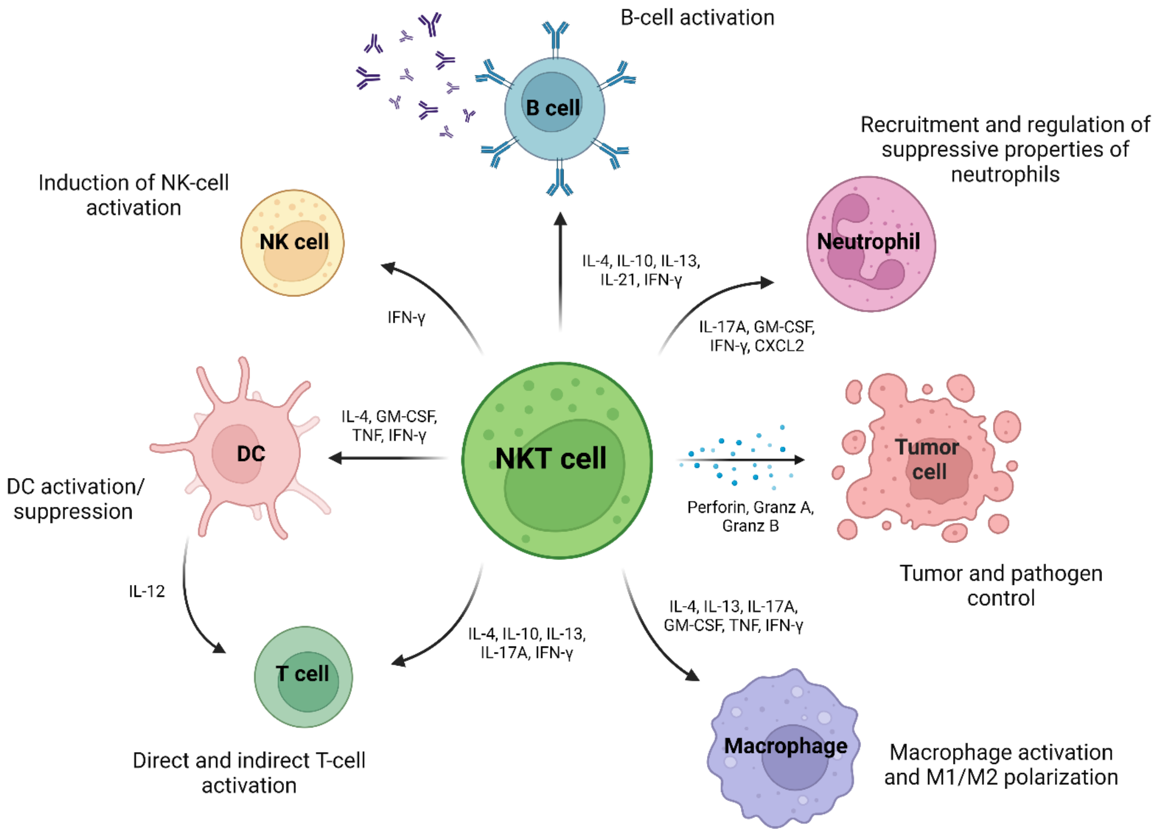

Figure 7: NKT-cell immunoregulatory and anti-tumor function

NKT cells are immunoregulatory cells orchestrating various immune responses. Using both NK and T-cell pathways, NKT cells interact with other cell types, leading to inflammatory states or tolerance. Further, NKT cells are fully equipped to perform tumor control through the release of cytokines and cytotoxic factors, such as IFN-γ, granzyme A, B and perforin. Figure generated with Biorender®. Adapted from Brennan, et al. [103].

NKT cells can also promote immunotolerance by indirectly inducing Th2-like T-cell differentiation through the release of IL-13 and IL-4 (Th2-like NKT cells) or direct the T-cell differentiation into Treg through the release of IL-10 by Treg NKT cells [95, 104, 105]. Furthermore, both direct TCR:CD1d interaction and IL-21-release by Tfh-like NKT cells induce B-cell activation following fast immunoglobulin production and affinity maturation [96, 106]. Interestingly, NKT cells may also activate NK and CD8 T cells through IFN-γ production by Th1-like NKT cells [107, 108]. Moreover, NKT cells can release large amounts of chemokines, such as the chemokine (C-C motif) ligand 5 (CCL5), eotaxin and the macrophage inflammatory protein (MIP) 1α and 1β, which attract NK cells, granulocytes and monocytes to inflammation sites [109].

1.3.3 iNKT cells and GvHD

Several studies have shown the potential of iNKT cells to prevent GvHD in both mice and humans. Lan et al. observed a higher frequency of NK1.1+TCRαβ+ or DX5+TCRαβ T cells in mice that underwent lymphoid irradiation before bone marrow transplantation [110]. The same could be observed using other conditioning strategies in Lewis rats [111]. In both studies, a resistance of NKT cells towards distinct conditioning strategies and a protective effect of these cells against GvHD could be noted. Importantly, despite the immunosuppressive effect of these cells, no negative effect regarding tumor clearance after allogeneic bone transplantation could be observed [112]. Moreover, murine GvHD seems to be controlled by a synergistic effect of Treg and NKT cells in an IL-4-dependent manner [113].

Another strategy applied was the use of the iNKT-cell stimulator α-GalCer in mice, aiming to induce activation and cell expansion *in vivo* and consequently their effect on GvHD. Duramad et al. showed that the intravenous application of liposomal α-GalCer led to significantly prolonged survival of mice with GvHD after allogeneic BM transplantation while maintaining the GvL effect. Mechanistically, this effect seemed to be related to a dose-dependent expansion of CD4+FoxP3+ Treg and iNKT cells in lymphoid organs and BM [114].

Using adoptively transferred CD4+ iNKT cells, Schneidawind et al. could confirm the efficacy of NKT cells in preventing GvHD through the expansion of

CD4+CD25+FoxP3+ Treg cells after allogeneic HSCT [65]. This effect was also reproducible using third-party murine iNKT cells [115].

In humans, analyses of different patient cohorts revealed interesting data correlating the incidence of GvHD and iNKT-cell numbers. For instance, Haraguchi et al. observed a positive correlation between low numbers of recovered NKT cells and a higher incidence of acute and chronic GvHD after both HSCT and BM SCT [116]. A correlation between iNKT-cell numbers in grafts and the incidence of GvHD was also analyzed in other studies. A clinical study evaluated a cohort of 57 patients and observed a significant positive correlation between low numbers of CD4- iNKT cells and the incidence of aGvHD after allogeneic-matched related transplantation [117]. Another study using a larger cohort (n=117) confirmed the frequency of CD4- iNKT cells as a predictive factor for the development of aGvHD [118]. Malard et al. evaluated the correlation between the frequency of iNKT cells, the incidence of GvHD and progression-free survival (GPFS) in a cohort of 80 patients undergoing allogeneic HSCT. The iNKT-cell dose was the only parameter to positively impact the GPFS. Interestingly, conversely to data obtained in murine systems, no correlation between the frequency of Treg cells and the GPFS could be observed [119].

Altogether, these data provide convincing evidence of the potential of iNKT cells for the prevention of GvHD, while maintaining the ability of grafts to induce GvL. In mice, the mechanism of action of these cells seems to be attached to the frequency of Treg cells, however, in humans the mechanism is still to be elucidated.

1.3.4 iNKT cells in tumor therapy

Besides their immunoregulatory properties, NKT cells are also armed to exert cytotoxicity against tumor cells by themselves or through their immunoregulatory properties. Studies have shown, for instance, that the application of iNKT-cell ligands such as α-GalCer demonstrates a potent effect against various solid cancer cells in murine models [120-123]. Other studies have also documented an important anti-tumor effect and prevention of metastasis in mice through NKT cells stimulated with α-GalCer-loaded DCs, leading to significantly enhanced overall survival (OS) [124, 125]. Moreover, the feasibility of adoptive transfer of *ex vivo* expanded human iNKT cells against leukemic cells has been assessed *in vitro* [126, 127].

Regarding the mechanisms involved in cytotoxicity induced by iNKT cells, different pathways have been described. Several studies have highlighted CD1d as a key molecule for iNKT-cell-mediated cytotoxicity against CD1d+ tumor cells, which could be further enhanced upon α-GalCer-treatment [75, 128, 129]. Interestingly, the indirect cytotoxicity of iNKT cells against CD1d- tumor cells through cross-presentation with CD1d+ cells in the tumor microenvironment has also been documented [130, 131]. Considering their biology, iNKT cells can also be activated via NK-cell mechanisms and promote tumor control [132]. Importantly, iNKT cells were shown to improve cytotoxicity and cytokine production by NK cells and cytotoxic T lymphocytes [75, 125, 133]. Upon activation through both CD1d-dependent and -independent pathways, perforin/granzyme B, but also TNF-α, FasL and TNF-related apoptosis-inducing ligand (TRAIL) pathways seem to mediate cytotoxicity [128, 134, 135].

The potential of iNKT cells for tumor control has also been studied in a clinical setting. Analogous to murine experiments, α-GalCer has also been tested in patients. In a phase I study, Giaccone et al. showed that α-GalCer was well-tolerated by patients with solid tumors. Despite that, no clinical response regarding tumor control was observed [136]. However, another phase I study showed that NKT-cell activation through adoptive transfer of α-GalCer-loaded DCs leads to a substantial overall response of both innate and acquired immune systems, with minor side effects. Although efficacy was not the focus of this work, several patients showed tumor necrosis, decreased tumor markers and improvement of hepatic function in compromised patients [137].

Yamasaki et al. tested the combination of α-GalCer-loaded APCs and *ex vivo* expanded iNKT cells in patients with head and neck squamous cell carcinoma (HNSCC) in phase II clinical study. In this study, objective tumor regression in 50% of the patients was observed [138]. In these and other studies, responses were mostly related to the frequency of iNKT cells and other IFN-γ-producing cells.

Thus, these data show that iNKT cells can be a promising tool for the treatment of tumoral diseases. Nevertheless, further pre-clinical and clinical analyses are needed for the assessment of their safety and efficacy as an immunotherapeutic strategy.

1.4 Chimeric antigen receptor (CAR)

1.4.1 Definition and structure

Chimeric antigen receptors (CAR) are modified molecules designed to enhance the specificity and functionality of effector immune cells by recognizing antigens independent of their MHC restriction. The design of CARs was first inspired by the structure of the canonical TCR, with their extracellular and intracellular domains, for potent antigen recognition and signal transduction. In this sense, the basic CAR structure is composed of an extracellular domain, where the antigen binding domain is located, a transmembrane domain (TM) and an intracellular domain, which is responsible for signal transduction [139]. The representation of the most basic CAR structure is depicted in figure 8.

Despite having the same purpose as in the TCR, the antigen binding domain usually derives from other very antigen-specific moieties. Single-chain variable fragments (scFv) derived from monoclonal antibodies are commonly used. Further, the use of other structures such as nanobodies and cytokines bound to the receptors has also been described [140, 141]. Traditionally, the antigen binding domain consists of a variable heavy (VH) and variable light (VL) chain, interconnected through a linker or hinge, which might provide flexibility and proper foldability to the receptor [142].

Attached to the antigen binding site is the TM, which provides stability to the CAR and promotes interaction with other receptors. TM structures commonly derive from type I proteins such as CD3ζ, CD28, CD4, or CD8α. Interestingly, different TM have distinct characteristics that seem to have important effects on CAR functionality. For instance, CD3ζ-derived sequences have been shown to facilitate the interaction with the endogenous TCR, which correlates with enhanced cell activation [143]. On the other hand, CD8α and CD28 moieties are associated with reduced levels of cytokine production and activation-induced cell death (AICD) [144].

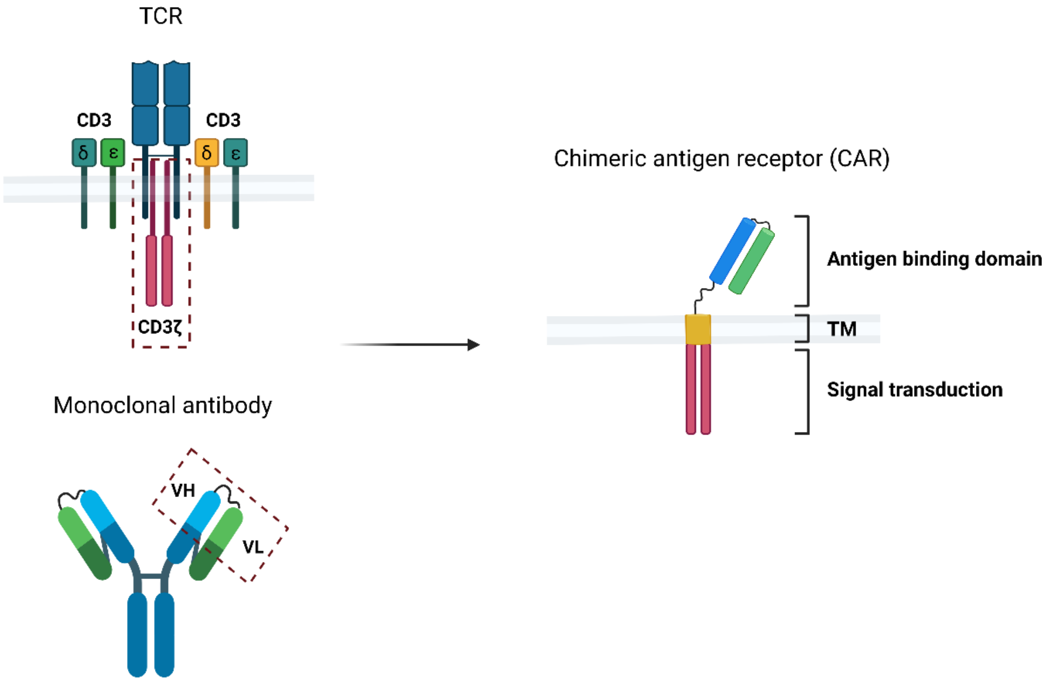

Figure 8: Basic structure of the chimeric antigen receptor
The elemental structure of a chimeric antigen receptor is based on an antigen binding site derived from antibodies and a domain for signal transduction, which resembles the machinery of the canonical TCR. Currently, several adaptations have been developed to improve the functionality of these molecules, such as the addition of costimulatory domains. Figure generated with Biorender®. Adapted from Makita, et al. [145].

At last, a CAR must possess an intracellular domain. Usually comprising an activation domain and one or more costimulatory domains, the intracellular domain is responsible for mediating signals in the cytoplasm of the effector cells. The most commonly used motifs are those from CD3ζ chains, which, however, are not able to mediate a sustainable T-cell response by themselves [146]. In this regard, the adoption of costimulatory domains to the CAR structure promoted an important enhancement of the functionality of CAR-bearing cells [147, 148]. CD28 and 4-1BB-derived sequences are usually used for this purpose and also show particularities. For example, CAR cells with CD28 domains tend to differentiate into memory cells and use mostly aerobic glycolysis, while with 4-1BB, CAR cells differentiate into central memory (T_{cm}) phenotype and have higher oxidative metabolism [149].
Regarding their structure, CARs can be divided into different generations (**Fig. 9**). The very first CARs were composed of only the CD3ζ domain as a responsible unit for

signal transduction. However, these CARs showed limited signaling and consequently also limited efficacy [146]. Later, Maher at al. designed a CAR containing motifs of the costimulatory receptor CD28 improving signaling, survival and persistence [147]. Meanwhile, CARs bearing more than one costimulatory domain have also been developed [150]. At last, a fourth-generation CAR, which allows the simultaneous induction of cytokine production by effector cells, has been proposed [151]. While the first two generations have been extensively studied, evidence of the efficacy and safety of the last ones is scarce.

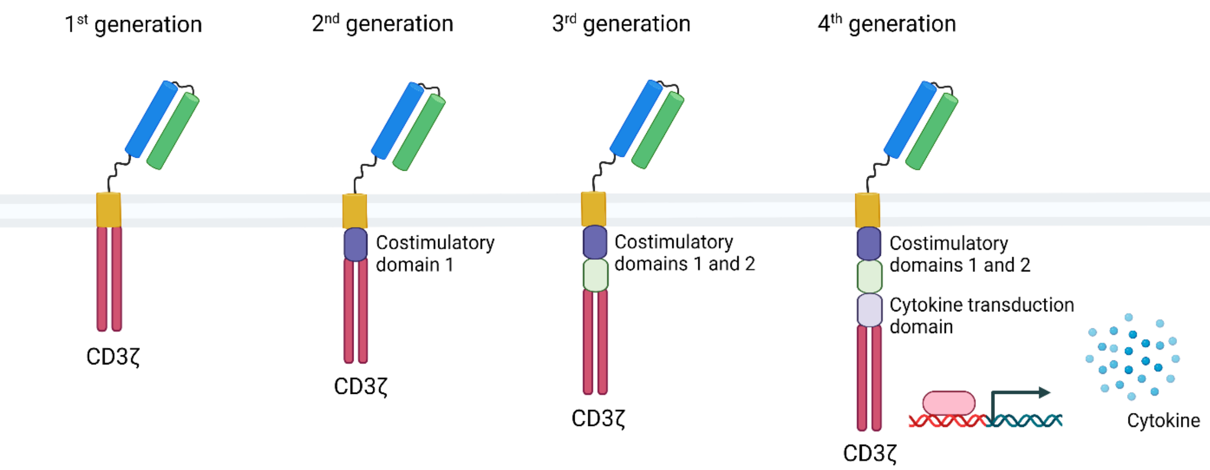

Figure 9: Structure of CAR of different generations

1st generation CARs did not show promising results. However, this has changed since the development of 2nd and 3rd generation CARs, bearing costimulatory receptors. Besides, 4th generation CARs have also been developed with to enhance cytokine production by effector cells and thus, enhance cytotoxicity. Figure generated with Biorender®. Adapted from Makita, et al. [145].

1.4.2 Clinical studies and challenges

A convincing body of evidence has demonstrated the efficacy and safety of CAR-bearing cells both *in vitro* and *in vivo*. The advent of 2nd generation CARs allowed the application of this technology in a clinical setting. Thus, CAR therapy has become a well-established therapeutic strategy, with high efficacy, especially against hematological malignancies.

Back in 2010, the very first patients with various B-cell malignancies were first treated with CAR-T cells directed against the CD19 antigen. Kochenderfer et al. documented the first efficient use of these effector cells against advanced follicular lymphoma. A selective disease regression could be noted for this patient, leading to the absence of B cells in the blood for at least 39 weeks, whereas other cell type counts recovered [152]. Another study was directed against advanced CLL, which is often accompanied by a poor prognosis. Three patients were treated with anti-CD19-CAR-T cells. The genetically modified cells showed a robust expansion *in vivo* and kept B-cell aplasia for at least six months. Importantly, two of three patients achieved complete remission (CR) [153]. In a study with two children with relapsed and refractory ALL, the application of anti-CD19-CAR T cells confirmed the potential for *in vivo* expansion of these effector cells and their capacity of maintaining B-cell aplasia. However, in both cases, severe side effects were observed. Nevertheless, both children achieved CR, although one of them relapsed after two months post-treatment [154].

Meanwhile, better levels of evidence have been achieved for the therapy with CAR-T cells. A phase II study was conducted to assess the remission rates of pediatric and young patients after CD19-CAR-T-cell treatment with tisagenlecleucel (tisa-cel) against B-ALL. For 75 patients, the overall remission rate was 81% within three months. OS at six and twelve months were 73% and 50%, respectively. Moreover, CAR-T cells were still detectable in blood 20 months post-treatment [155]. Another phase II trial evaluated the efficacy of another commercial CAR-T product, axicabtagene ciloleucel (axi-cel), against diffuse large B-cell lymphoma, B-cell lymphoma, or follicular lymphoma. An objective response rate was achieved by 82% of the 101 patients treated. Besides, 40% of those who had a response, remained in complete remission after 15.4 months [156].

Altogether, these data confirm the feasibility of CAR-T cells as immunotherapeutic tools. However, relapse is still a major concern. It has been hypothesized that CD19-CAR-T-cell failure is related to three main factors (**Fig. 10**). Loss of CD19 expression by target cells is estimated to affect 10 to 20% of ALL patients and happens through various mechanisms [157, 158]. An alternative to this problem would be the use of multiple-targeting CAR-T cells, for instance against both CD19 and CD20 antigens, usually expressed by B cells.

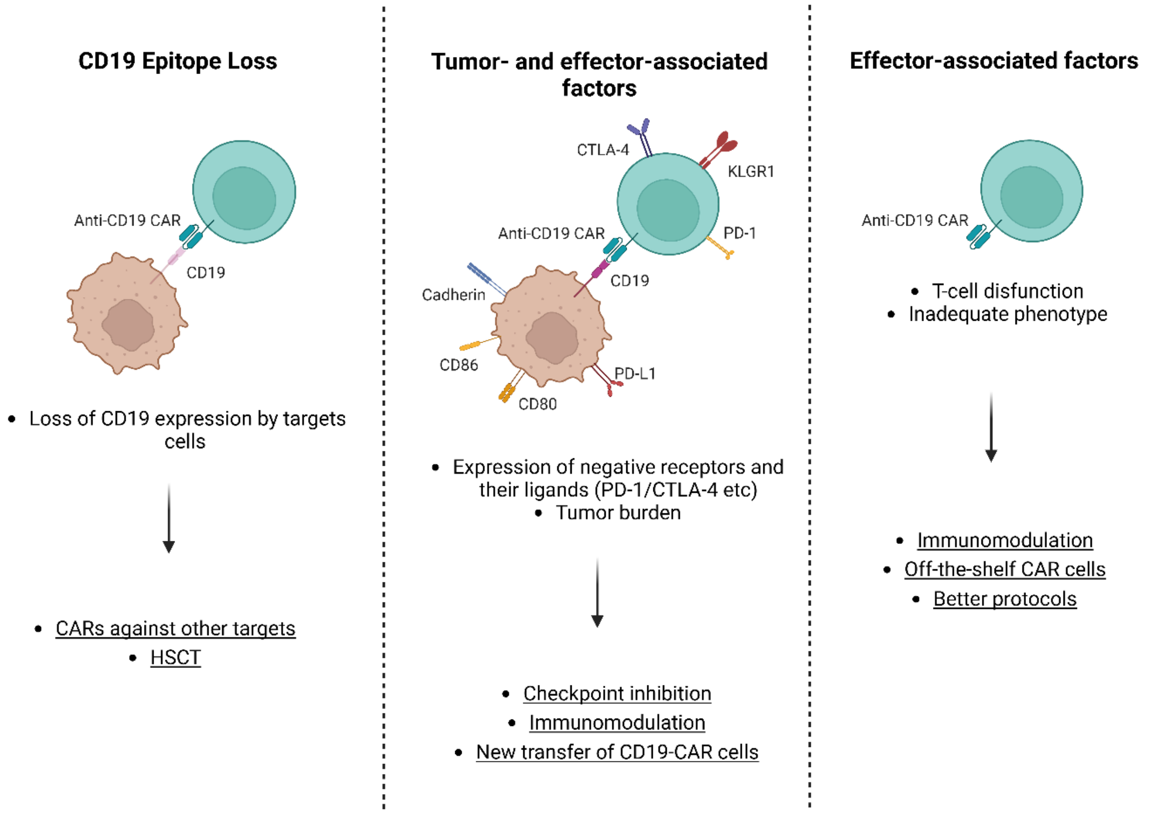

Figure 10: Challenges in the CAR-T-cell therapy

Despite the progress achieved in the last decade and the promising results both in pre-clinical and clinical settings, the potential of CAR-bearing cells is still limited. For instance, several patients experience relapse due to antigen loss by target cells, which takes place through different mechanisms. This could be addressed, for instance, by the design of CARs directed to other targets or more than one target in the same construct. Another problem is the factors associated with both tumor and effector cells, such as the expression of immunosuppressive receptors like PD-1/PD-L1 and CTLA-4/CD86/CD86. These factors affect the function of CAR-T-cells, leading to diminished cytotoxicity and persistence. Besides, lots of studies have focused on the development of better CAR products, in which effector cells possess a superior phenotype and better fitness at the end of the manufacturing process. Figure generated with Biorender®. Adapted from Byrne et al. [159].

Upregulation of inhibitory receptors such as PD-L1 and cadherin is a known mechanism of tumor evasion and is tightly associated with both target and effector cells. The interaction with their counterparts on the surface of effector cells leads to the suppression of these cells and eventual loss of function and persistence [160, 161]. This effect has also been noted in CAR-T-cell therapy [162, 163]. In this context, the combination of CAR-T cell therapy and checkpoint inhibition seems to be justifiable, with a few studies demonstrating its efficacy [164-166]. However, a phase I clinical

study showed no improved expansion or persistence of CAR-T cells upon the combination with PD-1 inhibition against neuroblastoma. But at least, treatment toxicity was low [167]. Importantly, this strategy has shown limited efficiency in patients who previously underwent allogeneic HSCT. Moreover, an increased risk for GvHD has been observed, limiting its application in this particular setting [168, 169].
Finally, there has been made a lot of effort to manufacture better CAR-T products. For instance, it has been shown that T-cell polyfunctionality correlates positively with clinical responses [170]. Besides, the design of the CAR seems to have a direct impact on T-cell function [171]. Likewise, T-cell activation leads to exhaustion and deletion of CD8+ cytotoxic T lymphocytes [172].

1.4.3 CAR-iNKT cells

The idea of harnessing iNKT cells to bear a CAR receptor is not novel and uniting their functionality both as killer cells and as immunoregulators sounds promising. Several studies have evaluated the feasibility of using CAR-iNKT cells in therapy against various malignancies such as B-cell lymphoma, neuroblastoma and myeloma [173-176].
In 2018, Rotolo et al. published a comprehensive study showing the potential of iNKT cells directed against the CD19 antigen. In this work, CD19-CAR-iNKT cells showed enhanced functionality in comparison to CD19-CAR-T cells both *in vitro* and *in vivo* [173]. Interestingly, the intravenous administration of CD19-CAR-iNKT cells, but not CD19-CAR-T cells, eradicated brain lymphoma. Furthermore, Simonetta et al. assessed the direct anti-tumor effect of allogeneic CD19-CAR-iNKT cells against B-cell lymphoma in immunocompromised mice. CD19-CAR-iNKT cells exerted robust tumor control and also elicited cross-priming of host CD8+ T cells, enhancing long-term tumor control. Importantly, this work shows the duality of CD19-CAR-iNKT cells as both direct cytotoxic agents but also as potent immunoregulators [108].
From a clinical point of view, only one phase I study has been published so far showing data on the application of CAR-NKT cells in patients. Autologous GD2-CAR-NKT cells with IL-15 were administered to three pediatric patients with relapsed or refractory neuroblastoma in a dose-escalation trial. The results showed no-dose limiting cytotoxicity, CAR-NKT-cell expansion *in vivo* and tumor infiltration. Besides, an

objective response could be observed for one patient, with bone metastasis regression [177]. Other ongoing studies have tried to assess the use of donor-derived and allogeneic CD19-CAR-iNKT cells against lymphoma and leukemia [178].

1.5 Aim of the work

Various studies using mouse models have demonstrated that iNKT cells prevent GvHD mostly through the expansion of FoxP3+ Treg cells [65, 110, 115]. However, despite a negative correlation between the frequency of iNKT cells and the incidence of GvHD, no variation in the frequency of Treg cells was observed in clinical studies [112, 119]. Therefore, the mechanism by which iNKT cells prevent allo-reactions in humans remains unclear.

Schmid et al. demonstrated that iNKT cells prevent T-cell activation and proliferation *in vitro* in a dose-dependent manner while eradicating tumor cells [126]. Thus, the first part of the present work aimed to explore the mechanisms by which human culture-expanded iNKT cells affect T-cell functionality *in vitro*. For that, the potential of iNKT cells to prevent allo-reactions was investigated through mixed lymphocyte reactions (MLR) and apoptosis assays *in vitro* using cells from healthy donors and GvHD patients.

Further, considering the efficacy of iNKT cells to promote tumor control, the second part of this work was dedicated to establishing and evaluating third-generation CD19-CAR-iNKT cells against CD19+ malignancies. A particular focus was set on the enhancement of their functionality through checkpoint inhibition and simultaneous GvHD control.

2 Material

2.1 Primary cells, bacteria and cell lines

2.1.1 Primary cells

Human buffy coats from healthy volunteers were obtained from the Center of Clinical Transfusion Medicine Tübingen. Samples from peripheral blood mononuclear cells (PBMCs) from patients with ALL were isolated after written informed consent had been obtained. The study was approved by our institutional review board following ethical standards and with the Helsinki Declaration of 1975, as revised in 2013 (IRB approvals 483/2015BO2 and 137/2017BO2).

2.1.2 Bacteria

Table 1: List of bacteria

Bacteria	Manufacturer
E.coli DH5α competent cells	Thermo Fisher Scientific Inc., Waltham, USA
Stellar *E.coli* competent cells	Takara Bio Europe S.A.S, Saint-Germain-en-Laye, France

2.1.3 Cell lines

Table 2: List of cell lines

Cell lines	Characteristics	Origin
HEK 293T	Embryonal kidney cell line	German Collection of Microorganisms and cell culture GmbH, Braunschweig, Germany
Jurkat	T-ALL cell line	American type culture collection (ATCC), Manassas, USA
K562- CD1d	Chronic myeloid leukemia (CML) cell line	Prof. Anastasios Karadimitris (Imperial College London), London, United Kingdom
K562-WT	CML cell line	Prof. Anastasios Karadimitris (Imperial College London), London, United Kingdom
Raji	Burkitt lymphoma (BL) cell line	ATCC, Manassas, USA
Raji-ctrl	BL cell line	Prof. Margot Thome-Miazza (University of Lausanne), Lausanne, Switzerland
Raji-PD-L1	BL cell line	Prof. Margot Thome-Miazza (University of Lausanne), Lausanne, Switzerland

Raji-PD-L2	BL cell line	Prof. Margot Thome-Miazza (University of Lausanne), Lausanne, Switzerland
SEM	ALL cell line	ATCC, Manassas, USA

2.2 Software

Table 3: List of software

Software	Developer
BD FACSDiva™	BD Biosciences, Franklin Lakes, USA
FlowJo v.10	TreeStar, Ashland, USA
GraphPad PRISM 8	GraphPad Software Inc., San Diego, USA
LegendPlex™	Qognit Inc., San Carlos, USA
IDEAS®	Luminex Corporation, Austin, USA

2.3 Instruments

Table 4: List of instruments

Instrument	Manufacturer
Amnis® ImageStream® X Mk II	Amnis/Luminex, Austin, USA
Autoclave	Wesa AG, Eupen, Belgium
Balance, M-Prove	Sartorius AG, Göttingen, Germany
BD FACSAria IIu™ III cell sorter	BD Biosciences, Franklin Lakes, USA
BD FACSCanto™ II cell analyzer	BD Biosciences, Franklin Lakes, USA
BD FACSLyric™ clinical cell analyzer	BD Biosciences, Franklin Lakes, USA
BD LSRFortessa™ cell analyzer	BD Biosciences, Franklin Lakes, USA
BD LSRFortessa™+HTS cell analyzer	BD Biosciences, Franklin Lakes, USA
Cell counter	IVO GmbH & Co, Oberviechtach, Germany
Centrifuge, 5920 R	Eppendorf, Hamburg, Germany
Centrifuge, Megafuge 1.0R	Thermo Fisher Scientific Inc., Waltham, USA
Centrifuge, Multifuge X3R	Thermo Fisher Scientific Inc., Waltham, USA
Freezing chambers (Mr. Frosty)	Thermo Fisher Scientific Inc., Waltham, USA
Fume hood	Waldner Laboreinrichtungen GmbH & Co. KG, Wangen, Germany
Heating block, AccuBlock Digital Dry Bath	Labnet International Inc., Edison, USA
Hot plate and magnetic stirrer, RCT	IKA®-Werke GmbH & Co. KG, Staufen, Germany

Ice machine, Scotsman AF100	Hubbard Systems Inc., Great Blakenham, UK
Incubator shaker, New Brunswick™ Innova ® 44	Eppendorf, Hamburg, Germany
Incubator, Heracell	Thermo Fisher Scientific Inc., Waltham, USA
Incubator, Heracell Vios 160i	Thermo Fisher Scientific Inc., Waltham, USA
MACS magnet, quadroMACS separator	Miltenyi Biotech, Bergisch Gladbach, Germany
Microscope, Axiovert 25	Carl Zeiss AG, Oberkochen, Germany
Microscope, Zeiss Primovert	Carl Zeiss AG, Oberkochen, Germany
Multichannel micropipette (10-100 µL, 20-200 µL)	Brand, Wertheim, Germany
Nitrogen tank, Chronos 420	Cryotherm, Kirchen, Germany
Orbital incubator, S150	Stuart Scientific, Staffordshire, UK
pH-Meter, MP220	Mettler-Toledo, Greifensee, Switzerland
Photometer, Nanodrop I	Thermo Fisher Scientific Inc., Waltham, USA
Pipettboy, Accu-Jet Pro	Integra Biosciences, Zizers, Switzerland
Pipettes	Brand, Wertheim, Germany Eppendorf, Hamburg, Germany
Plate shaker, DOS-10L	NeoLab, Heidelberg, Germany
Reaction tube magnet	CellSystems GmbH, Troisdorf, Germany
Refrigerator -20ºC	Liebherr, Ochsenhausen, Germany
Refrigerator -80ºC	Thermo Fisher Scientific Inc., Waltham, USA
Refrigerator +4ºC	Liebherr, Ochsenhausen, Germany
Safety bench class II, Herasafe 2030i	Thermo Fisher Scientific Inc., Waltham, USA
Stepper pipettes: HandyStep® S Multipipette stream Multipipette E3	 Brand, Wertheim, Germany Eppendorf, Hamburg, Germany Eppendorf, Hamburg, Germany
Ultrasound water bath, Sonorex Super RK 255 H	Bandelin Electronic GmbH & Co. KG, Berlin, Germany
Vacuum pump, Vacusafe	Integra Biosciences, Zizers, Switzerland
Vortex	NeoLab GmbH, Heidelberg, Germany
Water bath	GFL, Burgwedel, Germany
Water purification system, GenPure Pro	Thermo Fisher Scientific Inc., Waltham, USA

2.4 Glass products and consumables

2.4.1 Glass products

Table 5: List of glass products

Glass products	Manufacturer
Coverglas (20 x 24 x 0,4 mm)	NeoLab GmbH, Heidelberg, Germany
Erlenmeyer glass (500 mL)	Schott AG, Mainz, Germany
Glass bottles (250 mL, 500 mL, 1 L, 2 L)	Schott AG, Mainz, Germany
Neubauer counting chamber	Karl Hecht GmbH & Co KG, Sondheim vor der Rhön, Germany
Pasteur capillary pipettes (230 mm)	Wilhelm Ulbrich GdbR, Bamberg, Germany

2.4.2 Consumables

Table 6: List of consumables

Consumables	Manufacturer
Bacteria Petri dishes (100 mm)	Greiner Bio-One, Frickenhausen, Germany
Cell culture dishes (100 mm)	Greiner Bio-One, Frickenhausen, Germany
Cell filter (0.70 μm)	Falcon Corning, New York, USA
Centrifuge tubes (10 mL, 15 mL, 50 mL)	Sarstedt, Nümbrecht, Germany Greiner Bio-One, Frickenhausen, Germany Falcon Corning, New York, USA
Combi-tips (2.5 mL, 5 mL)	Brand, Wertheim, Germany Eppendorf, Hamburg, Germany
Counting chamber, C-Chip Neubauer improved	Carl Roth GmbH & Co. KG, Karlsruhe, Germany
CryoVials	Greiner Bio-One, Frickenhausen, Germany
Culture flasks (25 cm^3, 75 cm^3, 175 cm^3)	Falcon Corning, New York, USA
FACS tubes	Falcon Corning, New York, USA
FACS tubes with lid	Falcon Corning, New York, USA
Gloves, Peha-soft® powder free	Paul Hartmann AG, Heidenheim, Germany
Low blinding microtubes (1.5 mL)	Sarstedt, Nümbrecht, Germany
MACS columns (LS, LD, MS)	Miltenyi Biotech, Bergisch Gladbach, Germany
Non-treated cell culture plates (6, 24, 48-well) (U-bottom)	Falcon Corning, New York, USA
Packaging film, BemisTM Curwood ParafilmTM	Bemis Company Inc., Neenah, USA

Pipette tips (10 µL, 100 µL, 200 µL, 1000 µL, 1250 µL, 5000 µL)	Sarstedt, Nümbrecht, Germany TipOne, Starlap, Milton Keynes, UK
Polypropylene tubes (14 mL)	Greiner Bio-One, Frickenhausen, Germany
Polystyrene reservoir (25 mL)	VWR International, Radnor, USA
Precision wipes, Kimtech	Kimberly-Clark Worldwide Inc., Dallas, USA
Reaction tubes (eppis, 0.5 mL, 1.5 mL, 2 mL, 5 mL)	Sarstedt, Nümbrecht, Germany Eppendorf, Hamburg, Germany
Serological pipettes (2 mL, 5 mL, 10 mL, 25 mL, 50 mL)	Greiner Bio-One, Frickenhausen, Germany Sarstedt, Nümbrecht, Germany
Steril filter (0.20 µm)	Sarstedt, Nümbrecht, Germany
Syringes, BD Plastipak	BD Biosciences, Franklin Lakes, USA
TW-inserts (24-well, 0.4 µm)	Sarstedt, Nümbrecht, Germany
Treated cell culture plates (6, 12, 24, 48, 96-well) (U-, F-bottom)	Greiner Bio-One, Frickenhausen, Germany Falcon Corning, New York, USA

2.5 Chemicals, reagents and kits

2.5.1 Chemicals and reagents

Table 7: List of chemicals and reagents

Chemicals/Reagents	Manufacturer
2-Mercaptoethanol (2-ME)	Carl Roth GmbH & Co. KG, Karlsruhe, Germany
4-(2-hydroxyethyl)-1-piperazineethanesulfonic acid (HEPES)	Gibco Thermo Fisher Scientific, Dreieich, Germany
Agar Agar	Carl Roth GmbH & Co. KG, Karlsruhe, Germany
Ammonium chloride (NH_4Cl)	Sigma-Aldrich, Steinheim, Germany
Ampicillin	Sigma-Aldrich, Steinheim, Germany
Ampuwa	Fresenius Kabi, Bad Homburg, Germany
Bovine serum albumin	Biomol GmbH, Hamburg, Germany
Clicks medium (EHAA)	Fujifilm Irvine Scientific, Santa Ana, USA
Descosept	Dr. Schumacher GmbH, Malsfeld, Germany
Dimethyl sulfoxide (DMSO)	Sigma-Aldrich, Steinheim, Germany
DNase	Merck, Darmstadt, Deutschland
Dulbecco's phosphate-buffered saline (DPBS)	Gibco Thermo Fisher Scientific, Dreieich, Germany
Ethanol	VWR Chemicals, Radnor, USA
Ethylenediaminetetraacetic acid (EDTA)	Sigma-Aldrich, Steinheim, Germany

FcR blocking reagent	Miltenyi Biotech, Bergisch Gladbach, Germany
Fetal bovine serum (FBS)	Sigma-Aldrich, Steinheim, Germany
Gene juice® transfection reagent	Merck, Darmstadt, Germany
Geneticin G418	Gibco Thermo Fisher Scientific, Dreieich, Germany
Glycerol	Merck, Darmstadt, Germany
Iscove's modified Dulbecco's medium (IMDM)	Gibco Thermo Fisher Scientific, Dreieich, Germany
Isopropanol	Merck, Darmstadt, Germany
L-glutamine	Lonza, Verviers, Belgium
Lysogeny broth (LB) Lennox	Carl Roth GmbH & Co. KG, Karlsruhe, Germany
Minimum essential medium (MEM)	gibco Thermo Fisher Scientific, Dreieich, Germany
OneComp beads	eBioscience ThermoFisher Scientific, Dreieich, Germany
Pancoll	Pan-Biotech, Aidenbach, Germany
Penicillin/streptomycin (P/S)	Lonza, Verviers, Belgien
Perform	Schülke & Mayr AG, Frauenfeld, Germany
Polystyrene latex beads (3.0 μm)	Sigma-Aldrich, Steinheim, Germany
Potassium hydrogen carbonate ($KHCO_3$)	Sigma-Aldrich, Steinheim, Germany
Retronectin	Takara Bio Europe S.A.S, Saint-Germain-en-Laye, France
Roswell park memorial institute (RPMI) 1640	Gibco Thermo Fisher Scientific, Dreieich, Germany
RPMI medium 1640+Glutamax	Gibco Thermo Fisher Scientific, Dreieich, Germany
Sodium pyruvate	Gibco Thermo Fisher Scientific, Dreieich, Germany
Trypan blue 0.4%	Sigma-Aldrich, Steinheim, Germany
Water (high-performance liquid chromatography grade, HPLC grade)	Merck, Darmstadt, Germany

2.5.2 Kits

Table 8: List of kits

Kit	Manufacturer
Annexin V-FITC/Propidium iodide (PI) Kit	Miltenyi Biotech, Bergisch Gladbach, Germany
Anti-iNKT Microbeads, human	Miltenyi Biotech, Bergisch Gladbach, Germany
Blood DC Isolation Kit II, human	Miltenyi Biotech, Bergisch Gladbach, Germany
CD3 Microbeads, human	Miltenyi Biotech, Bergisch Gladbach, Germany

CellTrace™ Violet (CTV) – Cell proliferation kit	Thermo Fisher Scientific Inc., Waltham, USA
Carboxyfluorescein-Succinimidylester (CFSE) - Cell Division Tracker Kit	Biolegend, San Diego, USA
LEGENDplex™ Human CD8/NK panel (13-plex)	Biolegend, San Diego, USA
NucleoBond Xtra Maxi Plus EF	Macherey-Nagel GmbH & Co. KG, Düren, Germany

2.6 Media and buffers

2.6.1 Media

Table 9: List of media

Medium	Components
CAR medium	45% Clicks EHAA medium 45% RPMI 1640 0.5% L-glutamine 100 I.U. P/S 10% FBS
DC medium	RPMI 1640+Glutamax 10% FBS 0.08 µM 2-ME 0.1 mM MEM 0.1 mM sodium pyruvate 100 I.U. P/S
Freezing medium	RPMI 1640+Glutamax 20% FBS 10% DMSO
iNKT medium	RPMI 1640+Glutamax 10% FBS 5.5 µM 2-ME 0.1 mM MEM 0.1 mM HEPES 0.1 mM sodium pyruvate 100 I.U. P/S
LB agar plates	20 g LB Lennox 15 g agar-agar 1 L distilled water
LB Medium	20 g LB Lennox 1 L distilled water
Thawing medium	IMDM 10% FBS 100 I.U. P/S 10 µg/mL DNase
Transfection medium	IMDM 0.1 mM sodium pyruvate 10% FBS 100 I.U. P/S

2.6.2 Buffers

Table 10: List of buffers

Buffer	Components
Annexin V buffer	2.5 mL 20x annexin V buffer 47.5 mL ampuwa
Erylysis buffer	155 mM NH_4Cl 10 mM $KHCO_3$ 0.1 mM EDTA Millipore water to 1L
FACS buffer	DPBS 2% FBS
MACS buffer	DPBS 0.5% FBS 2 mM EDTA

2.7 Plasmids

Table 11: List of plasmids

Plasmids	Origin
MSCV-hCD19	AddGene Europe, Teddington, UK.
PegPAM	Prof. Malcolm Brenner (Baylor College of Medicine), Houston, USA
RDF	Prof. Malcolm Brenner (Baylor College of Medicine), Houston, USA
SFG.CD19-CD28/CD137ζ	Prof. Malcolm Brenner (Baylor College of Medicine), Houston, USA

2.8 Antibodies, tetramers and viability dyes (VD)

Table 12: List of antibodies, tetramers and VD

Antigen/Target	Clone	Fluorochrome	Dilution (1:x)	Manufacturer
7-AAD	-	-	100	BD Biosciences, Franklin Lakes, USA
Annexin V	-	FITC	100	Miltenyi Biotech, Bergisch Gladbach, Germany
CD127	A019D5	PE-Cy7	200	Biolegend, San Diego, USA
CD14	HCD14	AF700	100	Biolegend, San Diego, USA
CD19	HIB19	FITC	200	BD Biosciences, Franklin Lakes, USA

CD19	HIB19	BV421	200	Biolegend, San Diego, USA
CD1c	L161	APC-Cy7	20	Biolegend, San Diego, USA
CD1d	51.1	PE	20	Biolegend, San Diego, USA
CD25	BC96	BV711	80	Biolegend, San Diego, USA
CD28	CD28.2	BV650	50	Biolegend, San Diego, USA
CD3	HIT3a	APC	100	Biolegend, San Diego, USA
CD3	HIT3a	PerCP-Cy5.5	400	Biolegend, San Diego, USA
CD3	OKT3	BV605	400	Biolegend, San Diego, USA
CD303	201a	PerCP-Cy5.5	20	Biolegend, San Diego, USA
CD4	RPA-T4	BV421	400	Biolegend, San Diego, USA
CD4	OKT4	BV785	200	Biolegend, San Diego, USA
CD40	5C3	FITC	25	Biolegend, San Diego, USA
CD44	IM7	BV510	200	Biolegend, San Diego, USA
CD45RA	HI100	BV650	200	Biolegend, San Diego, USA
CD69	FN50	BV711	80	Biolegend, San Diego, USA
CD8	HIT8a	FITC	200	Biolegend, San Diego, USA
CD8	HIT8a	AF700	600	Biolegend, San Diego, USA
CD80	2D10	PE-Cy7	50	Biolegend, San Diego, USA
CD86	IT2.2	BV605	400	Biolegend, San Diego, USA
CTLA-4	BNI3	BV421	200	Biolegend, San Diego, USA
efluor 506	-	-	1000	Thermo Fisher Scientific Inc., Waltham, USA
eFluor 780	-	-	1000	Thermo Fisher Scientific Inc., Waltham, USA
Goat F(ab')2 anti-Human IgG (H+L)-(F(ab')2-fragment)	polyclonal	PE	40	Jackson Immunoresearch Europe Ltd, Ely, UK
HLA-DR	L243	BV650	100	Biolegend, San Diego, USA
IgG1 (mouse, κ) Isotype control (ctrl)	MOPC-21	APC	*	Biolegend, San Diego, USA
IgG2b (mouse, κ) Isotype ctrl	MPC-11	APC	*	Biolegend, San Diego, USA
IgG2b (mouse, κ) Isotype ctrl	MOPC-173	PE	*	Biolegend, San Diego, USA
KLRG1	14C2A07	PE-Cy7	100	Biolegend, San Diego, USA
LAG-3	11C3C65	FITC	50	Biolegend, San Diego, USA
Nivolumab	-	-	10000	Novartis AG, Basel, Switzerland

PBS57-CD1d tetramer	-	APC	1000	National Institutes of Health, Atlanta, USA
PBS57-CD1d tetramer	-	PE	1000	National Institutes of Health, Atlanta, USA
PD-1	EH12.2H7	BV711	100	Biolegend, San Diego, USA
PD-1	EH12.2H7	BV605	100	Biolegend, San Diego, USA
PD-L1	MIH2	APC	200	Biolegend, San Diego, USA
PD-L2	24F.10C12	PE	40	Biolegend, San Diego, USA
PI	-	-	20	Miltenyi Biotech, Bergisch Gladbach, Germany
TIGIT	A15153G	PerCP-Cy5.5	400	Biolegend, San Diego, USA
TIM-3	F38-2E2	BV510	50	Biolegend, San Diego, USA
Ultraleaf purified IgG4 Isotype ctrl	QA16A15	-	10000	Biolegend, San Diego, USA

* Same concentration used for the specific antibodies.

2.9 Cytokines and stimulators

Table 13: List of cytokines and stimulators

Cytokines and stimulators	Manufacturer
Dynabeads™ human-T-Activator CD3/CD28	Thermo Fisher Scientific Inc., Waltham, USA
GM-CSF	Miltenyi Biotech, Bergisch Gladbach, Germany
rhIL-2	Novartis AG, Basel, Switzerland
rhIL-4	Miltenyi Biotech, Bergisch Gladbach, Germany
α-GalCer	Abcam, Cambridge, UK

3 Methods

3.1 Cellular methods

3.1.1 Isolation of PBMCs

PBMCs were isolated from samples of concentrated peripheral blood (buffy coats) using density gradient centrifugation. A high-density polymer (Pancoll®, 1,077 g/mL) was used as a separation solution. After centrifugation, erythrocytes and granulocytes, which have a higher density than the polymer, form a cell pellet on the bottom. Plasma and thrombocytes, which are lighter, stay on the superior layer, while PBMCs form a layer between the plasma and the polymer. Buffy coat samples were diluted 1:3 with DPBS and overlaid on 15 mL Pancoll®. After centrifugation (800xg, 20 min, RT, without brake and acceleration), the PBMCs were collected, transferred to another tube and washed twice with 50 mL DPBS (450xg, RT, 5 min). The remaining thrombocytes were removed in the last washing step with 40 mL DPBS and centrifugation (130xg, RT, 10 min). After the washing steps, the supernatant was removed. The isolated PBMCs were resuspended in either DPBS or in an appropriate culture medium and counted using a trypan blue solution and a Neubauer counting chamber.

3.1.2 Determination of the cell number

The cell number was determined by trypan blue staining and counting. Dead cells, with a damaged cell membrane, are permeable to trypan blue and can be observed under the microscope for their blue color, while alive cells can be identified for their brightness.

10 µL cell suspension was stained with 10 µL trypan blue solution (dilution factor 2), transferred to a Neubauer counting chamber and counted under the microscope. Freshly isolated PBMCs were stained and counted only after pre-treatment with EryLysis buffer for 5 min at a 1:10 ratio for removal of the remaining erythrocytes (final dilution factor 20). The number of alive cells was determined by the formula below:

$$\text{Cell number} = \frac{\text{alive cells}}{\text{number of counted squares}} \text{ x dilution factor x } 10.000$$

3.1.3 Cell freezing and thawing

The supernatant of the cell suspension was removed after centrifugation (5 min, RT, 300xg). The cell pellet was resuspended in freezing medium (1-5x10^7 cells/mL) and aliquoted at 1 mL per cryovial. The vials were placed in a Mr. Frosty chamber with isopropanol to ensure a slow freezing process and transferred to a -80 ºC refrigerator. For long-term storage, the cells were stored in liquid nitrogen tanks. To thaw the cells, frozen cells were immersed in a water bath at 37 ºC until only a small solid ice core remained. The content of the vials was completely transferred to 40 mL DPBS. After centrifugation (5 min, RT, 450xg), the supernatant was completely removed and the cells were resuspended in an adequate medium. Since the freezing medium contains DMSO, which is cytotoxic, all steps were performed quickly to avoid cell death. Cells used for functional assays were kept overnight in thawing medium before usage.

3.1.4 Generation of monocyte-derived dendritic cells (mo-DCs)

Mo-DCs were generated from PBMCs considering the ability of monocytes to attach to plastic surfaces. Once the monocytes form an adhesive layer on plastic plates or flasks, other cell types, which remain in suspension, are removed and a cocktail with IL-4 and GM-CSF is used to induce their differentiation into mo-DCs. Freshly isolated PBMCs were resuspended in DC medium at a cell concentration of 4x10^6/mL. 1.5 mL/well of the cell suspension was seeded to 6-well plates. After 2h (37ºC, 5% CO_2), the medium was completely removed and the wells were washed with DPBS to remove non-adherent cells. 3 mL DC medium, supplemented with 100 ng/mL GM-CSF and 50 ng/mL IL-4, was added to each well. During 6 days, the medium was supplemented every other day with 100 ng/mL GM-CSF and 50 ng/mL IL-4. On day 6, the mo-DCs were flushed from the wells using DPBS and counted. The cells were tested for their maturity by flow cytometric analysis using the panel below (**table 14**). The gates were set on DCs (FSC-A vs. SSC-A), singlets (SSC-W vs. SSC-A) and viable cells. Maturity was assessed by the percentage of CD3-CD19-CD14-HLA-DR+CD40+CD80+CD86+ cells.

Table 14: Antibodies used to determine purity and maturation of mo-DCs

Antigen/Target	Fluorochrome	Dilution	Clone
CD14	AF700	100	HCD14
CD19	BV421	200	HIB19
CD1d	PE	40	51.1
CD3	APC	100	HIT3a
CD40	FITC	25	5C3
CD80	PE-Cy7	50	2D10
CD86	BV605	400	IT2.2
HLA-DR	BV650	100	L243
VD	eFluor 506	1000	-

3.1.5 Cultivation of cell lines

Cancer cell lines were cultured according to the guidelines of the German Collection of Microorganisms and Cell Cultures for cell seeding and maintenance.

3.1.6 *Ex vivo* expansion of iNKT cells

iNKT cells are rare T lymphocytes and comprise approximately 0.1-0.5% of the total lymphocytes in blood [179]. Therefore, for downstream applications, iNKT cells must be expanded from PBMCs to achieve higher cell numbers. In this work, a well-established protocol for the *ex vivo* expansion of human iNKT cells was used [126]. Briefly, freshly isolated PBMCs (3.1.1) were resuspended in iNKT medium supplemented with 100 I.U. rhIL-2 and 100 ng/mL α-GalCer to a cell concentration of 1.5×10^6 cells/mL. The remaining PBMCs were frozen to be used later as autologous feeder cells. The cells were incubated for 7 days (37ºC, 5% CO_2). On day 7, the iNKT-cell expansion was determined by flow cytometry using the following antibodies and reagents: CD3-PerCP-Cy5.5 (HIT3a), CD4-BV421 (RPA-T4), CD8-FITC (HIT8a), PBS57-CD1d-Tetramer-PE and eFluor 506. The staining was performed as in 3.2.1. The percentage of iNKT cells was determined by gating on lymphocytes (FSC-A vs.

SSC-A plots), single cells (FSC-A vs. FSC-H), viable (eFluor 506-) and CD3+PBS57-CD1d-Tetramer+ cells (iNKT cells).

Cultures, in which the percent of iNKT cells was higher than 1%, were further expanded for another 7 days, using thawed autologous feeder cells as stimulators. Feeder cells were prepared as follows. Frozen autologous PBMCs were thawed (3.1.3) and resuspended in iNKT medium ($0.5*10^6$ cells/mL). 100 ng/mL α-GalCer was added to the cells and after 4h (37ºC, 5% CO_2), the cells were irradiated with 30 Gy. iNKT-cell cultures were restimulated with α-GalCer-loaded feeder cells at a 1:2 ratio (iNKT cell:feeder cell) in fresh iNKT medium (final cell concentration=$1.5x10^6$ cells/mL), supplemented with 50 I.U./mL rhIL-2 and 50 ng/mL α-GalCer. The cells were cultured for another 7 days (37ºC, 5% CO_2) and on day 14, the percentage of iNKT cells was determined by flow cytometry as described above. In case of successful expansion (≥30% iNKT cells), the iNKT cells were isolated by MACS (3.3.1).

3.1.7 Generation of CD19-CAR-iNKT cells

On day 0, upfront isolated iNKT cells (3.3.1) were resuspended at $1x10^6$ cells/mL in CAR medium, supplemented with 200 I.U./mL rhIL-2 and 200 ng/mL α-GalCer. Autologous irradiated α-GalCer-loaded feeder cells (3.3.2) were added at a 1:2 ratio (iNKT cell:feeder cell) to induce cell activation (final cell concentration=$1.5x10^6$ cells/mL). The genetic modification was performed through retroviral transduction, using Retronectin® as a transduction enhancer. Retronectin® plates were prepared on day 2 by adding 10 µg/well Retronectin® solution (diluted in DPBS) to a non-tissue 24-well culture plate. The plates were stored at 4ºC for 24h. On day 3, Retronectin®-coated wells were loaded with retroviral supernatant. For that, the Retronectin® solution was removed from the wells and these were washed once with DPBS. 1 mL of the thawed retrovirus supernatant was promptly added to each well. The plates were centrifuged at 2000xg at 32ºC for 90 min. Meanwhile, the activated iNKT cells were harvested, washed and counted. The cell concentration was adjusted to $1x10^6$ cells/mL with CAR medium supplemented with 200 I.U./mL rhIL-2 and 200 ng/mL α-GalCer (calculated to the final volume of 2 mL). After centrifugation, the viral supernatant was removed from the Retronectin® plates and 1 mL of the cell suspension was quickly added to each well. 1 mL of retrovirus was further added to each well. A negative control was prepared by culturing iNKT cells under the same conditions but without any retroviral treatment (untransduced iNKT cells). The plates were centrifuged at 450xg for 5 min at RT to improve the contact of the cells with the retrovirus-Retronectin®-coated plate bottom. The cells were incubated for 72h (37ºC, 5% CO_2). After this time (day 6), the cells were harvested, washed three times to remove the viral supernatant and resuspended in CAR medium. The expansion step was performed by the addition of autologous irradiated α-GalCer-loaded feeder cells at a 1:2 ratio (CD19-CAR-iNKT cell/iNKT cell:feeder cell), 100 I.U./mL rhIL-2 and 100 ng/mL α-GalCer to the CD19-CAR iNKT cells or untransduced iNKT cells. This step was repeated twice, once a week (on days 6 and 13). On day 20, the transduction efficiency was determined by flow cytometry after $F(ab')_2$ antibody staining (3.2.2) using the panel in table 15. Lymphocytes were pre-gated using the FSC-A vs. SSC-A parameters. Further analysis was performed on singlets (SSC-W vs. SSC-A), viable (eFluor780-) iNKT cells (CD3+PBS57-CD1d-tetramer+). The gates for CD19-CAR-iNKT cells were set using untransduced iNKT cells as a negative control. A schematic representation of the protocol for the generation of CD19-CAR-iNKT cells is depicted in figure 11.

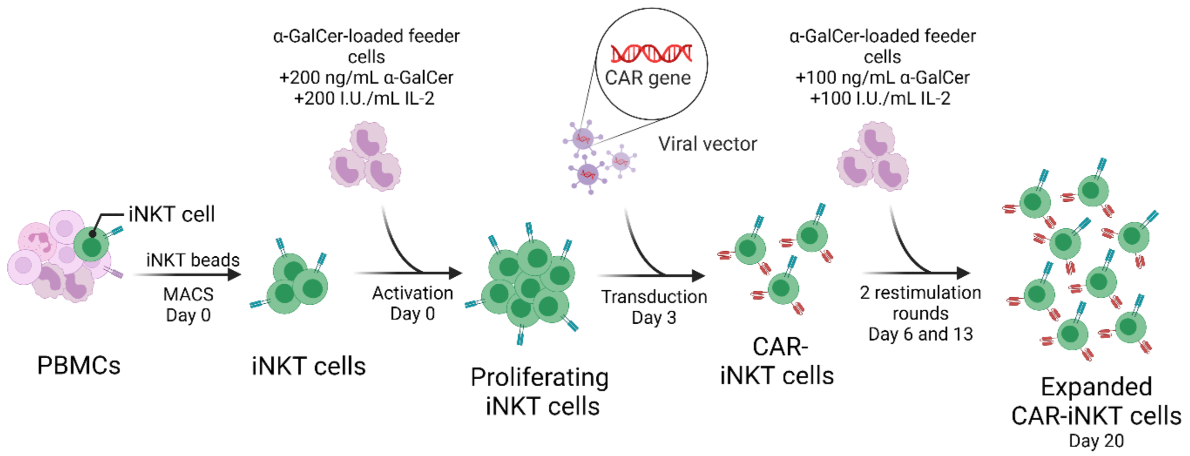

Figure 11: Protocol for the generation of CD19-CAR-iNKT cells

(A) Schematic representation of the generation of CD19-CAR-iNKT cells. iNKT cells are immunomagnetically isolated from PBMCs using anti-iNKT-cell Microbeads on day 0. The cells collected in the flow-through are loaded with α-GalCer for 4h and irradiated with 30 Gy (feeder cells). The enriched iNKT-cell fraction is activated with part of the feeder cells, 200 I.U./mL rhIL-2 and 200 ng/mL α-GalCer. The remaining feeder cells are frozen for posterior usage. On day 3, activated iNKT cells are transduced with retroviral supernatant containing the CAR gene. On day 6, CD19-CAR-iNKT cells are harvested and expanded in two stimulation rounds with α-GalCer-loaded feeder cells and 100 I.U./mL rhIL-2 and 100 ng/mL α-GalCer. On day 20, the transduction efficiency is determined by flow cytometry.

Table 15: FACS panel to determine the transduction efficiency of CD19-CAR-iNKT cells

Antigen/Target	Fluorochrome	Dilution	Clone
CD3	BV605	400	OKT3
CD4	BV421	400	RPA-T4
CD8	FITC	200	HIT8a
$F(ab')_2$ Fragment	PE	20	-
PBS57-CD1d-Tetramer	APC	1000	-
VD	eFluor 780	1000	-

3.1.8 Generation of CD19 expressing K562 cells

K562-wild-type (K562-WT) and K562-CD1d cells were kindly provided by Prof. Dr. Karadimitris from the Department of Medicine of the Imperial College London (London, United Kingdom). Besides CD1d, K562-CD1d cells also express the mCherry fluorochrome. Both cell lines were transduced to stably express the CD19 antigen. The day before transduction, the cells were split at 1:2. The transduction procedure was performed as described in 3.1.7, however with retroviral supernatant generated in 3.3.10 and without an activation step. After 72h, the cells were washed and analyzed by flow cytometry for CD19 expression using CD19-BV421 (HIB19) and eFluor 780. Debris was removed from the analysis by gating the larger cell population using the FSC-A vs. SSC-A parameters. Further analysis was performed on singlets (SSC-W vs. SSC-A) and viable cells (eFluor 780-).
$1x10^6$ transduced cells were stained under sterile conditions as described in 3.2.1 with CD19-BV421 (HIB19) and eFluor 780 and sorted in bulk using a BD FACSAria IIu^{TM} III cell sorter. The cells were discriminated from remaining contaminating cells using FCS-A vs. SSC-A gating followed by singlet gating using the FSC-W vs. FSC-H and SSC-W vs. SSC-H parameters. After the exclusion of dead cells (VD+ cells), cells were sorted into CD19+, CD1d+ (mCherry+) and CD19+CD1d+ (double positive, DP) cells. Sorted cells were further expanded for one week, frozen and stored in liquid nitrogen tanks.

3.2 Analytical methods

All flow cytometric analyses were performed using FACS LSRFortessa™, FACS LSRFortessa™+HTS or FACSCanto™ II. The generated data were analyzed using the software FlowJo. LegendPlex assays were measured using the FACSLyric™ with autosampler and analyzed with the LegendPlex software. ImageStream assays were measured using the Amnis® ImageStream® X Mk II and the data analysis was performed with the Software IDEAS®.

3.2.1 Extracellular staining

Cells were harvested into a FACS tube and washed with FACS buffer (450xg, 4ºC, 5 min). After the supernatant was removed, 50 µL FcR blocking reagent (1:100 in FACS buffer) was added to the cells to prevent unspecific interactions between antibodies and Fc receptors, which are expressed on the surface of B cells, DCs and monocytes. After incubation (5 min, RT, protected from light), 50 µL of the master mix or FACS buffer plus antibody of interest was added to the cells. The cells were incubated at 4ºC for 20 min and washed once with FACS buffer (450xg, 4ºC, 5 min). The supernatant was removed, and the cells were resuspended in 100 µL FACS buffer for analysis. The samples were analyzed within 2h.

3.2.2 F(ab')$_2$ antibody staining

The transduction efficiency of CD19-CAR-iNKT cells was determined by surface staining with an anti-human IgG (H+L) F(ab')$_2$ fragment (PE) and subsequent flow cytometric analysis. This antibody binds to the Ig region, which is designed as the hinge of the CAR receptor. For the staining, $1x10^6$ cells were transferred to FACS tubes, washed with FACS buffer and centrifuged twice for 5 min (450xg, RT) for the removal of any remaining medium. The cells were resuspended in 100 µL FACS buffer and 2.5 µL anti-human IgG (H+L) F(ab')$_2$ fragment (PE) were added to each sample. After incubation (20 min, RT, protected from light), the cells were washed twice with FACS buffer (450xg, RT, 5 min). The cells were stained extracellularly to determine the presence of other surface antigens (e.g., CD3) (3.2.1). The cells were resuspended in 100 µL FACS buffer and analyzed within 2h.

3.2.3 CD19 protein staining

The staining with the F(ab')$_2$ fragment is not compatible with experiments involving nivolumab. As the F(ab')$_2$ fragment binds to general Ig motifs, this antibody may also bind unspecifically to remaining nivolumab on the cell surface, resulting in false positive results for CAR cells. In these sets of experiments, CD19-CAR-iNKT cells were stained with a biotin-conjugated CD19 protein, which is recognized by the anti-CD19 binding domain of the CAR receptor. Subsequently, streptavidin conjugated to a fluorochrome allows the detection by flow cytometry. The staining procedure is performed as follows. The cells were harvested and washed once with FACS buffer and centrifuged for 5 min at 450xg at RT. The supernatant was removed and 1 µL CD19 protein was added to each sample. After 10 min (RT, protected from light), the cells were washed twice with FACS buffer. Streptavidin-PE was added together with the desired antibodies for extracellular staining, depending on the purpose of the analysis (3.2.1 or 3.2.4). The cells were resuspended in 100 µL FACS buffer and analyzed within 2h.

3.2.4 Annexin V staining

The annexin V staining was performed according to the manufacturer's instructions. Briefly, the cells were washed twice (450xg, RT, 5 min) with 100 µL 1x annexin buffer and then, stained with 100 µL master mix containing the annexin V reagent (1:100) and eventually other antibodies for extracellular staining. After 15 min (RT, protected from light), the cells were washed once (450xg, RT, 5 min) and resuspended with 100 µL annexin buffer for analysis (within 2h).

3.2.5 Multiplex analysis

Multiplex analysis was performed using a LegendPlex™ Human CD8/NK 13-plex Kit. The assay is a bead-based immunoassay that works like sandwich immunoassays. For that, beads of different sizes coated with different antibodies are used. The analytes attach to the antibodies on the bead surface and can be detected by flow cytometry using a biotinylated detection antibody and further with fluorochrome-attached streptavidin. Thus, the analytes can be analyzed according to the bead size and fluorescence. The assays were performed with supernatants collected and frozen after DC apoptosis induction and cytotoxicity assays (3.5.5, 3.5.8). The samples were prepared as instructed by the manufacturer. The standard control was prepared in seven concentrations (0, 2.4, 9.8, 39.1,156.3, 625, 2.500 and 10.000 pg/mL) diluted in assay buffer. The supernatants were thawed at RT before the assay. 15 µL of the samples or standard controls was added to each well of a polypropylene V-bottom 96-well plate together with 15 µL assay buffer and 15 µL beads. The plate was incubated at RT for 2h on a plate shaker (800 RPM, protected from light). The beads were washed with wash buffer twice. 15 µL of the detection antibodies was added to each well. The plate was incubated at RT for 1h on a plate shaker (800 RPM, protected from light). After this time, 15 µL of the streptavidin-PE was added to each well. After incubation (30 min, RT, 800 RPM, protected from light), the samples were washed twice with 200 µL wash buffer (450xg, 5 min, RT) and resuspended in 150 µL assay buffer. The flow cytometric analysis was performed within 2h.

3.2.6 Staining for ImageStream assays

ImageStream is a technique that combines flow cytometry and microscopy, which allows detailed imagery combined with the possibility of analyzing cell antigens through fluorescence measurements. After the incubation time, the cells were harvested and centrifuged at 200xg for 10 min at RT. The medium was removed and the cells were washed once (200xg, RT, 10 min) with FACS buffer. The cells were stained for CAR expression as described in 3.2.2. After the incubation time, the cells were washed twice (200xg, RT, 10 min) with annexin buffer. The annexin V staining was performed as described in 3.2.4. After the annexin V staining, the cells were washed once with annexin buffer, resuspended in 100 µL annexin buffer and analyzed within 2h.

3.3 Preparative methods

3.3.1 iNKT-cell isolation

iNKT cells were isolated either after *ex vivo* expansion of iNKT cells or upfront directly from PBMCs (for the generation of CD19-CAR-iNKT cells), using anti-iNKT microbeads from Miltenyi Biotech, according to the manufacturer's instructions. Briefly, PBMCs or *ex vivo* expanded iNKT cultures were first resuspended in MACS puffer (400 µL/1x10^6 cells). Anti-iNKT microbeads were added to the cell suspension at a concentration of 100 µL of anti-iNKT microbeads per 1x10^8 total cells. After incubation (15 min, 4ºC), the cells were washed with MACS buffer (10 min, 4ºC, 300xg) and loaded into a LS column posed in a magnet. The column was washed 3 times with MACS buffer. After the removal of the column from the magnet, the isolated iNKT cells were flushed from the column with MACS buffer into a collection tube.

3.3.2 Preparation of α-GalCer-loaded feeder cells

The flow-through fraction of the upfront iNKT-cell isolation (3.3.1) was collected in a 50 mL falcon tube. After centrifugation (5 min, RT, 450xg) and removal of the supernatant, the cells were resuspended in CAR medium supplemented with 100 ng/mL α-GalCer at 1.5x10^6 cells/mL. After incubation (4h, 37ºC, 5% CO_2), the cells were irradiated with 30 Gy. Part of the cells were used on the same day for iNKT-cell activation (3.1.7) and the remaining cells were frozen (3.1.3) to be used in later stimulation steps.

3.3.3 T-cell isolation

T cells were isolated from PBMCs using CD3 microbeads according to the manufacturer's instructions. PBMCs were resuspended in MACS buffer (1x10^7 cells/80 µL). CD3 microbeads were added to the cell suspension (20 µL/1x10^7 cells). After incubation (15 min, 4ºC), the cells were washed with MACS buffer (10 min, 4ºC, 300xg) and loaded into a LS column posed in a magnet. The column was washed 3 times with MACS buffer. The column was removed from the magnet and attached T cells were flushed into a collection tube.

3.3.4 Preparation of Dynabeads® CD3/CD28

The calculated necessary amount of beads ($4x10^4$ beads/µL) was transferred to a 2 mL reaction tube. The beads were washed with 1 mL DPBS+1% BSA and posed in a magnet. Once the beads were attached to the tube walls, the supernatant was removed and after the removal from the magnet, the beads were resuspended in the desired amount of iNKT medium. T cells were stimulated at a 1:1 (bead:T cell) ratio.

3.3.5 Blood DC isolation

Blood DCs were isolated from PBMCs using the Blood Dendritic Cell isolation kit II according to the manufacturer's instructions. The first separation aims to enrich the monocyte, B cell and dendritic cell fraction while eliminating T cells. The second separation allows further enrichment of the DC fraction. PBMCs were resuspended in MACS buffer ($1x10^8$ cells/300 µL). 100 µL FcR blocking reagent and 100 µL non-DC depletion cocktail were added to the cells. After incubation (15 min, 4ºC), the cells were washed with MACS buffer (10 min, 4ºC, 300xg) and loaded into a LD column posed in a magnet. After three washing steps with MACS buffer, the cells collected in the flow-through were collected. For the DC enrichment, the cells in the flow-through were washed (10 min, 4ºC, 300xg) and resuspended in MACS buffer to a cell concentration of $1x10^8$ cells/300 µL. 100 µL of the DC enrichment cocktail was added to the cells. After incubation (15 min, 4ºC), the cells were washed with MACS buffer (10 min, 4ºC, 300xg) and loaded into a MS column posed in a magnet. After three washing steps (10 min, 4ºC, 300xg), the column was removed from the magnet and the cells were flushed into a collection tube.

3.3.6 Blood DC cell sorting

To isolate different blood DC subsets, the MACS-isolated blood DCs (3.3.5) were stained with the antibodies CD1c-APC-Cy7 (L161) and CD303-PerCP-Cy5.5 (201a), as described above (2.2.1), under sterile conditions. The cells were sorted in bulk using a BD FACSAria IIu™ III cell sorter. DCs were first gated using the FCS-A vs. SSC-A parameter followed by singlet gating using FSC-W vs. FSC-H and SSC-W vs. SSC-H gating. Conventional DCs (cDC) were sorted as CD1c+ and plasmacytoid DCs (pDC) were sorted as CD303+ cells.

3.3.7 CFSE staining

Cell proliferation was determined by CFSE dilution. The CFSE dye binds covalently to free amine groups in diverse internal cell structures. The fluorescence is diluted when stained cells proliferate, resulting in a weaker signal amongst daughter cells and thus, allowing the determination of their proliferation state. For the staining, isolated cells were resuspended in 1 mL DPBS and stained with 5 µM CFSE for 5 min, protected from light. After incubation, the reaction was stopped with 10 mL FBS and the cells were centrifuged for 5 min (300xg, RT). Afterward, the cells were washed twice with DPBS with 5% FBS (300xg, RT, 5 min) and then resuspended in an adequate medium.

3.3.8 CellTrace Violet (CTV) staining

For cytotoxicity assays, target cells were differentiated from other cell types by a CTV staining. Conversely to several surface antigens, CTV is not downregulated and can be identified even in case of cell death. Similar to CFSE, CTV dye also binds covalently to free amine groups in diverse cell structures. Before the staining, target cells were centrifuged (5 min, RT, 450xg) and the supernatant was completely removed. The cells were resuspended in 1 mL DPBS and stained with 500 nM CTV for 20 min (37ºC, protected from light). After this time, 4 mL cell culture medium was added to the cells to stop the reaction. After 10 minutes, the cells were centrifuged (5 min, RT, 450xg) and the supernatant was removed. Afterward, the cells were resuspended in appropriate cell medium.

3.3.9 Preparation of SFG.CD19-CD28/CD137ζ-CAR retrovirus supernatant

293T HEK cells were thawed (3.1.3) and plated in 10 mm cell culture dishes for 7 days before transfection with transfection medium supplemented with geneticin G418. The cells were split 1:10 every other day or by achieving 80-90% confluency. 18h before transfection, the cells were split 1:10 with transfection medium. The transfection was supported by the transfection enhancer GeneJuice®. For each plate, 470 µL IMDM medium were mixed with 30 µL Gene Juice®. Separately, the plasmids RDF (envelope, 2.5 µg), PeqPAM (gag/pol, 3.75 µg) and SFG.CD19-CD28/CD137ζ (CAR, 3.75 µg) (**Fig. 12**) were mixed. The mixture IMDM/GeneJuice® was added dropwise to the plasmid mixture. After 15 min, 500 µL of this mixture was added dropwise to each plate containing 293T HEK cells. After a 48h-incubation (37ºC, 5% CO_2), the supernatants containing viral particles were collected and transferred to 50 mL falcon tubes. The supernatants were centrifuged for 5 min (4ºC, 250xg) twice for the removal of any possible remaining cells, aliquoted in 1.5 mL Eppendorf tubes and stored at -80ºC. Fresh medium was added to the plates, which were incubated for another 24h (37ºC, 5% CO_2). After this time, the supernatant collection was repeated.

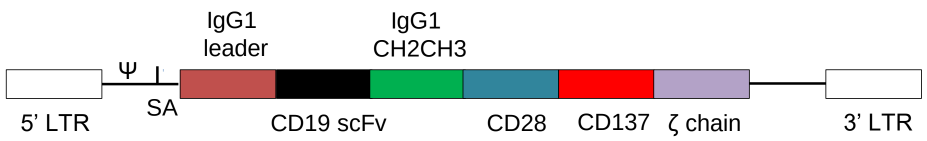

Figure 12: Structure of the 3rd generation CAR

The CAR construct used in this work expresses a 3rd generation CAR. The leader sequence and the hinge were derived from usual IgG1 sequences. The antigen-binding site is a single-chain variable fragment (scFV) of an anti-CD19 antibody (clone FMC63). Co-stimulatory domains derive from CD28 and CD137 sequences and the signaling domain derives from CD3ζ-chain sequences.

3.3.10 Preparation of CD19 retrovirus supernatant

The preparation of the CD19 retrovirus supernatant was performed as described in 3.3.9. However, the SFG.CD19-CD28/CD137ζ-CAR construct was substituted by an MSCV-hCD19 construct.

3.3.11 Plasmid transformation

The plasmid-DNA was amplified in *E. coli* (DH5α or Stellar cells). After *E. coli* was thawed on ice, 10 ng plasmid DNA was added carefully to 50 µL bacterial cells. After incubation on ice (30 min), the bacteria were placed in a water bath (42ºC) for 45 seconds and brought back on ice for 2 min. 400 µL SOC medium was added to the cells and the bacteria were incubated on a heating block for 45 min (300 RPM, 37ºC). The *E. coli* were seeded on LB agar plates supplemented with ampicillin (1:1000) and incubated for 8h (37ºC).

3.3.12 Plasmid preparation (Maxi-Prep)

Isolated colonies were picked from the LB agar plates and seeded in 5 mL LB medium supplemented with ampicillin (1:1000). The cultures were incubated for 8h on a shaker (300 RPM, 37ºC) and transferred to 300 mL LB medium supplemented with ampicillin (1:1000). The *E. coli* were allowed to grow for another 8h (300 RPM, 37ºC). The plasmid-DNA isolation was performed using the Macherey-Nagel™ Nucleobond™ Xtra Maxi plus EF kit according to the manufacturer's instructions. Briefly, the bacteria cultures were harvested and centrifuged for 20 min at 4400xg (4ºC). The supernatant was completely removed and the cell pellet was resuspended with resuspension buffer, followed by lysis buffer addition. The tubes were inverted 4-6 times and incubated at RT for 5 min. After this time, neutralization buffer was added to the cells. The tube was inverted 10-15 times and incubated on ice for 5 min. The complete suspension was loaded into a column pre-soaked with equilibration buffer. The column was washed three times with wash buffers and then eluted to a 50 mL tube with elution buffer. The plasmid-DNA was precipitated with isopropanol, transferred to a finalizer filter and washed with ethanol 70%. After the ethanol was completely removed, the plasmid DNA attached to the finalizer was eluted to an Eppendorf tube with HPLC-grade water. The plasmid-DNA concentration was determined using a Nanodrop photometer. For the preparation of glycerol stocks, 150 µL *E. coli* (Maxi cultures) were mixed with 850 µL glycerol and brought immediately to -80ºC.

3.5 Functional methods

3.5.1 Mixed lymphocyte reactions (MLR)

The inhibitory effect of iNKT cells on T-cell function was analyzed through MLR, using an established protocol that simulates basic GvHD conditions *in vitro* [180]. For that, third-party iNKT cells were tested in MLR using either DCs or Dynabeads® CD3/CD28 as stimulators and CFSE-stained T cells as responders for 7 days. DCs and T cells were either derived from healthy donors or GvHD patients. For healthy donors, DCs and T cells were HLA-mismatched. T cells were analyzed by flow cytometry for activation markers (CD69 or CD25) and proliferation (CFSE). Upon cell contact with the stimulators, T cells become activated and proliferate, which should be impaired by iNKT-cell addition.

Stimulators were prepared as described in 3.1.4, 3.3.5 and 3.3.6 or 3.3.4 and resuspended in iNKT medium at a concentration of $1x10^5$ cells or beads/100 µL. T cells were isolated as described in 3.3.3, stained with CFSE (3.3.7) and resuspended in iNKT medium at a concentration of $1x10^5$ cells/50 µL. iNKT cells were obtained as described in 3.1.6 and 3.3.1. from healthy donors and resuspended in iNKT medium to achieve concentrations ranging between $1x10^5$-$10x10^5$ cells/50 µL (final ratios 1:1:1, 1:1:5 and 1:1:10, beads/DCs:T cell:iNKT cell). On day 0, 100 µL stimulators was seeded into a 96-well plate with 50 µL CFSE-stained T cells in the presence or absence of iNKT cells (50 µL). T cells co-cultured only with stimulators (ratio 1:1) were used as positive control and T cells cultivated alone were used as negative control. The cells were measured by flow cytometry on day 1 (CD69, early activation), day 3 (CD25, late activation) and day 7 (CFSE dilution, proliferation). For data analysis, gates were set on lymphocytes using the FSC-A vs. SSC-A parameters, singlets (SSC-W vs. SSC-A) and viable cells (eFluor 780-). On days 1 and 3, T cells were discriminated from iNKT cells (which tend to downregulate their iTCR between 24-72h upon activation preventing detection by a tetramer staining) by further gating on CD3+CFSE+ cells and at last on CD3+CD69/CD25+ cells. The proliferation was determined using the CD3 and CFSE parameters on day 7. The panel below (**Table 16**) was used for each measurement.

Table 16: FACS panel to determine T-cell activation and proliferation in MLR with iNKT and/or CD19-CAR-iNKT cells

Antigen/Target	Fluorochrome	Dilution	Clone
CD127	PE-Cy7	200	A019D5
CD3	BV605	400	OKT3
CD4	BV421	400	RPA-T4
CD69/CD25	BV711	80	FN50/BC96
CD8	AF700	200	HIT8a
CFSE	CFSE	-	-
PBS57-CD1d-Tetramer	APC	1000	-
VD	eFluor 780	1000	-

Analysis of the effect of cDCs and pDCs on T-cell function

The effect of cDCs and pDCs on T cells was also determined in a MLR and subsequent flow cytometric analysis of usual activation markers and CFSE dilution. Blood DCs were prepared and seeded as described above. T cells were prepared as described above and resuspended in 100 μL iNKT medium and added to the stimulators. The cells were measured on day 1 and day 3 for T-cell activation (CD69 and CD25) and on day 7 for proliferation (CFSE dilution) using the panel in table 16.

Analysis of the inhibitory effect of CD19-CAR-iNKT cells on T cells

The analysis of the inhibitory effects of CD19-CAR-iNKT cells on T cells was performed as described above, using mo-DCs as stimulators. CD19-CAR-iNKT cells were generated as described in 3.3.1 and 3.1.7 and replaced iNKT cells in the assay. Untransduced iNKT cells were used as a further control.

3.5.2 Transwell (TW) assays

To determine whether the inhibitory properties of iNKT cells take place in directly or indirectly, iNKT cells were added to the MLR directly or separated by a TW insert. Stimulators were prepared as described in 3.1.4, 3.3.5 and 3.3.6 and resuspended in iNKT medium at a concentration of $1x10^6$ cells or beads/350 µL. T cells were isolated as described in 3.3.3, stained with CFSE (3.3.7) and resuspended in iNKT medium at a concentration of $1x10^6$ cells/350 µL. iNKT cells were obtained as described above (3.1.6 and 3.3.1) from third-party donors and resuspended in iNKT medium to achieve concentrations ranging between $1x10^6$-$10x10^6$ cells/300 µL. On day 0, 350 µL DCs was seeded together with 350 µL CFSE-stained T cells in a 24-well plate. 300 µL iNKT cells were added directly to the MLR or into the TW insert. T cells co-cultured only with stimulators (1:1 ratio) were used as positive control and T cells cultivated alone were used as negative control. The cells in the MLR were measured by flow cytometry on day 1 (CD69, early activation), day 3 (CD25, late activation) and day 7 (CFSE dilution), using the panel in table 16. The gating strategy is described in 3.5.1. A schematic demonstration of the MLR is shown in figure 13.

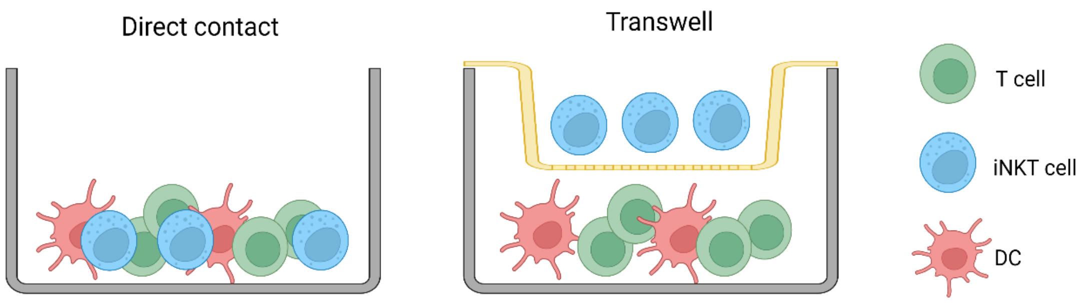

Figure 13: Schematic representation of a MLR using a direct setting and with cell populations separated through a transwell insert
On the left, a representation of the assay with direct cell contact is depicted. For that, DCs, T cells and iNKT cells are co-cultured together. For the transwell assay, a transwell insert separates iNKT cells (top) from DCs and T cells (bottom) but still allows the exchange of soluble factors. Figure generated with Biorender®.

3.5.3 DC apoptosis assay

DC apoptosis was determined by annexin V and VD staining. When cells undergo apoptosis, they translocate phosphatidylserine molecules to the outer leaflet, and these can be detected at an early stage as annexin V+VD- cells (early apoptotic) or a later stage as annexin V+VD+ (late apoptotic) by flow cytometry [181].
For DC apoptosis assays, generated or isolated DCs were incubated with CD19-CAR-iNKT cells and/or iNKT cells at different effector-to-target ratios (E:T). After 4h, the cells

were harvested and stained as described in 3.2.4, using the panel in table 17. For the assays with blood DCs, the cells were stained according to the panel in table 18.

Table 17: FACS panel to determine iNKT and/or CD19-CAR-iNKT-cell-mediated DC apoptosis

Antigen/Target	Fluorochrome	Dilution	Clone
Annexin V	FITC	100	-
CD3	APC	100	HIT3a
PBS57-CD1d-Tetramer	PE	1000	-
VD	PI/7-AAD	40/100	-

Table 18: FACS panel to determine iNKT-cell-mediated apoptosis of blood DCs

Antigen/Target	Fluorochrome	Dilution	Clone
Annexin V	FITC	100	-
CD1c	APC-Cy7	20	L161
CD1d	PE	40	51.1
CD3	APC	100	HIT3a
CD303	PerCP-Cy5.5	20	201a
PBS57-CD1d-Tetramer	PE	1000	-
VD	PI	40	-

Debris was excluded from the analysis using the FSC-A vs. SSC-A parameters. Only singlets (SSC-W vs. SSC-A) and CD3-PBS57-CD1d-tetramer- cells were analyzed. Percent of viable cells stands for the percent of annexin V-VD- cells. Cytotoxic activity was determined by the formula below.

$$\text{cytotoxic activity [\%]} = (1 - (\frac{\text{\% viable cells after culture with effector cells/}}{\text{\% viable cells after culture without effector cells}}) * 100$$

3.5.4 Characterization of CD19-CAR-iNKT cells

Phenotype and exhaustion

The phenotype and exhaustion profile after expansion of the generated CD19-CAR-iNKT cells were determined by flow cytometry. For each analysis, the cells were harvested and stained for the CAR expression (3.2.2) and subsequently for usual extracellular antigens (3.2.1), using the panels shown in tables 19 and 20.

Table 19: FACS panel to determine the phenotype of CD19-CAR-iNKT cells

Antigen/Target	Fluorochrome	Dilution	Clone
CD25	BV711	40	BC96
CD3	BV605	400	HIT3a
CD4	BV785	200	OKT4
CD44	BV510	200	IM7
CD45RA	BV650	200	HI100
CD69	PE-Cy7	50	FN50
CD8	AF700	400	HIT8a
F(ab')$_2$ Fragment	PE	20	-
PBS57-CD1d-tetramer	APC	1000	-
VD	eFluor780	1000	-

Table 20: FACS panel to determine the exhaustion profile of CD19-CAR-iNKT cells

Antigen/Target	Fluorochrome	Dilution	Clone
CD28	BV650	50	CD28.2
CD3	BV605	400	HIT3a
CD4	BV785	200	OKT4
CD8	AF700	400	HIT8a
CTLA-4	BV421	200	BNI3
F(ab')$_2$ Fragment	PE	40	-
KLRG1	PE-Cy7	100	14C2A07
LAG-3	FITC	50	11C3C65
PBS57-CD1d-tetramer	APC	1000	-
PD-1	BV711	100	EH12.2H7
TIGIT	PerCP-Cy5.5	400	A15153G
TIM-3	BV510	50	F38-2E2
VD	eFluor780	1000	-

The percentage of positive cells for each marker was determined by gating on lymphocytes (FSC-A vs. SSC-A plots), single cells (FSC-A vs. FSC-H), viable (eFluor 780-), CD3+PBS57-CD1d-Tetramer+ cells (iNKT cells) and CAR+ cells. At last, every single marker was plotted against the CD3+ population.

3.5.5 Cytotoxicity assays

iNKT-cell or CD19-CAR-iNKT cell-mediated cytotoxicity against cell lines (SEM, Jurkats, K562, Raji cells) and ALL blasts from patients was determined by co-culture with CTV-stained target cells and subsequent annexin V staining. CTV-stained target cells (3.3.8) were incubated with untransduced iNKT cells or CD19-CAR-iNKT cells at different E:T ratios. The incubation times varied between 4h and 24h. Where stated, 10 µg/mL nivolumab or its IgG4 isotype control were added to the assays. To determine the specificity of the CD19-CAR-iNKT cells and their different pathways of action using modified K562 cells, 100 ng/mL α-GalCer or DMSO was added to the assays. The cells were harvested and stained with annexin V (3.2.4) using annexin V-FITC and eFluor 780.

Debris was removed from the analysis using the FSC-A vs. SSC-A parameters. Only singlets (SSC-W vs. SSC-A). The percentage of viable CTV+ cells stands for annexin V-VD- cells. The percentage of cytotoxic activity was determined by the formula below.

$$\text{cytotoxic activity [\%]} = \left(1 - \left(\frac{\text{\% viable CTV+ after culture with effector cells/}}{\text{\% viable CTV+ after culture without effector cells}}\right) * 100\right.$$

3.5.6 ImageStream assays

For the ImageStream assays, SEM cells were incubated with CD19-CAR-iNKT cells at a 1:1 ratio for 4h. After this time, cells were stained as described in 3.2.4 using the panel below for annexin V and extracellular staining. 10,000 cells were acquired using Amnis® ImageStream® X Mk II. Since the goal was to analyze interactions between CD19-CAR-iNKT cells and target cells, only doublets were included in the analysis, which was performed by the technical assistant Simone Pöschel.

Table 21: Antibodies/dyes used in the ImageStream assay

Antigen/Target	Fluorochrome	Dilution	Clone
Annexin V	FITC	100	-
CD19	BV421	200	HIB19
F(ab')$_2$ fragment	PE	40	-
PBS57-CD1d tetramer	APC	100	-
VD	7-AAD	100	-

3.5.7 Proliferation assays

The proliferation of CD19-CAR-iNKT cells upon antigen contact was determined by CFSE dilution. For that, CD19-CAR-iNKT cells were stained with CFSE (3.3.7) and incubated with irradiated (100 Gy) CTV-stained modified Raji cells for 5 days. Effector cells cultivated without stimulus were used as negative control. The cells were harvested and stained for CAR expression using a CD19 protein (3.2.3. and 3.2.1, **table 22**) and analyzed by flow cytometry. Where stated, 10 µg/mL nivolumab or its IgG4 isotype control was added to the reactions. Lymphocytes were gated using the FSC-A vs. SSC-A parameters. Only singlets (SSC-W vs. SSC-A), alive (eFluor 780-), CD19-CAR-iNKT cells (CD3-PBS57-CD1d-tetramer+CAR+) were analyzed. The results are expressed as the median fluorescence index (MFI).

Table 22: FACS panel to determine cell proliferation upon specific antigen encounter

Antigen/Target	Fluorochrome	Dilution	Clone
Anti-Biotin	PE	40	-
CD3	PerCP-Cy5.5	400	HIT3a
CD4	BV785	400	RPA-T4
CD8	AF700	200	HIT8a
CFSE	CFSE	-	-
CTV	CTV	-	-
PBS57-CD1d-Tetramer	APC	1000	-
VD	eFluor 506	1000	-

3.5.8 Rechallenge assays

To analyze the long-term cytotoxicity of CD19-CAR-iNKT cells against PD-L1/PD-L2 expressing Raji cells, CD19-CAR-iNKT cells were stimulated in a rechallenge or repetitive antigen encounter assay. One of the biggest challenges in CAR-T cell therapy is the eventual loss of activity of these against target cells due to several factors such as the exhaustion caused by inhibitory receptors [182]. $5x10^5$ CD19-CAR-iNKT cells were seeded in a 48-well plate. PD-L1/2 expressing Raji cells were irradiated at 100 Gy and added to CD19-CAR-iNKT cells at a 2:1 ratio (E:T). For the following rounds of stimulation, the cells were harvested, counted and restimulated weekly with irradiated Raji cells at a 2:1 ratio. Cytotoxic activity and cytokine release were used as readouts. Unstimulated cells (day 0) or stimulated cells (day 7 and day 14) were counted and seeded at a concentration of $4x10^4$ cells/well. Non-irradiated target cells are added at a 2:1 ratio. The co-culture followed for 24h. Supernatants from these cytotoxicity assays were collected for multiplex analysis, while the cells were stained with the panel in table 23 and analyzed by flow cytometry. A schema of the assay is shown in figure 14. Where stated, 10 µg/mL nivolumab or an IgG4 isotype control was added to the assay.

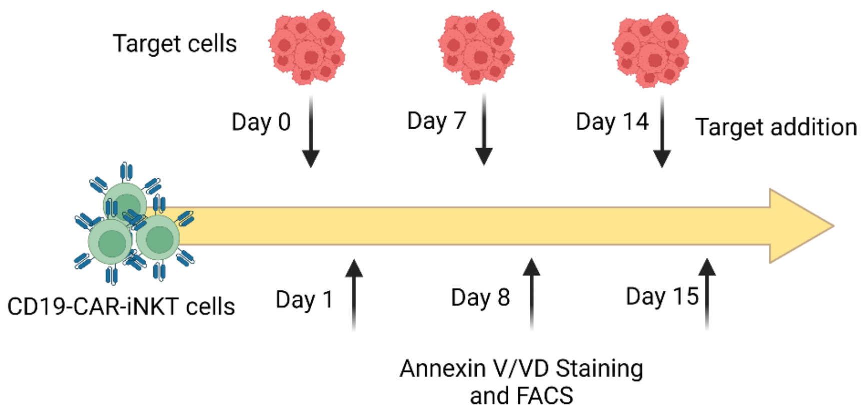

Figure 14: Schema of a rechallenge assay

CD19-CAR-iNKT cells were stimulated three times with irradiated PD-L1/2-expressing Raji cells. On days 0, 7 and 14, part of the CD19-CAR-iNKT cells was challenged with irradiated target cells. The other part of the effector cells was set in a cytotoxicity assay with PD-L1/2 Raji cells. After 24h, the cells were harvested and analyzed by flow cytometry. Generated with Biorender®.

Table 23: FACS panel to determine cytotoxicity and CD19-CAR-iNKT-cell function

Antigen/Target	Fluorochrome	Dilution	Clone
Annexin V	FITC	100	-
CD3	PerCP-Cy5.5	400	HIT3a
CTV	CTV	-	-
F(ab')$_2$ fragment/Anti-Biotin	PE	40	-
PBS57-CD1d-Tetramer	APC	1000	-
VD	eFluor 780	1000	-

4 Results

4.1 Analysis of the inhibitory properties of culture-expanded iNKT cells on T-cell function

4.1.1 iNKT cells do not impair the functionality of T cells stimulated with Dynabeads® CD3/CD28

Schmid et al. showed that iNKT cells impair T-cell activation and proliferation when the latter ones are stimulated with mo-DCs [126, 180]. However, it was still unclear whether this effect is related to the direct iNKT-cell interaction with T cells or with DCs. To address this question, T cells were co-incubated with Dynabeads® CD3/CD28 for 7 days. iNKT cells were added to the MLR at different ratios. The cells were analyzed by flow cytometry for activation markers on day 1 (CD69), on day 3 (CD25) and proliferation on day 7 (CFSE dilution). T cells alone were used as the negative control and T cells co-cultured with Dynabeads® CD3/CD28 were used as the positive control. As expected, T cells stimulated only with Dynabeads® CD3/CD28 showed high levels of early and late activation markers (97.1±0.32% for CD69 and 92.7%±2.25% for CD25) and proliferation (98.5±0.12%) (**Fig. 15A-C**). Indeed, as observed by Schmid et al., T-cell activation and proliferation were also barely affected by iNKT cells when T cells were stimulated by Dynabeads® CD3/CD28 (**Fig. 15**) [126, 183]. A significant effect on activation could only be achieved for CD69 expression at higher ratios, with a decrease of 4.74%±1.28% (**Fig. 15A**).
These data reinforce the concept that the inhibitory effect of iNKT cells on T-cell function might be rather related to their interaction with DCs than with T cells.

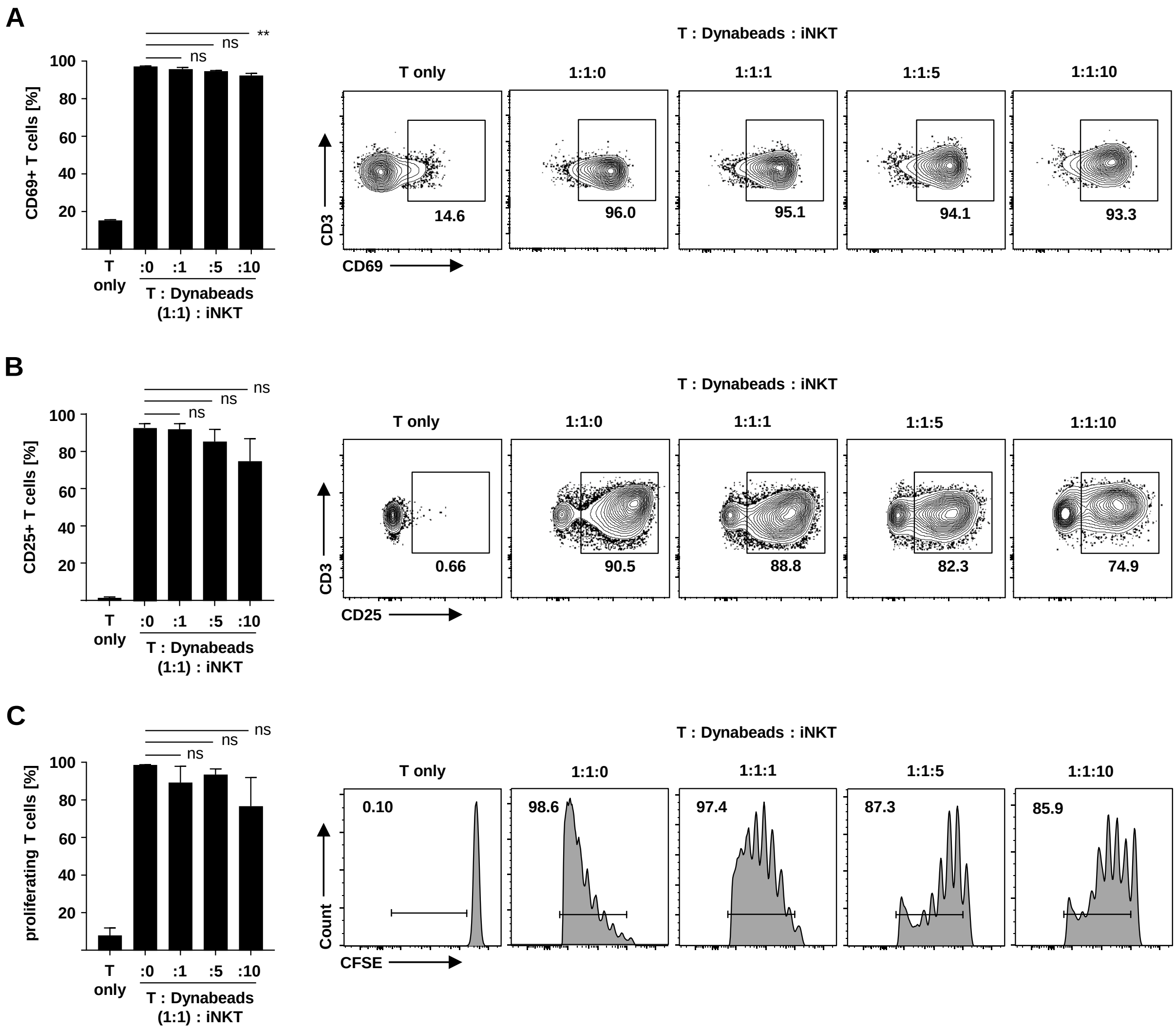

Figure 15: T-cell activation and proliferation promoted by Dynabeads® CD3/CD28 are less affected by iNKT cells

Magnetically isolated T cells were stimulated with Dynabeads® CD3/CD28 at a 1:1 ratio (T cell:beads) and analyzed by flow cytometry for T-cell activation (CD69 on day 1 and CD25 on day 3) and proliferation (CFSE dilution on day 7). Where stated, iNKT cells were added to the cultures at different ratios (from 1:1:1 to 1:1:10, T cell:DC:iNKT cell). Figures **(A)**, **(B)** and **(C)** show histograms with the mean of pooled data of at least three independent experiments and dot plots of alive T cells (VD-) analyzed on days 1, 3 and 7. Co-cultures without iNKT cells were used as the positive control and T cells cultured alone were used as the negative control. Exclusion of iNKT cells followed gating on CFSE positive populations on days 1 and 3 and PBS57-CD1d-tetramer negative populations on day 7. Error bars show SEM. One-way ANOVA. Not significant (ns) p>0.05, ** p≤0.01.

Modified from Schmid & Moraes-Ribeiro et al. [184]

4.1.2 iNKT cells hinder T-cell function through direct cell contact

To further elucidate the cellular mechanisms, DCs and T cells were co-cultured for 7 days at a 1:1 ratio in a MLR in an HLA mismatched setting. iNKT cells were added to the MLR at different ratios, either directly or separated by a TW insert. The insert prevents direct contact between cells but still allows the exchange of soluble factors between both environments. As in the experiment described in 4.1.1, T cells were analyzed for T-cell activation and proliferation on days 1, 3 and 7 by flow cytometry. Further, T cells cultured alone were used as the negative control, and T cells co-incubated with DCs were used as the positive control.

The data confirm that T-cell activation and proliferation were most affected by direct addition of iNKT cells to the MLR (**Fig. 16**). A decrease of early activation could be noted at higher ratios of iNKT cells added directly to the MLR (25.5%±6.09% for the ratio 1:1:5 and 20.4%±5.33% for 1:1:10). No significant difference could be observed when iNKT cells were added separately to the MLR even at higher ratios (42.8%±4.64% at 1:1:10) in comparison to the positive control (46.8%±3.80%) (**Fig. 16A**). The CD25 expression was significantly affected by adding iNKT cells directly even at lower ratios (22.7%±8.23%, 9.35%±2.70% and 4.42%±1.47% for 1:1:1, 1:1:5 and 1:1:10, respectively) in comparison to both positive control (DC+T, 45.2%±3.01%) and to cells tested with a TW insert (45.6%±5.97%, 38.7%±6.47% and 36.8%±8.12, for 1:1:1, 1:1:5 and 1:1:10, respectively) (**Fig. 16B**). The analysis of the CFSE dilution revealed a significant decrease of T-cell proliferation caused by direct addition of iNKT cells to the MLR at the 1:1:5 and 1:1:10 ratios (24.4%±7.94% and 17.6%±6.35%, respectively) in comparison to the positive control (61.0%±9.25%). No significant effect could be observed in the analysis with the TW insert (**Fig. 16C**). All values are expressed as $\bar{x}$±SEM.

Thus, these data confirm that iNKT cells impair T-cell function mostly in a dose and cell-contact-dependent manner.

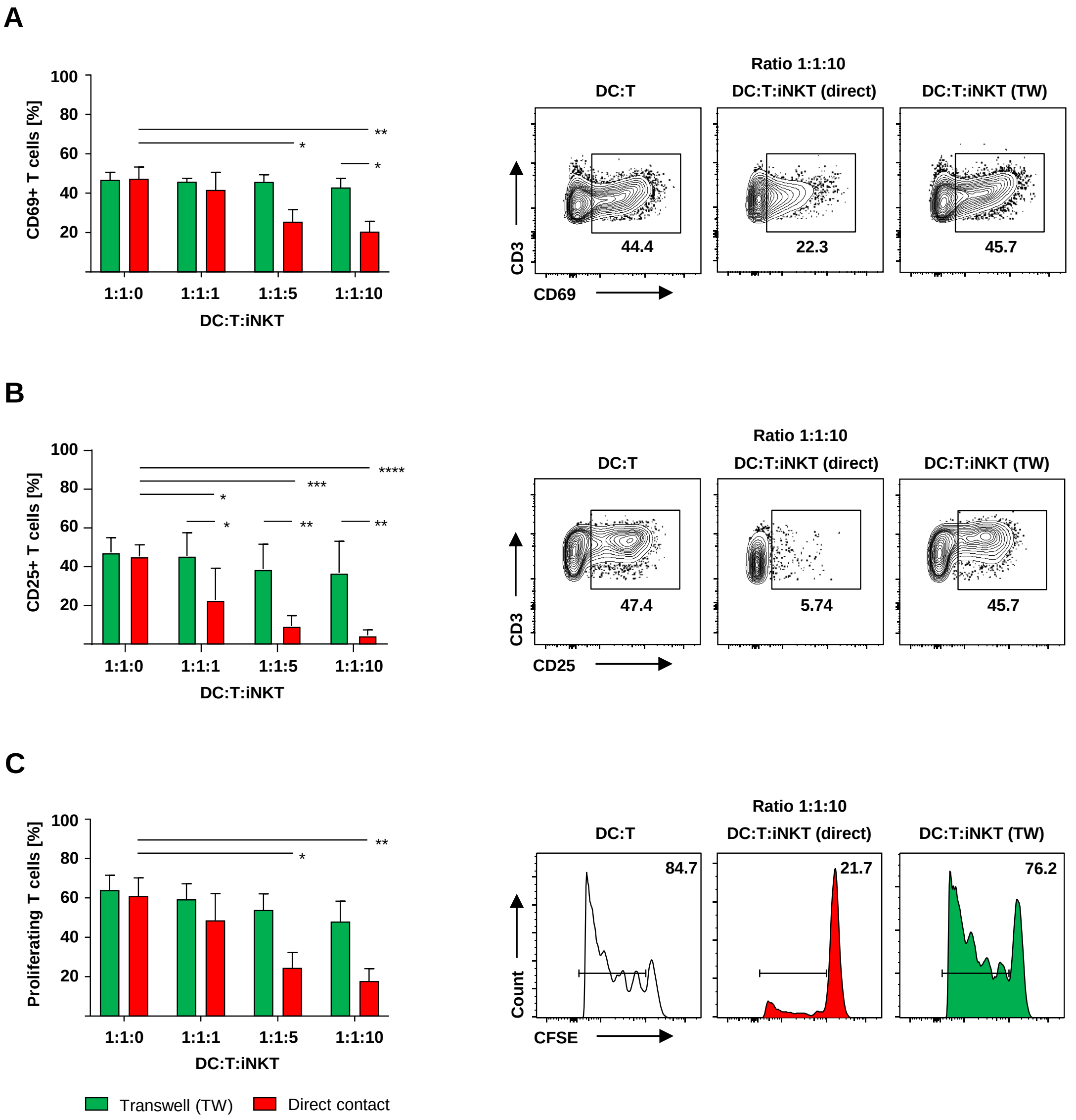

Figure 16: iNKT cells prevent T-cell activation and proliferation in a dose- and contact-dependent manner

T cells were co-cultured with mo-DCs at a 1:1 ratio (T cell:DC) and analyzed by flow cytometry for early and late T-cell activation (CD69 on day 1 and CD25 on day 3, respectively) and proliferation (CFSE dilution on day 7). iNKT cells were added to the cultures at different ratios (from 1:1:1 to 1:1:10, T cell:DC:iNKT cell) directly or separated by a TW insert. **(A)** shows histograms and representative dot plots (only 1:1:10 ratio) of early activation of T cells after 24h co-culture. **(B)** depicts T-cell activation on day 3 with pooled data and representative dot plots (1:1:10) and **(C)** demonstrates histograms and dot plots of proliferating T cells after co-incubation with mo-DCs for 7 days. Data in green show the results of assays performed with a TW insert and those in red with direct cell contact. Co-cultures without iNKT cells were used as the positive control and T cells cultured alone were used as the negative control. Exclusion of iNKT cells followed gating on CFSE positive populations on days 1 and 3 and PBS57-CD1d-tetramer negative populations on day 7. Only alive (VD-) T cells were analyzed. Histograms show the mean of pooled data of four different donors, analyzed independently. Error bars show SEM. Two-way ANOVA. * p≤0.05, ** p≤0.01, *** p≤0.001 and **** p≤0.0001. Data without depicted statistical analysis are not statically significant (p>0.05).

Modified from Schmid & Moraes-Ribeiro et al. [184]

4.1.3 iNKT cells induce apoptosis of blood DCs

It has been previously shown that iNKT cells might promote tolerance by inducing DC apoptosis [184]. Schmid analyzed cell populations in graft samples that were used for patient transplantation. While analyzing DCs in these samples, a CD1d^{high} and a CD1d^{low} DC population were noticed. Further characterization revealed that the CD1d^{high} showed a CD1c+ phenotype, which characterizes conventional DCs (cDCs), while the CD1d^{low} population turned out to be plasmacytoid DCs (CD303+, pDCs) [126, 183].

In the first set of experiments, mo-DCs were used as stimulators, since they are more readily accessible for large assays. Now, aiming to simulate a more physiological environment and considering the presence of DCs in grafts, a second batch of experiments was performed using magnetically isolated blood DCs instead of mo-DCs. Like the experiments performed by Schmid, third-party culture-expanded iNKT cells were challenged with isolated blood DCs for 4h [183]. Subsequently, the cells were stained and analyzed by flow cytometry for apoptosis and CD1c and CD303 expression. DCs incubated alone were used as negative control (**Fig. 17**).

In this setting, iNKT cells also efficiently induced apoptosis of blood DCs, with specific apoptosis induction ranging between 58.7-91.2% (76.1%±4.36%, $\bar{x}$±SEM) (**Fig.17A-B**). Interestingly, the analysis of the remaining viable cells revealed that cDCs (CD1c+ DCs) were mostly affected by iNKT cells, while pDCs (CD303+) seem to be spared (**Fig.17C**). Further, analysis of CD1d expression on MACS-isolated blood DCs confirmed that cDCs express significantly higher levels of CD1d in comparison to pDCs. This observation could explain why iNKT cells preferentially induce apoptosis of cDCs.

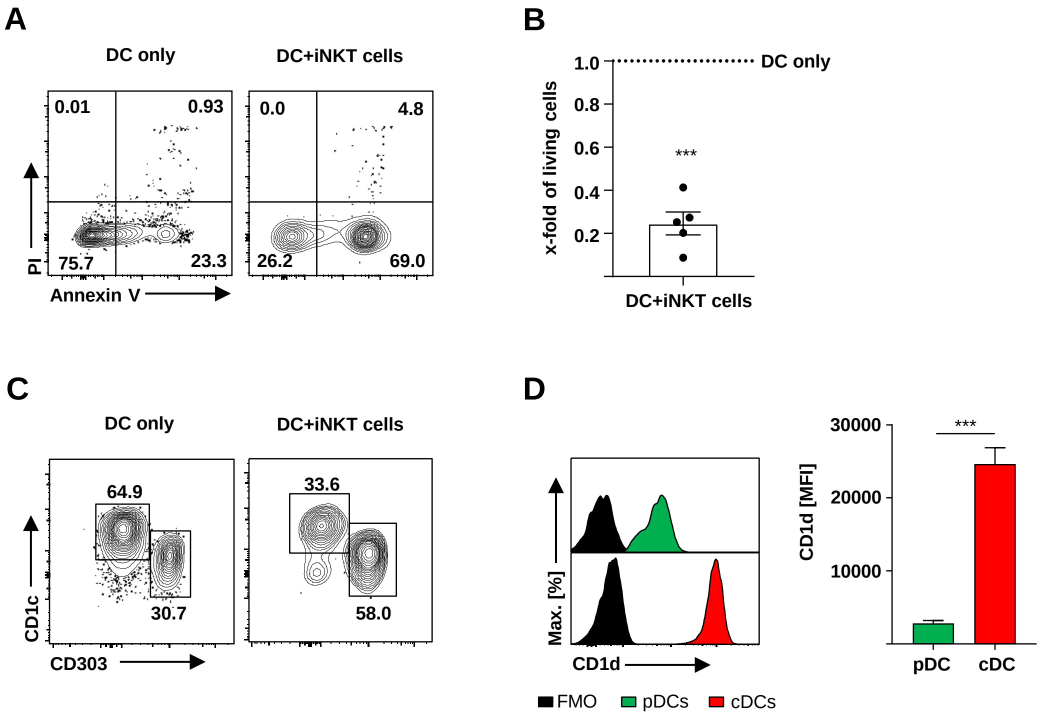

Figure 17: Culture-expanded iNKT cells induce apoptosis of blood DCs

MACS-isolated blood DCs were co-cultured for 4h with iNKT cells at a 1:5 ratio (DC:iNKT cells). The cells were stained with annexin V, PI, anti-CD3, anti-CD1c and anti-CD303 antibodies and analyzed by flow cytometry. Representative dot plots showing blood DC apoptosis induction by iNKT cells are depicted in **(A)**. Pooled data showing the remaining living DCs (annexin V-PI-) normalized to the control DC only are shown in **(B)**. Representative dot plots in **(C)** show the prevalence of pDCs (CD303+ DCs) amongst living DCs. CD3+ iNKT cells were excluded from the analysis by gating on CD3- cells only. In **(D)**, representative histogram and pooled data (expressed as MFI) of CD1d expression of pDCs (green) and cDCs (red) after MACS isolation are shown. Pooled data show the results for at least three different donors analyzed independently. Error bars show the standard error of the mean (SEM). Paired *t*-test. *** $p<0.001$. FMO: fluorescence minus one; MFI: median fluorescence index.

Modified from Schmid & Moraes-Ribeiro et al. [184]

4.1.4 Only cDCs, but not pDCs, induce T-cell activation and proliferation

DCs are known as the most efficient APCs and therefore, are considered the most important bridge between innate and adaptive immunity. Among their tasks in the immune system, DCs present antigens to T cells and initiate immune responses important for host defense [185, 186]. Given different DC subsets and their distinct physiological functions, the role of cDCs and pDCs for T-cell activation and proliferation was under debate. To address this matter, blood DCs were sorted and co-cultured with isolated T cells at a 1:1 ratio in a mismatched setting. T cells were analyzed for early and late activation (CD69 and CD25, respectively) and T-cell proliferation (CFSE). T cells cultivated alone were used as the negative control. The results are shown in figure 18.

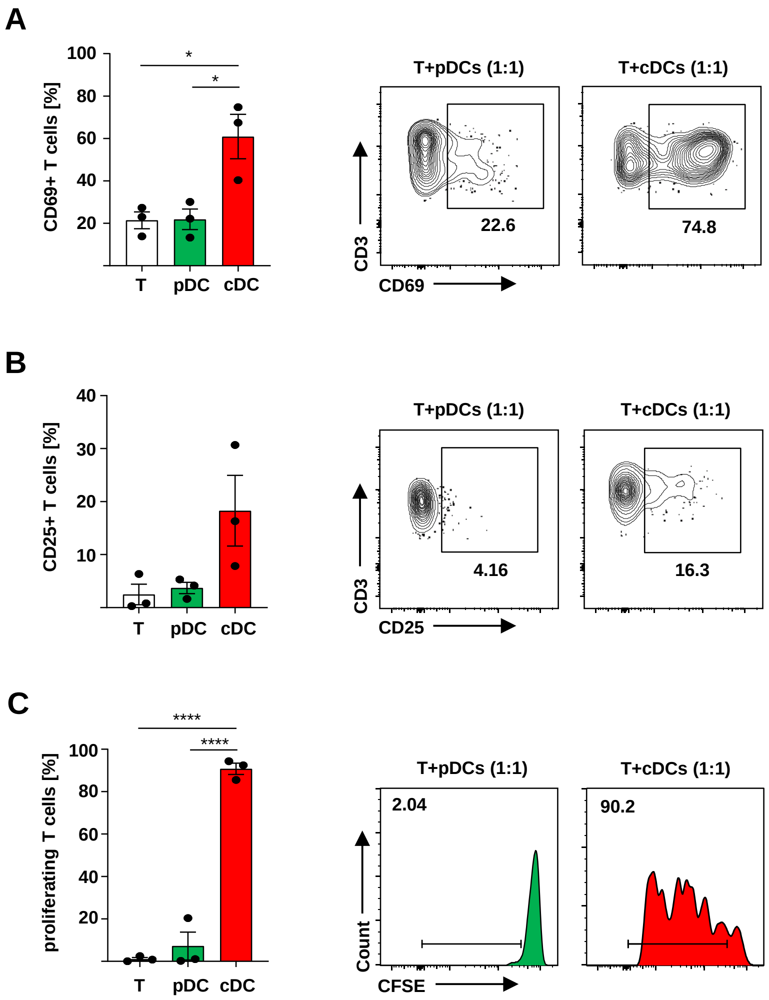

Figure 18: Only cDCs induce T-cell activation and proliferation

T cells were co-incubated with MACS-isolated blood DCs for 7 days at a 1:1 ratio (T cell:DC) in a mismatched setting. The cells were analyzed by flow cytometry on days 1 and 3 for activation (CD69 and CD25, respectively) and on day 7 for proliferation (CFSE dilution). **(A)** and **(B)** show pooled data and representative dot plots demonstrating CD69 and CD25 expression by T cells, respectively. **(C)** shows CFSE dilution for T cells. DCs were excluded from the analysis by gating on alive CD3+ cells. The experiments were performed at least three times independently and the mean of the pooled data is displayed. Error bars show SEM. One-way ANOVA. * $p \leq 0.05$, **** $p \leq 0.0001$. Non-significant statistical analysis ($p > 0.05$) is not depicted.

Modified from Schmid & Moraes-Ribeiro et al. [184]

The CD69 expression varied for pDCs between 13.3%-30.1% (21.8%±4.86%, $\bar{x}$±SEM), while for cDCs, the expression was significantly increased compared to both negative control (T cell only) and pDCs and varied between 40.4%-74.8% (60.8%±10.4%) (**Fig. 18A**). The late activation was overall lower in comparison to CD69. The average CD25 expression was 3.71%±1.08% for pDCs and 18.2%±6.65% for cDCs. Although the increased expression for cDCs was not significant, a trend could be observed for all tested donors (**Fig. 18B**). Strikingly, proliferation was mostly affected by cDCs. While no significant proliferation could be induced by pDCs (7.21%±6.57%), 90.8%±2.67% of T cells showed higher proliferation rates upon contact with cDCs (**Fig. 18C**). All values are expressed as $\bar{x}$±SEM.
Altogether, these data show that only cDCs induce significant alloreactive responses but not pDCs.

4.1.5 iNKT cells prevent activation and proliferation of T cells stimulated with blood DCs.

Using mo-DCs, it was demonstrated that iNKT cells prevent T-cell activation and proliferation by inducing DC apoptosis. Next, it was evaluated whether iNKT cells also prevent T-cell activation and proliferation promoted by circulating DCs. In the first set of experiments, MACS-isolated blood DCs were co-cultured together with T cells in a mismatched setting in the presence or absence of third-party culture-expanded iNKT cells for 7 days. T cells were analyzed by flow cytometry for T-cell activation (CD69 and CD25, on days 1 and 3, respectively) and proliferation (CFSE, on day 7). T cells co-cultured with DCs were used as the positive control. The results are shown in figure 19.
For CD69, the activation was decreased by 48.1±16.2% (**Fig. 19A, D**) and for CD25 by 65.1%±7.03% in comparison to the DC plus T-cell control (**Fig. 19B, D**). For CFSE dilution, the iNKT cells decreased the proliferation by 60.3%±4.17% (**Fig. 19C-D**). As in experiments using mo-DCs, these experiments show that iNKT cells can prevent iNKT-cell activation and proliferation induced by blood DCs.

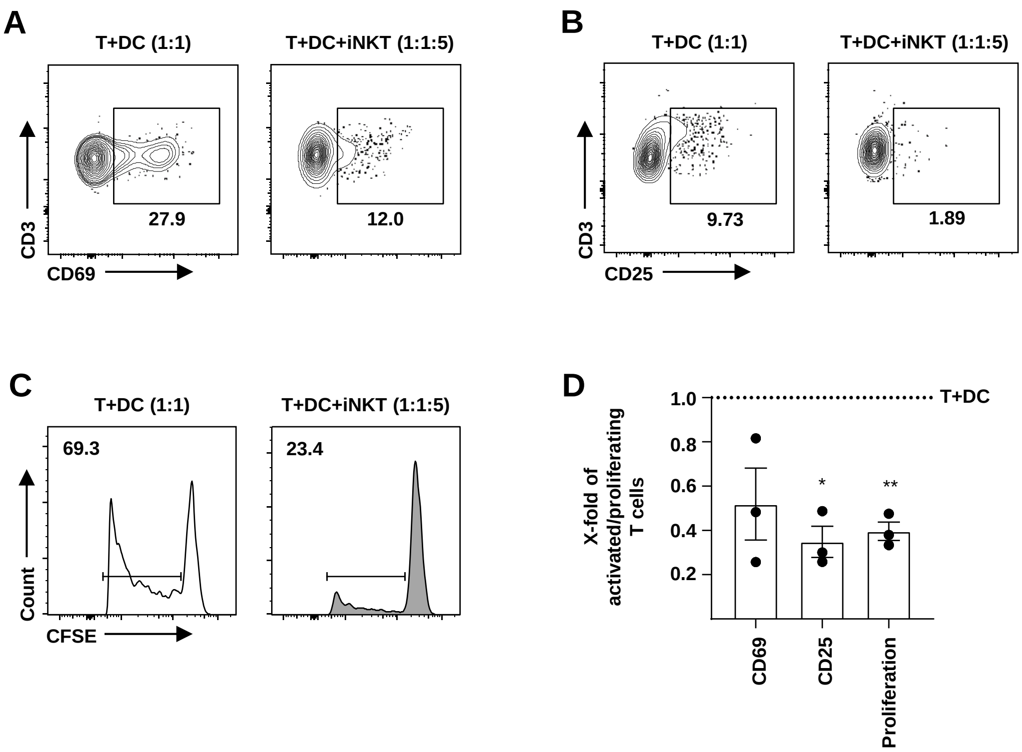

Figure 19: iNKT cells prevent T-cell activation and proliferation induced by blood DCs

T cells were co-incubated with blood DCs at a 1:1 ratio (T cell:DC) for 7 days. The cells were analyzed by flow cytometry on days 1 and 3 for activation (CD69 and CD25, respectively) and on day 7 for proliferation (CFSE dilution). Where stated, 5-fold iNKT cells were added to the cultures. Representative dot plots showing early and late activation and proliferation without or in presence of iNKT cells are depicted in **(A)**, **(B)** and **(C)**. **(D)** Histogram shows pooled data of mean from three experiments. The data were normalized to their respective T+DC control. DCs were excluded from the analysis by gating on the alive CD3+ population. Exclusion of iNKT cells followed gating on CFSE positive populations on days 1 and 3 and PBS57-CD1d-tetramer negative populations on day 7. The experiments were performed at least three times independently. Error bars show SEM. Paired *t*-test. * p≤0.05, ** p≤0.01. Non-significant statistical analysis (p>0.05) is not shown.

Modified from Schmid & Moraes-Ribeiro et al. [184]

As observed in 4.1.3 and 4.1.4, cDCs are the blood DCs that are most affected by iNKT cells, but the best T-cell stimulators. Thus, it seemed that the inhibitory effect of iNKT cells on T-cell function might be related to their ability to induce cDC apoptosis and further avoid T-cell activation and proliferation. To confirm this effect, cDCs were sorted from MACS-isolated blood DCs. Sorted cDCs were co-cultured with iNKT cells for 7 days and analyzed by flow cytometry as described in the previous experiments.

T cells only were used as the negative control, while T cells cultivated with DCs were used as the positive control.

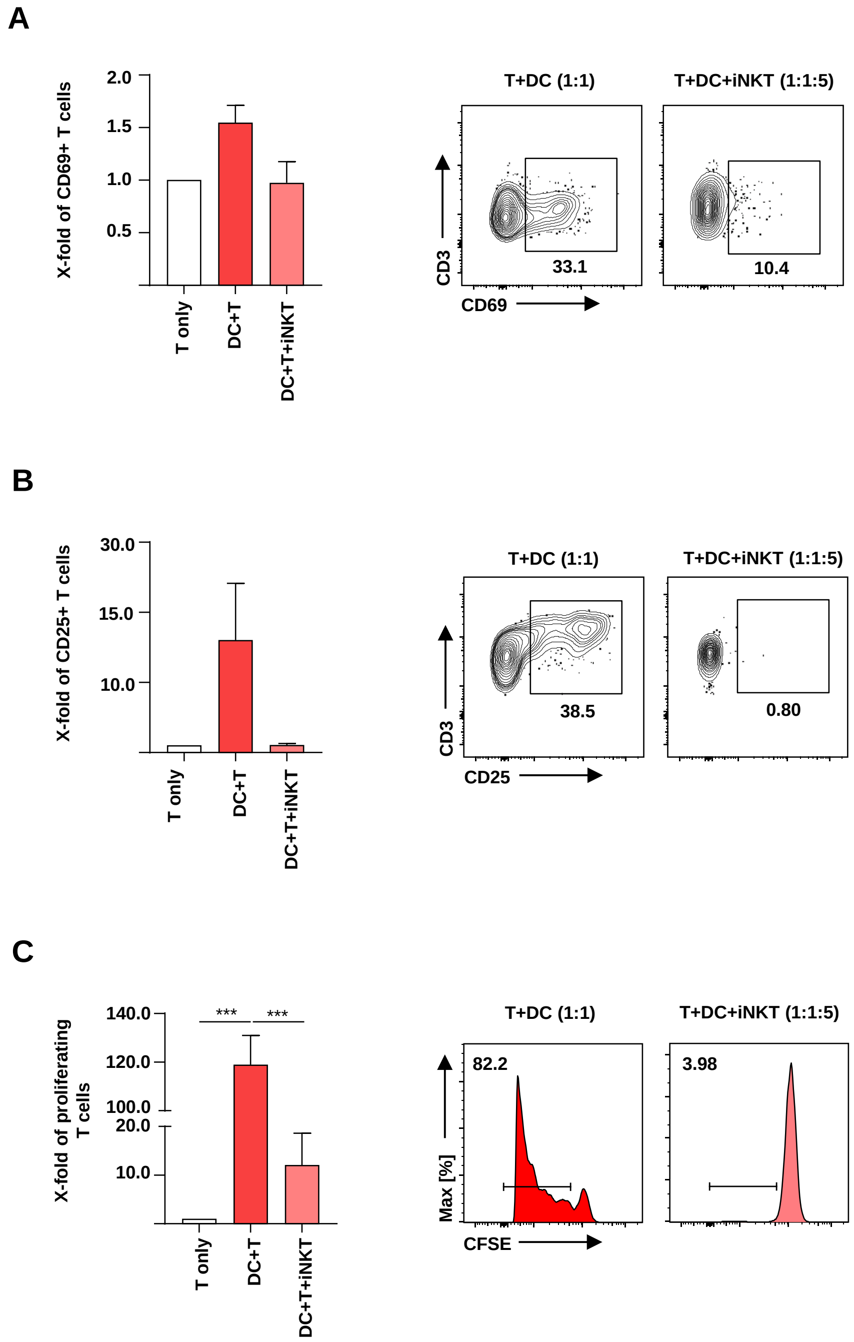

Figure 20: iNKT cells prevent T-cell activation and proliferation induced by blood cDCs
MACS-isolated blood DCs were sorted into cDCs (CD1c+). T cells were co-cultured with sorted blood cDCs at a 1:1 ratio (T cell:DC) for 7 days. The cells were analyzed by flow cytometry for early and late T-cell activation and proliferation. Where stated, iNKT cells were added to the cultures at a 1:1:5 ratio (T cell:DC:iNKT cell). Representative dot plots and histograms of pooled data (mean) showing early and late (CD69 and CD25, respectively) activation and proliferation (CFSE dilution) without or in presence of iNKT cells are depicted in **(A)**, **(B)** and **(C)**, respectively. Pooled data (mean) show the results of three

different donors analyzed independently. Due to intrinsic donor variability, the data were normalized to their respective T-cell-only control. DCs were excluded from the analysis by gating on the alive CD3+ population. Exclusion of iNKT cells followed gating on CFSE positive populations on days 1 and 3 and PBS57-CD1d-tetramer negative populations on day 7. Error bars show SEM. One-way ANOVA. *** $p \leq 0.001$. Non-significant statistical analysis ($p > 0.05$) is not shown.

Modified from Schmid & Moraes-Ribeiro et al. [184]

The data obtained in this set of experiments are shown in figure 20 and confirmed the high potential of cDCs to promote T-cell activation (1.54-fold±0.16 for CD69 expression and 16.0-fold±8.11 for CD25 expression) (**Fig. 20A-B**) and proliferation (118.90-fold±12.07) (**Fig. 20C**), which could be completely (T-cell activation) or partially (T-cell proliferation) reversed by iNKT-cell addition.

4.1.6 iNKT cells promote DC apoptosis and impair T-cell function in a patient-based setting

To confirm the inhibitory properties of iNKT cells on T-cell function, their proapoptotic effect on DCs and consequently their inhibitory effects on T-cell activation and proliferation were analyzed in a patient-based system. For that, blood samples from patients who participated in a simultaneous clinical study undergoing allo-HSCT were selected for the analysis. PBMCs were isolated, frozen and stored in nitrogen tanks.
For this set of experiments, patients who developed GvHD at any time during the study were selected. Blood DCs were isolated from PBMCs collected prior to HSCT. T cells were isolated from PBMCs collected after transplantation after the patient achieved complete chimerism before the patients had developed any GvHD signs and received any treatment. Due to the different factors, such as bad sample condition, small cohort, and consequently, few patients that eventually developed GvHD, only samples from two patients could be analyzed. iNKT cells were obtained from third-party healthy donors.
First, blood DCs were co-incubated with iNKT cells for 4h. The cells were subsequently stained with annexin V, PI, anti-CD3, anti-CD1c and anti-CD303 and analyzed by flow cytometry for DC apoptosis and antigen expression. DCs incubated alone were used

as the negative control. Freshly isolated DCs were further analyzed for their CD1d expression. The results are shown in figure 21.

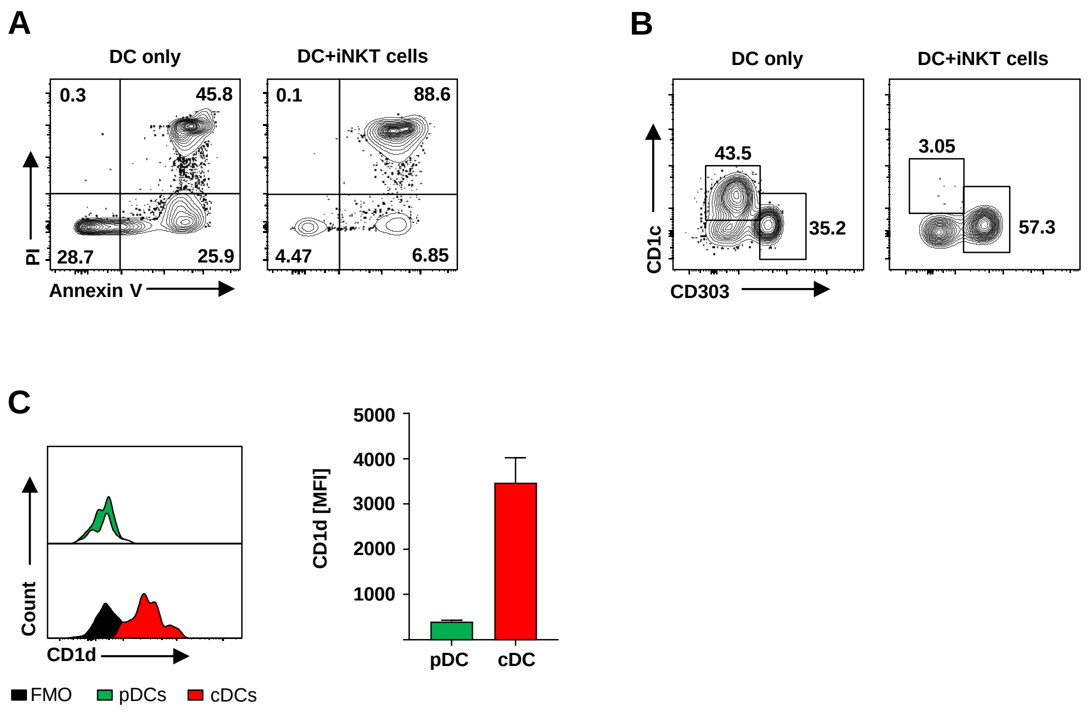

Figure 21: iNKT cells preferentially induce apoptosis of patient cDCs

Blood DCs were immunomagnetically isolated from frozen PBMCs collected from patients who underwent allo-HSCT and developed GVHD. Blood DCs were co-incubated with third-party iNKT cells at a 1:5 ratio for 4h. After this time, the cells were stained with annexin V, PI, anti-CD1c, anti-CD303 and anti-CD3 antibodies and analyzed by flow cytometry. **(A)** shows apoptosis induction of blood DCs co-cultured with iNKT cells. **(B)** shows the proportion of living (annexin V-VD-) cDCs and pDCs after co-culture with iNKT cells. Representative plots and histogram showing the CD1d expression on blood DCs after magnetic isolation are shown in **(C)**. Data from one donor are shown. The pooled mean of technical replicates is displayed. Error bars show standard deviation (SD).

Modified from Schmid & Moraes-Ribeiro et al. [184]

These results demonstrate that iNKT cells from third-party donors are also able to induce patient-derived DC apoptosis (24%) (**Fig. 21A**). Similar to our experiments using healthy donors' cells, iNKT cells also preferentially induced apoptosis of cDCs, decreasing its relative frequency among DCs from 43.5% to 3.05% (**Fig. 21B**). The analysis of the CD1d expression on these cells also revealed higher expression by cDCs (**Fig. 21C**).

Next, blood DCs and T cells from patients were co-cultured together for 7 days and analyzed for T-cell activation (CD25) and proliferation (CFSE dilution). iNKT cells were added to the MLR at a 1:1:5 ratio (T cell:DC:iNKT cell). T cells only were used as the negative control and T cells cultured with DCs were used as the positive control. The results are shown in figure 22.

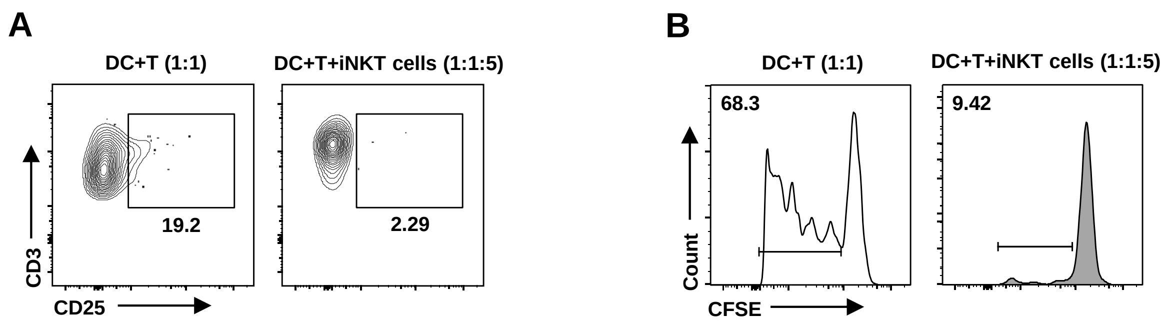

Figure 22: iNKT cells prevent activation and proliferation of patient-derived T cells
Blood DCs and T cells were immunomagnetically isolated from patient PBMCs. Similar to experiments involving mo-DCs and blood DCs from healthy donors, patient DCs and T cells were co-cultured for 7 days (1:1 ratio) in the presence or absence of iNKT cells (added 5-fold the number of DCs and T cells). The cells were analyzed on day 3 for T-cell activation and on day 7 for proliferation (CFSE dilution) by flow cytometry. Representative plots from a patient for T-cell activation are shown in **(A)** and for T-cell proliferation in **(B)**.

Modified from Schmid & Moraes-Ribeiro et al. [184]

The flow cytometric analysis showed that T-cell activation and proliferation could be efficiently reduced by 16.9% (CD25 expression) and 58.8% (CFSE dilution) (**Fig. 22A-B**). Data from a second patient is shown in appendix data 1.
Altogether, these data show that iNKT cells impair T-cell function through apoptosis of DCs from both healthy donors and patients in a direct cell contact-dependent manner.

4.2 Genetic optimization of iNKT cells for tumor control by insertion of a chimeric antigen receptor (CAR)

4.2.1 Characterization of CD19-CAR-iNKT cells

Despite being very rare in peripheral blood, iNKT cells can be easily expanded *ex vivo* to achieve higher cell numbers, which are necessary for clinical applications [126]. For the generation of CD19-CAR-iNKT cells, the original protocol for T cells had to be adapted considering several unique properties of iNKT cells. An important step in this process is cellular activation, which allows the entrance of the retroviral component into the cells during transduction. Several protocols have used CD3/28 antibodies to induce the activation of conventional T cells. Rotolo et al. also showed that iNKT cells can be optimally activated and expanded with CD3/CD28 beads [173]. However, the same could not be observed in our experiments, since beads reduced the viability of the generated cells (**Appendix data 2**).

The protocol, which was established for this work, consisted of upfront iNKT-cell isolation and activation using autologous α-GalCer-loaded feeder cells, IL-2 and α-GalCer as already described, but with some modifications [174]. After transduction with a retroviral SFG.CD19-CAR construct, iNKT cells were expanded during two stimulation rounds (weekly) with feeder cells, IL-2 and α-GalCer. This protocol allowed a significant expansion of iNKT cells (47.5-fold±9.27 for CD19-CAR-iNKT cells and 95.0-fold±23.1 for untransduced iNKT cells) with good transduction efficiency (57.7%±4.96). However, a significantly better expansion could be observed for untransduced iNKT cells (**Fig. 23A-B**).

The analysis of iNKT cells on day 0 and of untransduced iNKT cells and CD19-CAR-iNKT cells on day 20 revealed a preferential expansion of CD4+ cells and a decrease of the CD8+ population, while no consistent pattern could be identified for CD4-CD8- (DN) cells (**Fig. 23C**). Moreover, the generated CD19-CAR-iNKT cells presented a resting (CD25-) and effector memory (CD44+CD45RA-) phenotype (**Fig. 23D**). Importantly, flow cytometric analysis of expanded cells showed that this protocol did not induce cell exhaustion, despite the prolonged culture time (**Fig. 23E**).

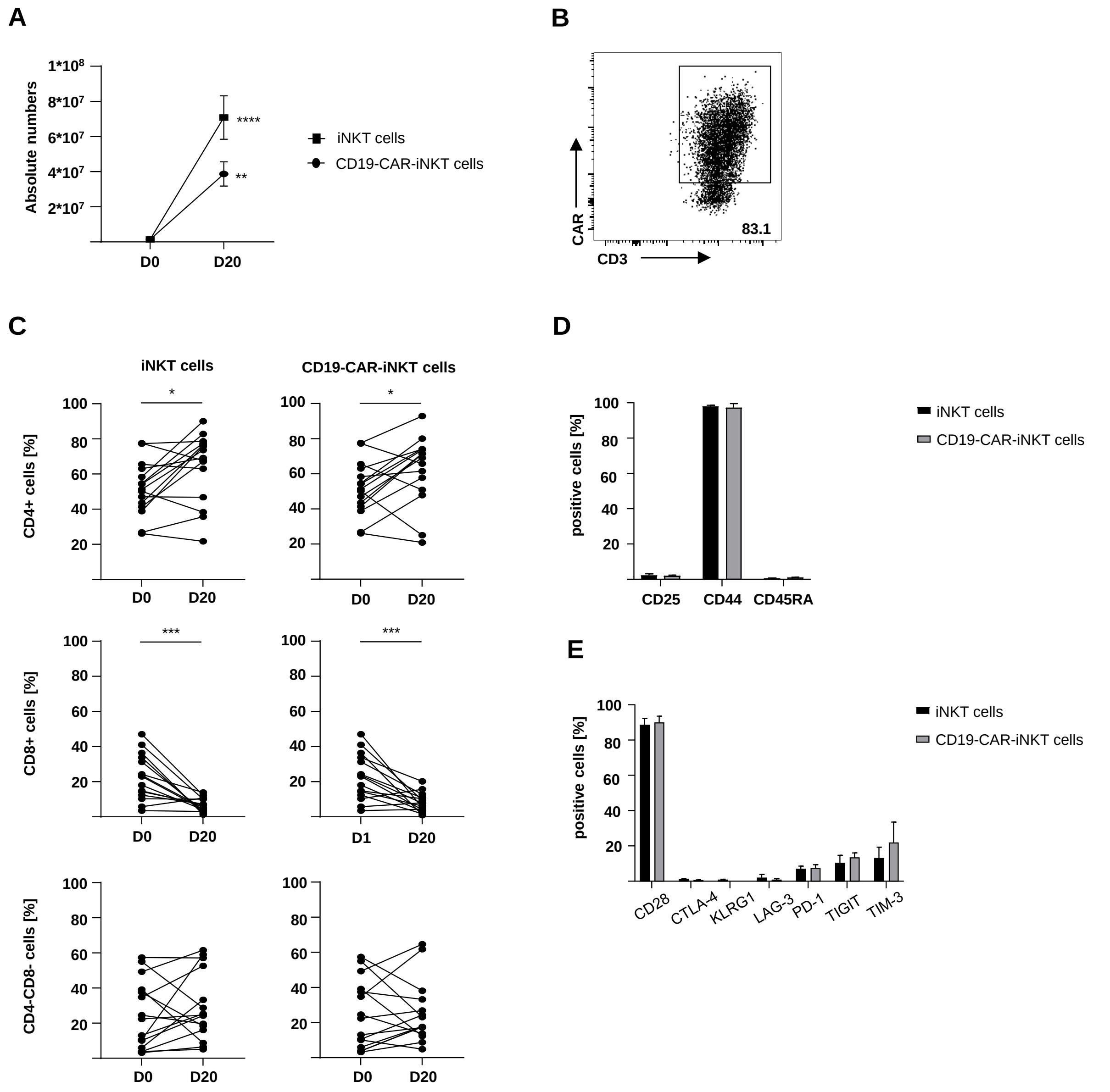

Figure 23: CD19-CAR-iNKT cells can be efficiently generated and expanded *ex vivo*

CD19-CAR-iNKT cells were generated after upfront iNKT-cell isolation and retroviral transduction. Activation and expansion were performed using autologous α-GalCer-loaded feeder cells, IL-2 and α-GalCer. On day 20, the surface phenotype of CD19-CAR-iNKT cells was analyzed by flow cytometry. **(A)** Absolute numbers of expanded iNKT cells and CD19-CAR-iNKT cells on day 20 (mean, n=10). The expansion was determined by flow cytometry and cell counting. **(B)** Representative data show transduction efficiency for one donor. **(C)** Percentage of positive CD4 (above), CD8 (middle) and double negative (CD4-CD8-, below) of untransduced iNKT cells and CD19-CAR-iNKT cells before expansion/activation (D0) and after expansion (D20). **(D)** shows the mean of pooled data for the expression of CD25, CD44 and CD45RA expression of iNKT cells or CD19-CAR-iNKT cells (n=4) after expansion (D20). Expression (mean) of different exhaustion markers by iNKT cells and CD19-CAR-iNKT cells (n=4) on day 20 is shown in **(E)**. Only alive iNKT cells/CD19-CAR-iNKT cells (VD-) were included in the analysis. Error bars show SEM. Two-way ANOVA for (**A**) and paired t-test for (**C**). * p≤0.05 ** p≤0.01, *** p≤0.001, **** p≤0.0001. Non-significant statistical analysis (p>0.05) is not shown.

4.2.2 CD19-CAR-iNKT cells show robust cytotoxicity against CD19+ tumor cells

To assess their functional fitness, CD19-CAR-iNKT cells were challenged against SEM (CD19+ ALL cell line), Raji (BL cell line) cells, ALL patient blasts (about 95% blast in PBMCs) and K562 (CD19- CML cell line) at different ratios for 4h. Subsequently, the cells were stained with annexin V and analyzed by flow cytometry. Untransduced iNKT cells were used as a negative control. Alternatively, CD19-CAR-iNKT cells were challenged with SEM for 4h and analyzed by ImageStream. The results are shown in figure 24.

Strikingly, CD19-CAR-iNKT cells showed a robust efficiency in eradicating tumor cells in comparison to the untransduced iNKT-cell control. For instance, the calculated cytotoxic activity against SEM at a 5:1 ratio (E:T) achieved 6.79%±1.24% (untransduced iNKT cells) and 84.3%±8.62% (CD19-CAR-iNKT cells), while for Raji cells, it was 7.15%±4.07% (untransduced iNKT cells) and 65.8%±4.23% (CD19-CAR-iNKT cells). Patient blasts were very sensitive to CD19-CAR-iNKT cells, which showed 81.3%±3.29% of cytotoxic activity at a 5:1 ratio (6.69%±6.79% for untransduced iNKT cells). Importantly, no significantly different cytotoxic activity between untransduced iNKT cells and CD19-CAR-iNKT cells was observed against the CD19- cell line K562 (12.3%±2.53% for untransduced iNKT cells and 21.3%±5.08% for CD19-CAR-iNKT cells at 5:1), showing high antigen specificity of CD19-CAR-iNKT cells (**Fig. 24A-B**). All values are expressed as $\bar{x}$±SEM.

Further, apoptosis induction of SEM by CD19-CAR-iNKT cells was also confirmed by ImageStream analysis (**Fig. 24C**).

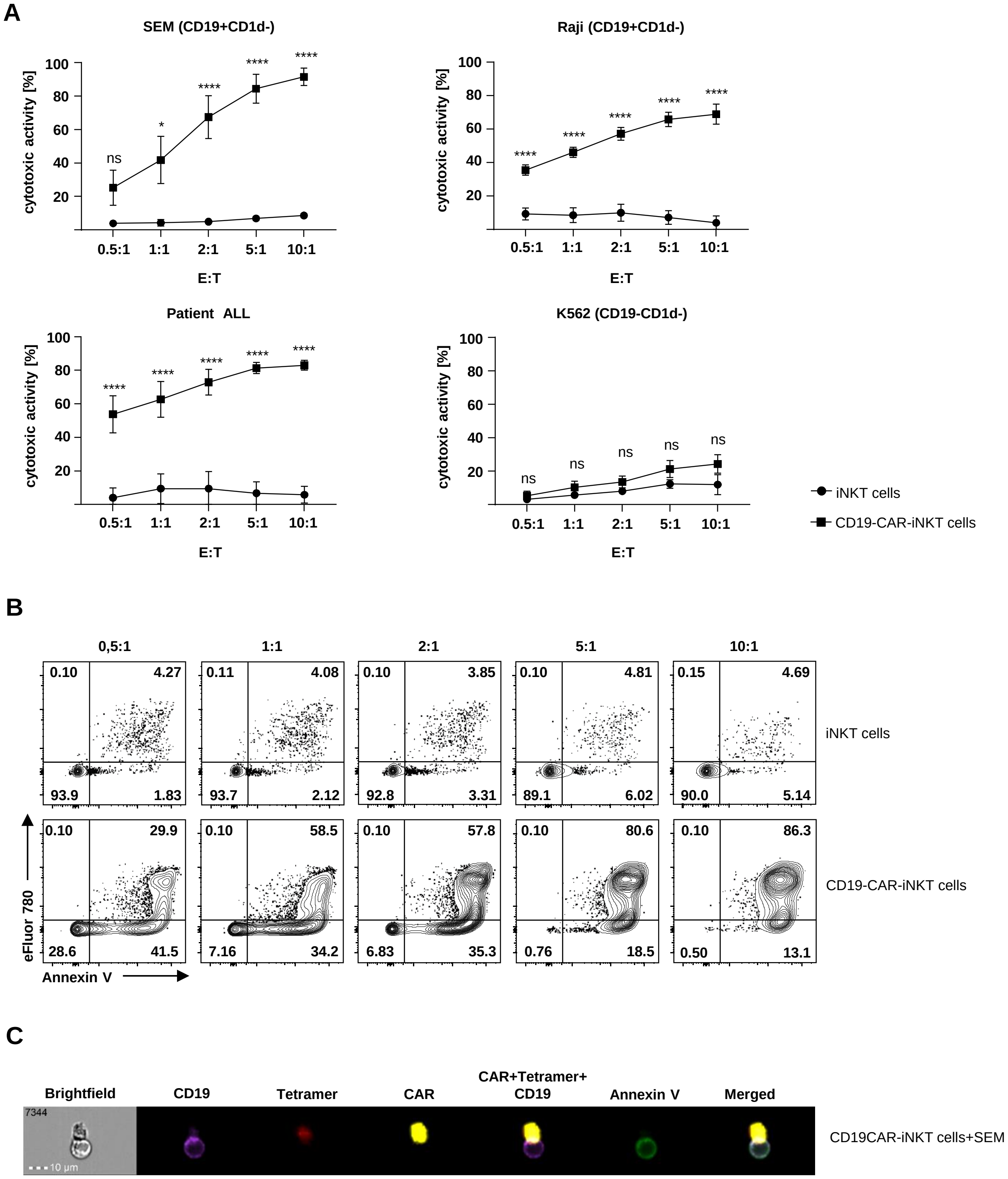

Figure 24: CD19-CAR-iNKT cells show robust cytotoxicity against ALL and lymphoma cells

CD19-CAR-iNKT cells were challenged with CTV-stained SEM (ALL), Raji (BL), patient (ALL) and K562 (CML) cells for 4h at different E:T ratios. The cells were stained with annexin V and eFluor 780 (VD) and analyzed by flow cytometry. Further, SEM co-cultured with CD19-CAR-iNKT cells were also analyzed by ImageStream after annexin V staining. **(A)** shows pooled data (mean) of the cytotoxic activity of CD19-CAR-iNKT cells against SEM, Raji and ALL patient blasts in comparison to untransduced iNKT cells (n=3). **(B)** shows representative dot plots of the cytotoxicity assay with SEM at different ratios. ImageStream analysis of CD19-CAR-iNKT cells (tetramer+, red and CAR+, yellow) inducing cell death (annexin V+, green) of SEM cells (CD19+, purple) in a contact-dependent manner is shown in **(C)**. CD19-CAR-iNKT cells were excluded from the classical flow cytometric analysis by gating on single CTV+ populations only. For the ImageStream analysis, only CD19+ PBS57-loaded CD1d tetramer+ CAR+ doublets were analyzed. The experiments were performed at least three times independently. Error bars show SEM. Two-way ANOVA. ns p>0.05, * p≤0.05, **** p≤0.0001.

Next, the CD1d-mediated cytotoxicity of CD19-CAR-iNKT cells was evaluated by challenging them with CD19-CD1d+ Jurkat cells upon treatment with α-GalCer or its vehicle DMSO. After 4h, the cells were stained with annexin V and analyzed by flow cytometry. The results are depicted in figure 25.

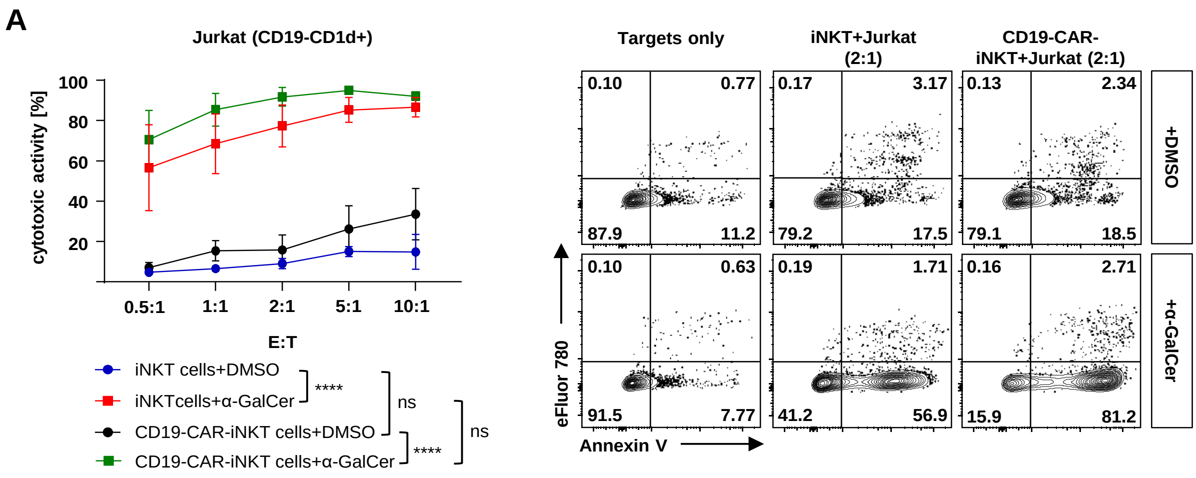

Figure 25: CD19-CAR-iNKT cells maintain their robust CD1d-mediated cytotoxicity
CD19-CAR-iNKT cells were challenged with CTV-stained Jurkat cells (T-ALL) at different E:T ratios. 100 ng/mL α-GalCer or DMSO (diluent) was added to the cells. After 4h, the cells were stained with annexin V and eFluor 780 and analyzed by flow cytometry. Pooled data (mean) showing cytotoxicity of CD19-CAR-iNKT cells with and without α-GalCer treatment (left, n=3) and representative dot plots (right) are depicted. Representative data show cells after gating on all cells (FSC-A vs SSC-A), singlets (SSC-A vs SSC-W) and CTV+ cells. The experiments were performed at least three times independently. The error bars show SEM. Two-way ANOVA. ns p>0.05, **** p≤0.0001.

Interestingly, neither CD19-CAR-iNKT cells nor untransduced iNKT cells treated with DMSO only reacted against the tumor cells, although a non-significant trend can be observed in favor of CD19-CAR-iNKT cells. This effect was abolished upon α-GalCer-addition and a significant robust cytotoxic activity could be observed. No significant difference in the cytotoxicity between untransduced iNKT cells and CD19-CAR-iNKT cells using the α-GalCer-treatment could be observed (**Fig. 25A**).

These data show that CD19-CAR-iNKT cells behave differently in face of CD19 and/or CD1d-dependent stimuli. To elucidate which mechanisms and molecules are involved in their cytotoxicity under different stimuli, untransduced iNKT cells and CD19-CAR-iNKT cells were challenged with WT and modified K562 cells. Modified cells were generated through viral transduction to stably express CD19 (K562-CD19), CD1d (K562-CD1d) and both (K562-DP) (**Fig. 26A**). Since preliminary data showed no activity of untransduced iNKT cells against the K562 wild type, α-GalCer was also added to the assays to promote this interaction. DMSO was used as a negative control. After 4h, cells were stained and analyzed by flow cytometry. Supernatants were further analyzed by multiplex. The results are shown in figure 26. Statistic data of figure 26B can be found in appendix data 3.

Conversely to the assays using K562 and Jurkat cells (**Fig. 24**), CD19-CAR-iNKT cells showed a significantly enhanced cytotoxicity against K562-WT cells in comparison to untransduced iNKT cells. α-GalCer did not have any additional effect. CD19-CAR-iNKT cells also showed strong cytotoxicity against K562-CD19 cells in a dose-dependent manner. In this setting, α-GalCer did not induce any further enhancement of cytotoxic activity. When tested against K562-CD1d, CD19-CAR-iNKT cells show overall superior cytotoxicity compared to untransduced iNKT cells. Despite a small effect when only treated with DMSO, cytotoxicity of untransduced iNKT cells against the target cells could also be enhanced upon α-GalCer treatment. Further, α-GalCer significantly increased the function of CD19-CAR-iNKT cells against CD1d+ target cells. Similarly, α-GalCer also significantly enhanced the cytotoxicity of both iNKT cells and CD19-CAR-iNKT cells against K562-DP cells (**Fig. 26B**).

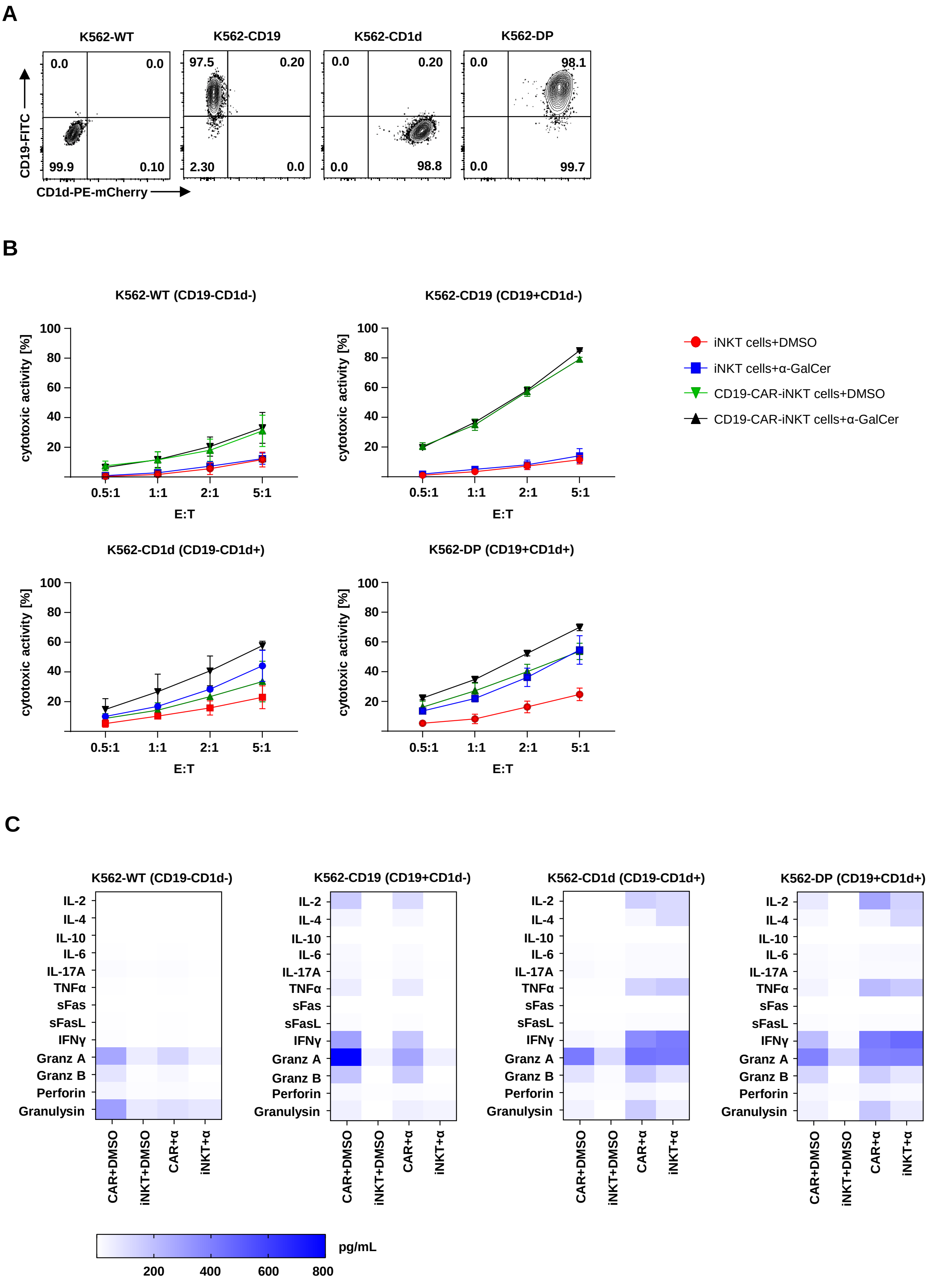

Figure 26: CD19-CAR-iNKT cells show robust cytotoxicity against modified cells lines using both CAR and CD1d pathways

K562-WT and K562-CD1d cells were transduced to express the CD19 antigen. Untransduced iNKT cells and CD19-CAR-iNKT cells were challenged with CTV-stained modified K562 cells for 4h. DMSO (diluent) or 100 ng/mL α-GalCer were added to the cells. The cells were stained with annexin V and eFluor 780 and analyzed by flow cytometry. Supernatants were collected for multiplex analysis. **(A)** shows representative dot plots of the CD19 and CD1d expression by sorted modified K562. Pooled data (mean, n=3) showing cytotoxicity of CD19-CAR-iNKT cells with and without α-GalCer treatment against K562-WT (left, above), K562-CD19+CD1d- (right, above), K562-CD19-CD1d+ (left, below) and K562-CD19+CD1d+ (right, below) are shown in **(B)**. Assays with iNKT cells and DMSO treatment are shown in red, iNKT cells with α-GalCer are shown in blue, CD19-CAR-iNKT cells with DMSO treatment are shown in green and CD19-CAR-iNKT cells with α-GalCer are shown in black. Pooled data were obtained after gating on all cells (FSC-A vs SSC-A), singlets (SSC-A vs SSC-W) and annexin V-VD-CTV+ cells. **(C)** Heat maps showing pooled data (mean) in pg/mL (n=3) of cytokine release by untransduced iNKT cells and CD19-CAR-iNKT cells upon treatment with DMSO and α-GalCer and challenge with K562-WT and modified K562 cells after 4h. The experiments were performed at least three times independently. Error bars show SEM. Granz A= granzyme A, Granz B= granzyme B.

LegendPlex analysis revealed a cytokine pattern, which supports the observations in figure 26B. A slight release of effector molecules such as granzyme A and granulysin seemed to be involved in the cytotoxic effect of CD19-CAR-iNKT cells against K562-WT cells and might explain the background cytotoxicity observed in all tested conditions in the cytotoxicity assays. For cells tested against CD19+ cells, an α-GalCer-independent release of IL-2, TNF-α, IFN-γ and effector molecules could be observed only by CD19-CAR-iNKT cells. On the other hand, assays using K562-CD1d cells confirmed the necessity of α-GalCer for the cytotoxic effect. Against double positive target cells, the same pattern as for CD19+ cells could be observed. Interestingly, α-GalCer seemed to boost the IL-2 release of CD19-CAR-iNKT cells, while higher levels of IFN-γ could be detected for untransduced iNKT cells under this condition. Further, α-GalCer seemed to boost TNF-α release by both effector cells.
Altogether, these results demonstrate the cytotoxic potential of CD19-CAR-iNKT cells for ALL and lymphoma control, which could be enhanced through the engagement of the TCR:CD1d machinery.

4.2.3 PD-1 expression of CD19-CAR-iNKT cells is increased after contact with CD19+ target cells

It has been documented that iNKT cells may become exhausted and consequently, anergic upon stimulation with α-GalCer [187, 188]. The characterization of the cells generated using the protocol described in this work showed low levels of exhaustion markers (4.2.1), despite prolonged culture time and several stimulation rounds with α-GalCer. Further, analysis of the cytotoxicity revealed that ALL cells are highly sensitive to CD19-CAR-iNKT cells while Raji cells seem to be more resistant (4.2.2).

Aiming at the complete elimination of the target cells, the co-incubation time was increased to 24h. After harvest and staining, the cells were analyzed by flow cytometry. CD19-CAR-iNKT cells showed robust cytotoxic activity against Raji cells, however, no target-cell eradication could be observed (**Fig.27A**). Further analysis of the effector cells during the assay revealed an increased expression of the inhibitory receptor PD-1 (**Fig.27B**).

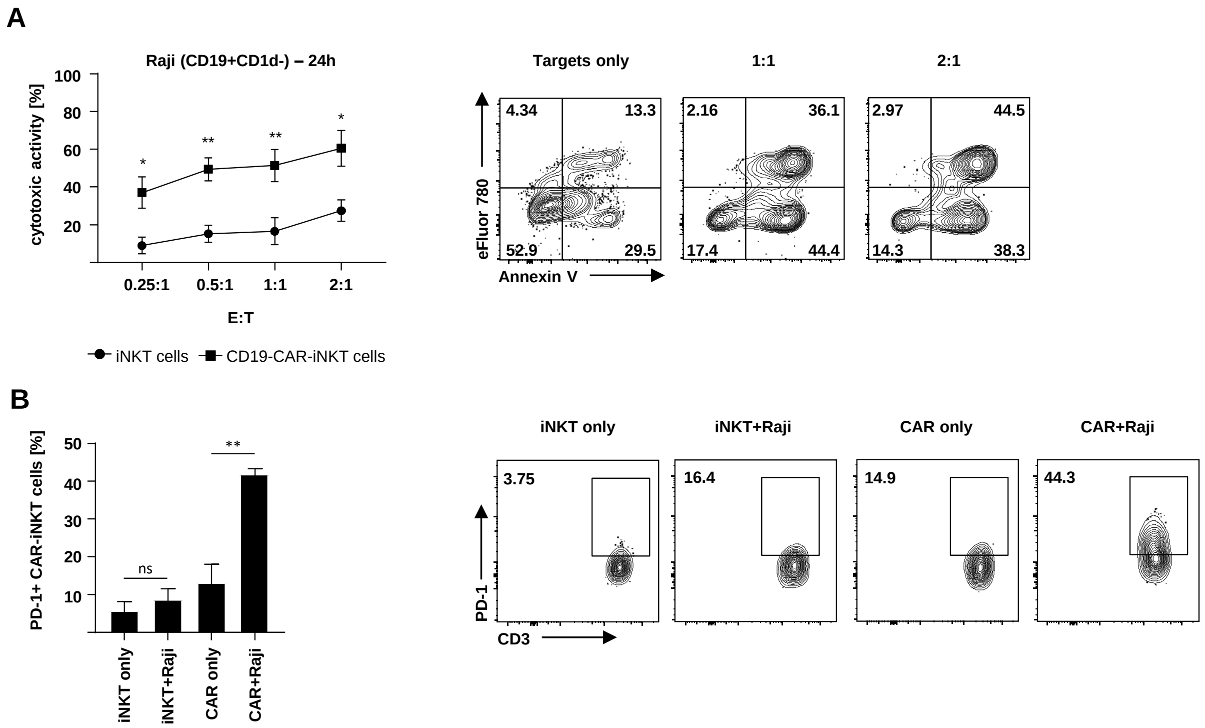

Figure 27: PD-1 expression is increased on CD19-CAR-iNKT cells upon antigen contact

CD19-CAR-iNKT cells were challenged with CTV-stained Raji cells (BL) at different E:T ratios. After 24h, the cells were stained with annexin V, eFluor 780 and usual T-cell markers and analyzed by flow cytometry. **(A)** shows pooled data (mean, n=3) of the cytotoxic activity of untransduced iNKT cells/CD19-CAR-iNKT cells against lymphoma cells for 24h (left) and representative plots for one donor for targets only and target cells challenged with CD19-CAR-iNKT cells at 1:1 and 2:1 ratios (E:T) (right). Annexin V/VD gates were set on singlets and CTV+ cells. **(B)** shows pooled data (n=3) of the PD-1 expression on untransduced iNKT cells/CD19-CAR-iNKT cells upon contact with Raji cells (left) and representative data for one donor (right). PD-1+ cells were analyzed from lymphocytes, singlets, alive iNKT cells (CD3+PBS57-CD1d-tetramer+) and CAR+ or not. The experiments were performed at least three times independently. Error bars show SEM. Two-way ANOVA. ns $p>0.05$, * $p\leq0.05$, ** $p\leq0.01$.

4.2.4 PD-1:PD-L1/2 interaction hinders the functionality of CD19-CAR-iNKT cells

The inhibitory receptor PD-1 is expressed after T-cell activation as a mechanism of defense to prevent exaggerated T-cell responses, and is downregulated once the antigen has been cleared. Therefore, its expression does not necessarily represent a negative characteristic of the physiological response. However, PD-1 expression in combination with other markers, e.g. thymocyte selection-associated HMG BOX (TOX), T-box expressed in T cells (T-bet) and eomesodermin (EOMES), might also indicate that effector cells might be following an exhaustion pathway [189, 190]. Functional exhaustion of T cells leads to decreased cytotoxicity and cytokine production [189, 191]. In this work, the behavior of CD19-CAR-iNKT cells upon encounter with both CD19 antigen and PD-1 ligands was assessed through functional assays. Thus, CD19-CAR-iNKT cells were tested against Raji cells modified to overexpress either PD-L1 (Raji-PD-L1) or PD-L2 (Raji-PD-L2). Raji cells transduced with an empty vector were used as control (**Fig. 28A**). After 24h-co-culture, the cells were stained and analyzed by flow cytometry. Further, the supernatants were analyzed by multiplex.

The cytotoxic assays revealed that Raji-ctrl were the most susceptible to CD19-CAR-iNKT cells, followed by Raji-PD-L2 cells. The most distinct effect could be observed for Raji-PD-L1 cells, however, none of these observations were shown to be statistically significant (**Fig. 28B**). Nevertheless, multiplex analyses demonstrated a significant decrease in the release of several cytokines when CD19-CAR-iNKT cells were challenged with Raji-PD-L1 and Raji-PD-L2 cells (**Fig. 28C**).

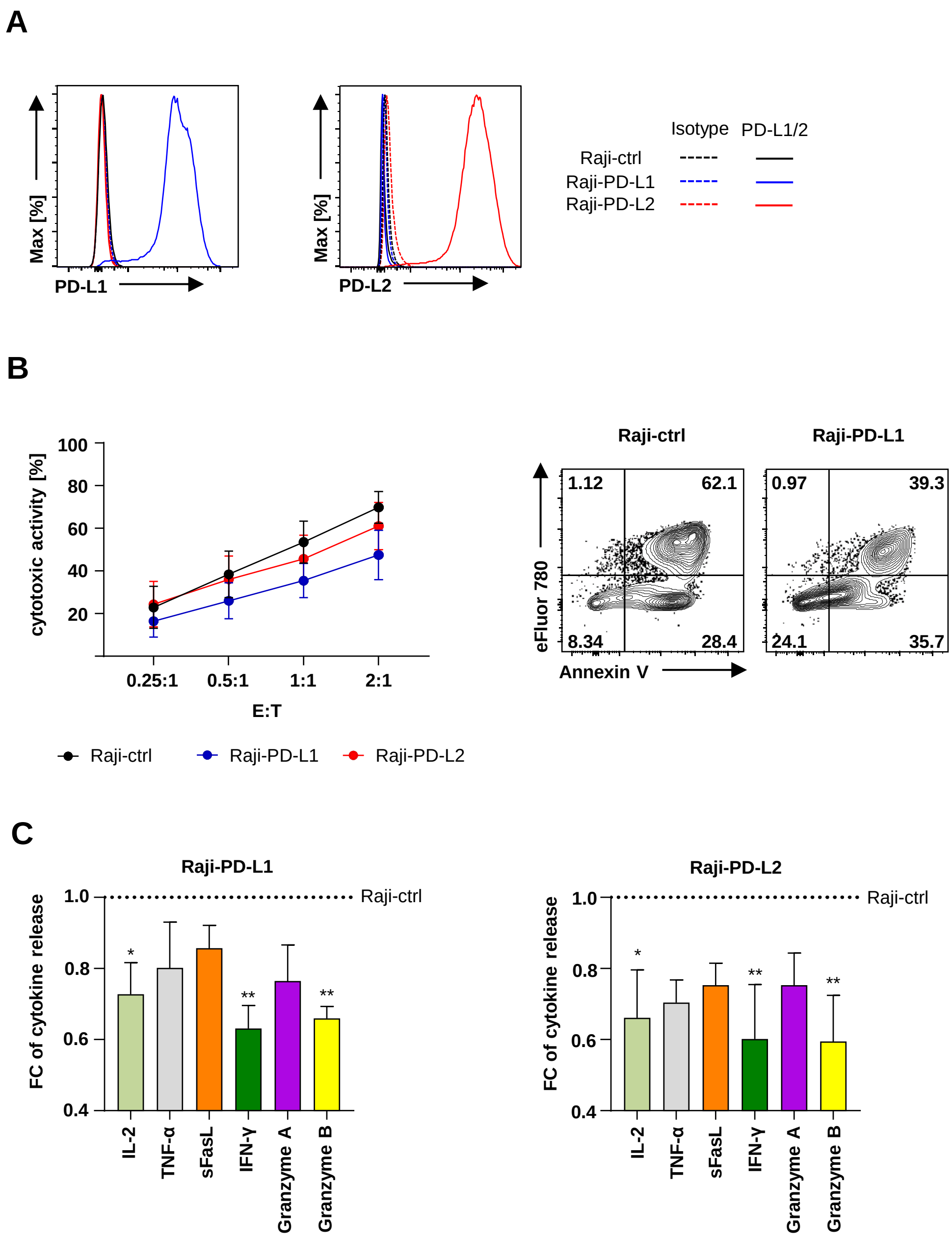

Figure 28: Functionality of CD19-CAR-iNKT cells is impaired through contact with PD-L1/PD-L2 expressing Raji cells

Raji cells were modified to express stably PD-L1 and PD-L2 molecules. For the cytotoxicity assays, CD19-CAR-iNKT cells were challenged with CTV-stained modified Raji cells at different E:T ratios. After 24h, the cells were stained with annexin V and eFluor 780 and analyzed by flow cytometry. For multiplex analysis, supernatants of the cytotoxicity assays were collected and analyzed with the LEGENDplex™ Human CD8/NK panel (13-plex). **(A)** shows PD-L1 (left) and PD-L2 (right) expression by modified Raji cells. Raji-ctrl are depicted in black, Raji-PD-L1 are depicted in blue and Raji-PD-L2 in red. Cell stained with isotype controls are shown as dashed lines, while specific staining is shown with full lines. Gates were set on singlets and alive CD19+ cells. Pooled data (mean, n=4) of the cytotoxic activity of CD19-CAR-iNKT cells against modified lymphoma cells for 24h (left) and representative plots (right) for one

CD19-CAR-iNKT-cell donor challenged with Raji-ctrl (red), Raji-PD-L1 (black) and Raji-PD-L2 (blue) are shown in **(B)**. Annexin V/eFluor 780 gates were set on singlets and CTV+ cells. **(C)** shows pooled data (mean, n=3) of the IL-2 (light green), TNF-α (light gray), sFasL (orange), IFN-γ (green), granzyme A (purple) and granzyme B (yellow) release by CD19-CAR-iNKT cells upon contact with modified Raji-PD-L1 (left) and Raji-PD-L2 cells (right). Data were normalized to the assay using Raji-ctrl. The experiments were performed at least three times independently. Error bars show SEM. Two-way ANOVA. * $p \leq 0.05$, ** $p \leq 0.01$. Statistically non-significant data analysis ($p > 0.05$) is not depicted.

Aiming to enhance this effect, CD19-CAR-iNKT cells were tested in a repetitive antigen encounter or rechallenge assay. The goal of this assay was to push the cells to their limit and thus, challenge their persistence. Thereby, CD19-CAR-iNKT cells were challenged with target cells once a week for three times. Further, a part of the cells was also tested once a week for their cytotoxicity against the same target cells in a 24h incubation period and analyzed by flow cytometry and multiplex assay.
The cytotoxicity assays confirmed the results for the first stimulation round (as shown in figure 29), whereby CD19-CAR-iNKT cells were less efficient against Raji-PD-L1 cells compared to Raji-ctrl and Raji-PD-L2. The subsequent stimulation rounds showed that Raji-ctrl were still more susceptible to CD19-CAR-iNKT cells than PD-L1/2-expressing cells, however, an important overall decrease in the cytotoxicity of CD19-CAR-iNKT cells could be observed for all target cells in the third stimulation round (**Fig. 29A**). Results for a second donor is depicted in appendix 4. For this donor, a substantial difference between the different targets can be observed, being the Raji-PD-L1 cells the most resistant to CD19-CAR-iNKT cells. However, no visible difference could be observed between the different conditions for the third stimulation. Multiplex analysis of the first and third stimulation rounds revealed an interesting decrease over time in cytokine production with Raji-PD-L1 cells. A significant effect could only be observed for several cytokines in the third stimulation. Interestingly, a significant decrease of IL-2, IFN-γ and granzyme B release by cells challenged with Raji-PD-L2 cells could already be observed even for the first stimulation, despite the negative correlation with the results of the cytotoxicity assays, but in agreement with the data obtained in figure 28.

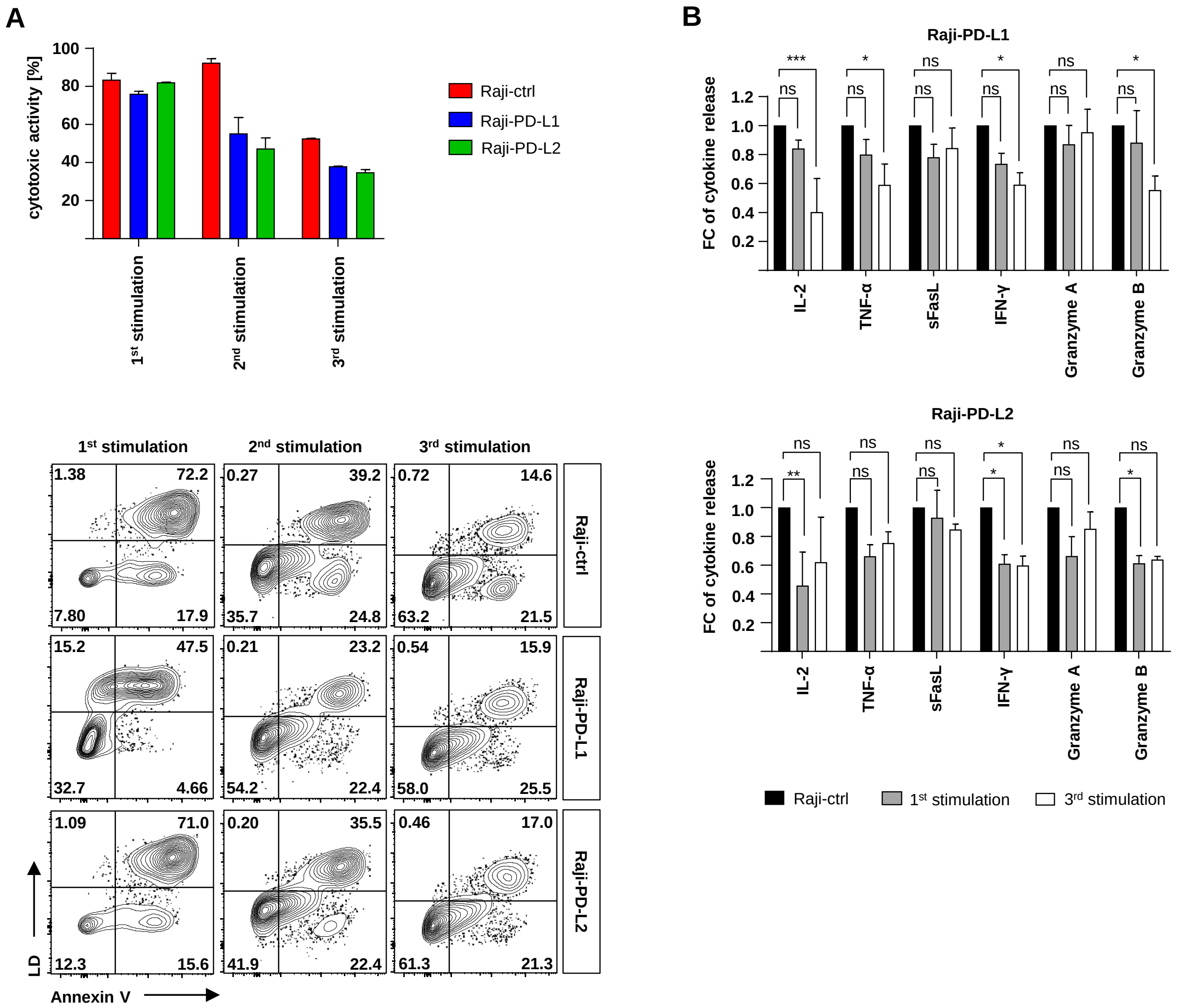

Figure 29: Functionality of CD19-CAR-iNKT cells is impaired upon repetitive antigen contact

CD19-CAR-iNKT cells were challenged with irradiated target cells every 7 days throughout three stimulation rounds. Every seven days, a part of the CD19-CAR-iNKT cells was analyzed for their cytotoxicity against PD-L1/2+ Raji cells at a 2:1 ratio (E:T). After 24h-co-incubation, the cells were harvested and analyzed by flow cytometry. The supernatants were collected for multiplex analysis. **(A)** shows the cytotoxicity course of CD19-CAR-iNKT cells for one donor throughout three stimulations with Raji-Ctrl (red), Raji-PD-L1 (blue) and Raji-PD-L2 (green) (above) and representative dot plots (below). Target cells were discriminated from CD19-CAR-iNKT cells through the FSC-A vs SSC-A gate and CTV+ staining. Only singlets were analyzed. Results of the multiplex analysis performed for the 1st (gray) and 3rd stimulation (white) rounds of CD19-CAR-iNKT cells being challenged against Raji-PD-L1 (above) and Raji-PD-L2 (below) are depicted in **(B)**. The figures show data obtained for IL-2, TNF-α, sFasL, IFN-γ, granzyme A and B after the 1st (gray) and 3rd (white) stimulation rounds. Data is represented in fold-change (FC) of cytokine release normalized to the assay with Raji-Ctrl (red) as targets (n=3). Pooled data show the mean of the biological replicates. The experiments were performed at least three times independently. Error bars show SEM. Two-way ANOVA. ns $p>0.05$, * $p\leq0.05$, ** $p\leq0.01$, *** $p\leq0.001$.

In summary, these results show that antigen-specific contact induces PD-1 expression on CD19-CAR-iNKT cells challenged with CD19+ BL. Moreover, the PD-1:PD-L1/2 interaction was shown to induce a negative effect on cytokine release by CD19-CAR-iNKT cells and on their cytotoxicity.

4.2.5 Checkpoint inhibition increases cytokine release and proliferation of CD19-CAR-iNKT cells, but does not impact short-term cytotoxicity

Due to the PD-1 expression by CD19-CAR-iNKT cells and the subsequently reduced functionality, the use of PD-1 checkpoint inhibition to overcome this effect was considered. The concept of using checkpoint inhibition to enhance CAR-T-cell function is not novel. However, despite promising results in tumor control, a higher risk for the development of GvHD in an allogeneic transplant setting has been observed in clinical studies, which significantly compromises the overall outcomes of the therapy [168, 169]. CD19-CAR-iNKT cells have not been evaluated in this context yet and could represent an elegant alternative to CAR-T cells even in an allogeneic setting since they are not able to induce GvHD. Thus, the potential of PD-1 checkpoint inhibition to enhance CD19-CAR-iNKT-cell function was evaluated *in vitro*.

CD19-CAR-iNKT cells were challenged with PD-L1/2+ Raji cells at several E:T ratios. The cells were further treated with the PD-1 checkpoint inhibitor nivolumab. After 24h, the cells were stained and analyzed by flow cytometry for cytotoxicity and the supernatants were analyzed by multiplex cytokine assay. Moreover, CD19-CAR-iNKT-cell proliferation was tested against modified Raji cells and checkpoint inhibition. An IgG4 isotype antibody was used as the negative control. The results are shown in figure 30.

Analyses of the short-term cytotoxicity demonstrated that checkpoint inhibition does not affect on the lytic function of CD19-CAR-iNKT cells (**Fig. 30A**). However, multiplex analysis revealed that checkpoint inhibition could not only block the negative effect of the PD-1:PD-L1/2 interaction but also even significantly enhanced the release of IL-2, TNF-α, IFN-γ and granzyme B by CD19-CAR-iNKT cells challenged with both PD-L1 and PD-L2 positive BL cells (**Fig. 30B**). Interestingly, no negative effect on cell proliferation had been observed for CD19-CAR-iNKT cells tested against modified Raji cells (IgG4-control data). Nevertheless, checkpoint inhibition increased the proliferation of CD19-CAR-iNKT cells upon antigen contact significantly (**Fig. 30C**).

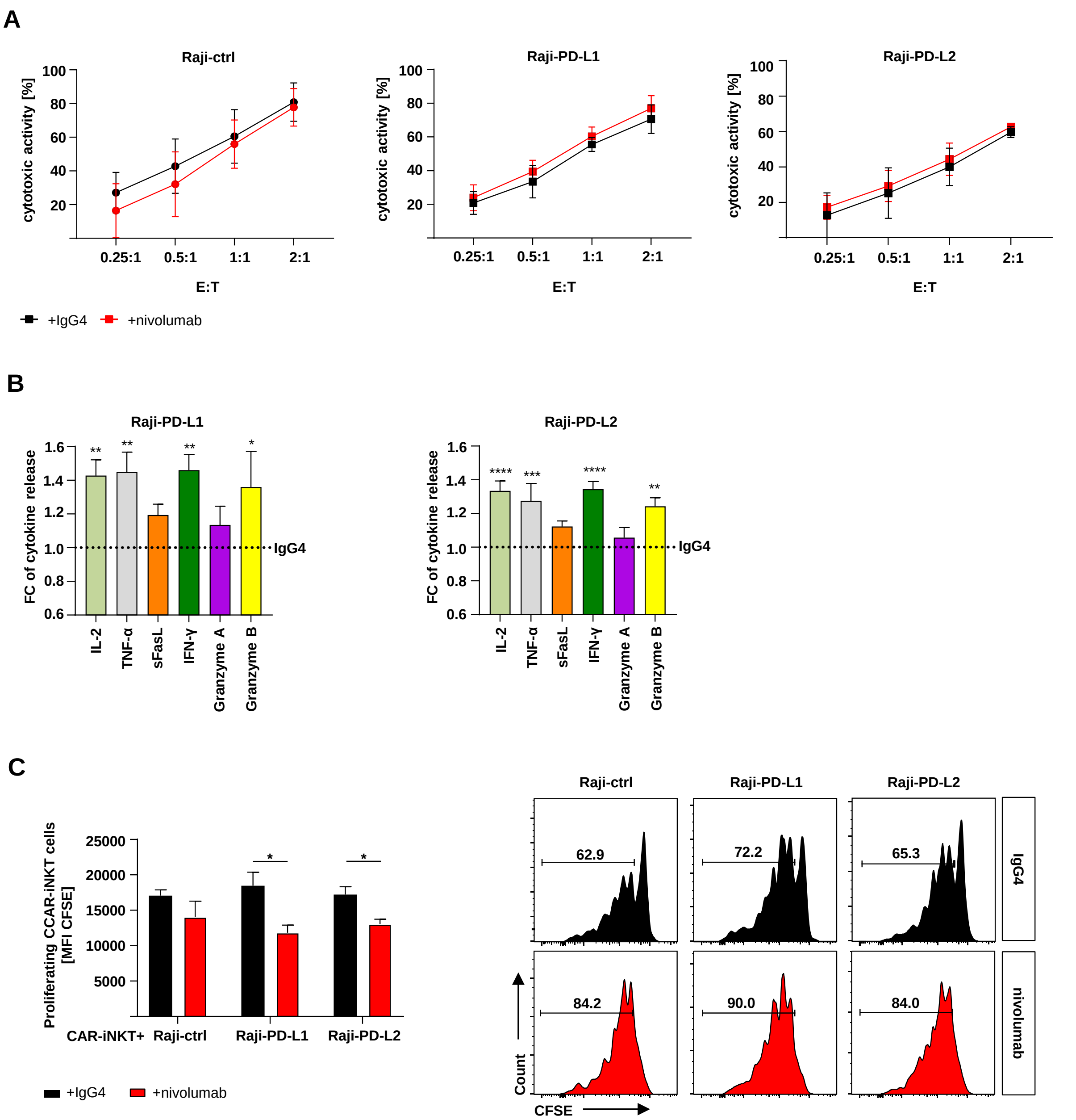

Figure 30: Checkpoint inhibition increases cytokine release and proliferation of CD19-CAR-iNKT cells, but does not impact short-term cytotoxicity

CD19-CAR-iNKT cells were challenged with CTV-stained modified Raji cells (BL) at different E:T ratios. Where stated, the cells were treated with nivolumab or its IgG4 control. After 24h, the cells were stained with annexin V, eFluor 780 and analyzed by flow cytometry. For multiplex analysis, supernatants of the cytotoxicity assays were collected and analyzed with the LEGENDplex™ Human CD8/NK panel (13-plex). For proliferation assays, nivolumab- or IgG4-treated CFSE-stained CD19-CAR-iNKT cells were challenged for 5 days with irradiated modified Raji cells and analyzed by flow cytometry. Pooled data (mean, n=4) of the cytotoxic activity of CD19-CAR-iNKT cells against Raji-ctrl (left), Raji-PD-L1 (middle) and Raji-PD-L2 (right) cells for 24h are shown in **(A)**. Black lines show assays with IgG4-control treatment and red lines show data for the treatment with nivolumab. Annexin V/eFluor 780 gates were set on single CTV+ cells. **(B)** shows pooled data (mean, n=5) of the IL-2 (light green), TNF-α (light gray); sFasL (orange), IFN-γ (green), granzyme A (purple) and granzyme B (yellow) release by CD19-CAR-iNKT cells upon contact with modified Raji-PD-L1 (left) and Raji-PD-L2 cells (right), under nivolumab- or IgG4-control treatment. Data were normalized to their respective IgG4-control data. **(C)** depicts the mean of pooled data (left) of the proliferation of nivolumab- (red) or IgG4 (black)-treated CD19-CAR-iNKT cells upon challenge with modified Raji cells and representative data for one donor (right). Gates were set on lymphocytes, singlets and alive CD19-CAR-iNKT cells. The results are expressed as MFI. The experiments were performed at least three times independently. Error bars show SEM. Two-way ANOVA. * $p \leq 0.05$, ** $p \leq 0.01$, *** $p \leq 0.001$, **** $p \leq 0.0001$. Non-significant statistical analysis ($p > 0.05$) is not depicted.

Next, checkpoint inhibition was also evaluated in the context of rechallenge assays. These were performed as described in 3.5.8 and 4.2.4. Additionally, the cells were treated with nivolumab (10 µg/mL). An IgG4 isotype antibody was used as a negative control. The data are depicted in figure 31.

Data obtained for one donor revealed a slight increase in the cytotoxicity of CD19-CAR-iNKT cells treated with nivolumab. This effect could be observed for all stimulation rounds with Raji-PD-L1 cells and in the second round for Raji-ctrl and Raji-PD-L2 cells. (**Fig. 31A**). For a second donor, a slight positive effect of cells treated with nivolumab could be observed only in the third stimulation round (**appendix data 5**).

Multiplex data of the first and third stimulations showed an overall decrease in the cytokine release by CD19-CAR-iNKT after three stimulation rounds that could not be rescued by checkpoint inhibition. Nevertheless, an interesting increase in the release of IL-2, TNF-α, sFasL, IFN-γ and granzyme A by CD19-CAR-iNKT cells challenged with Raji-PD-L1 cells upon nivolumab-treatment could be observed at both time points. A significant difference could be further observed for the release of granzyme B (**Fig. 31B**).

In summary, these data show that PD-1 checkpoint inhibition displays only a minor effect at the short- and long-term cytotoxicity. Nonetheless, cell proliferation and cytokine release seem to profit from this strategy.

+

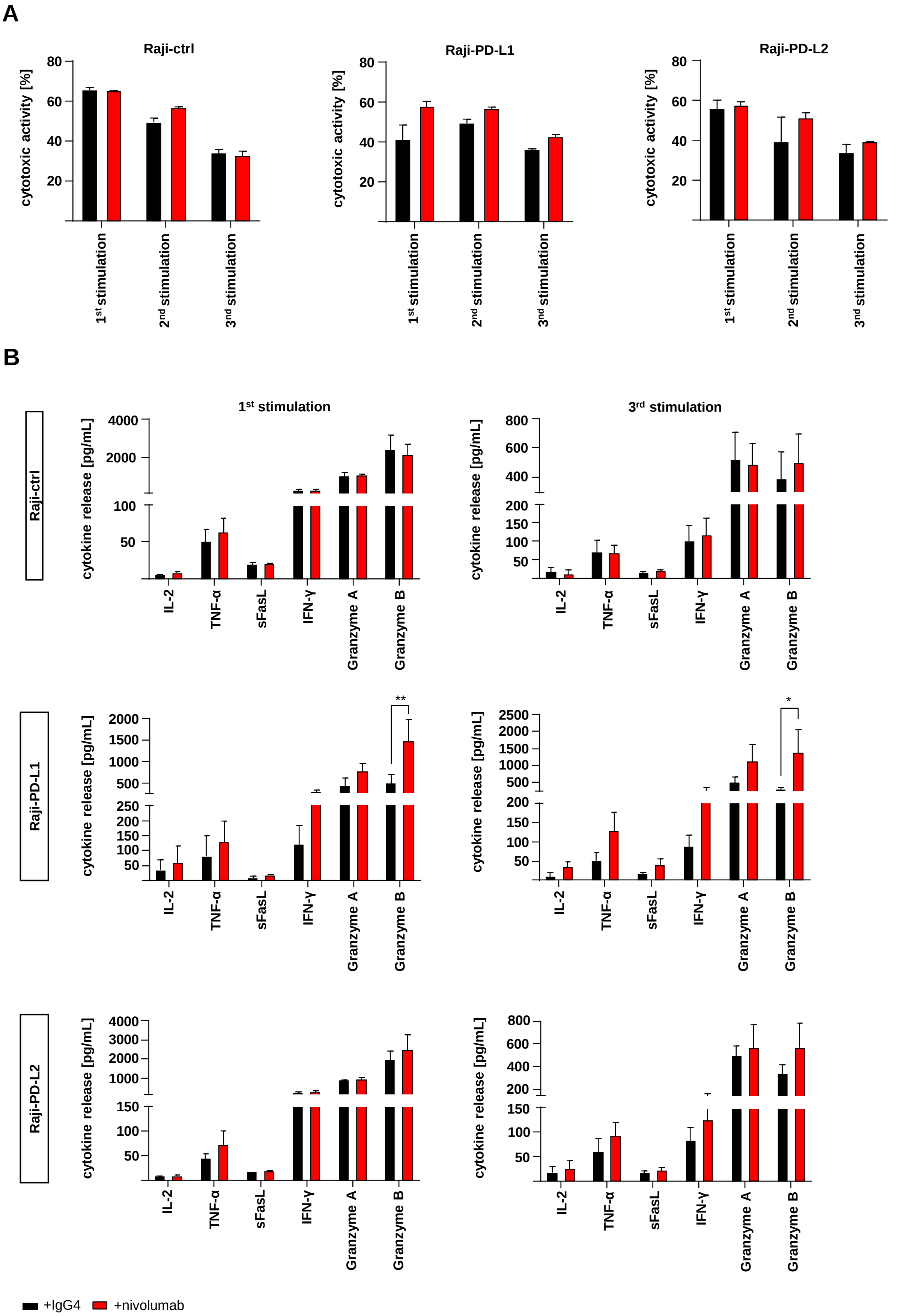
A
Raji-ctrl
Raji-PD-L1
Raji-PD-L2
cytotoxic activity [%]
80
60
40
20
1st stimulation
2nd stimulation
3rd stimulation
B
1st stimulation
3rd stimulation
Raji-ctrl
Raji-PD-L1
Raji-PD-L2
cytokine release [pg/mL]
IL-2
TNF-α
sFasL
IFN-γ
Granzyme A
Granzyme B
**
*
+IgG4
+nivolumab

Figure 31: Checkpoint inhibition partially improves the cytotoxicity and ability of cytokine release of CD19-CAR-iNKT cells after repetitive antigen encounter

CD19-CAR-iNKT cells were challenged with irradiated target cells every 7 days throughout three stimulation rounds. Every seven days, part of the CD19-CAR-iNKT cells were analyzed for their cytotoxicity against PD-L1/2+ Raji cells. After 24h, the cells were harvested and analyzed by flow cytometry. The supernatants were collected for multiplex analysis. Where stated, 10 µg/mL nivolumab or an IgG4 isotype control was added to the assays. **(A)** shows representative data for the cytotoxicity of CD19-CAR-iNKT cells (mean of technical replicates, n=1) throughout three stimulations with Raji-ctrl (left), Raji-PD-L1 (middle) and Raji-PD-L2 (right) upon IgG4 isotype control (black) or nivolumab (red) treatment. Single target cells were discriminated of CD19-CAR-iNKT cells through the FSC-A vs SSC-A gating and CTV+ staining. Results of the multiplex analysis performed for the 1st (left) and 3rd stimulation (right) rounds of CD19-CAR-iNKT cells being challenged against Raji-ctrl (above), Raji-PD-L1 (middle) and Raji-PD-L2 (below) are depicted in **(B)**. The figures show data obtained for IL-2, TNF-α, sFasL, IFN-γ, granzyme A and B. The data are represented in pg/mL of cytokine release (n=4). Samples treated with IgG4 isotype control are shown in black and nivolumab are shown in red. The experiments were performed at least three times independently. Error bars show SEM. Two-way ANOVA. * p≤0.05, ** p≤0.01. Non-significant statistical analysis (p>0.05) is not depicted.

4.2.6 CD19-CAR-iNKT cells maintain the immunoregulatory properties of conventional iNKT cells

As already demonstrated, iNKT cells are immunoregulatory cells that might prevent GvHD after HSCT. It has been shown that iNKT cells promote immune tolerance in humans by the preferential apoptosis induction of specific DC subsets, thus avoiding T-cell activation, while certain processes pertinent to the host defense might still take place through the action of other DC subsets [184].

Through cytotoxic assays against CD1d+ cell lines, it was shown that CD19-CAR-iNKT cells still keep their important immunoregulatory function, while exerting potent anti-tumor function. As a proof-of-concept, the analysis of the inhibitory properties of CD19-CAR-iNKT cells was also performed. This kind of analysis would be of extreme importance in case of allogeneic transplantation. Due to the non-existence of GMP-products for the isolation of these cells in the context of a translational approach, the presence of remaining T cells in the final product would be possible and could induce GvHD, which however could be prevented by CD19-CAR-iNKT cells. For that, the capacity of CD19-CAR-iNKT cells of promoting mo-DC apoptosis and preventing T-cell activation and proliferation was analyzed. The assays were performed as demonstrated in 4.1.3-6. Further, the supernatants were analyzed by multiplex assays. Untransduced iNKT cells were used as controls. The obtained data is shown in figure 32.

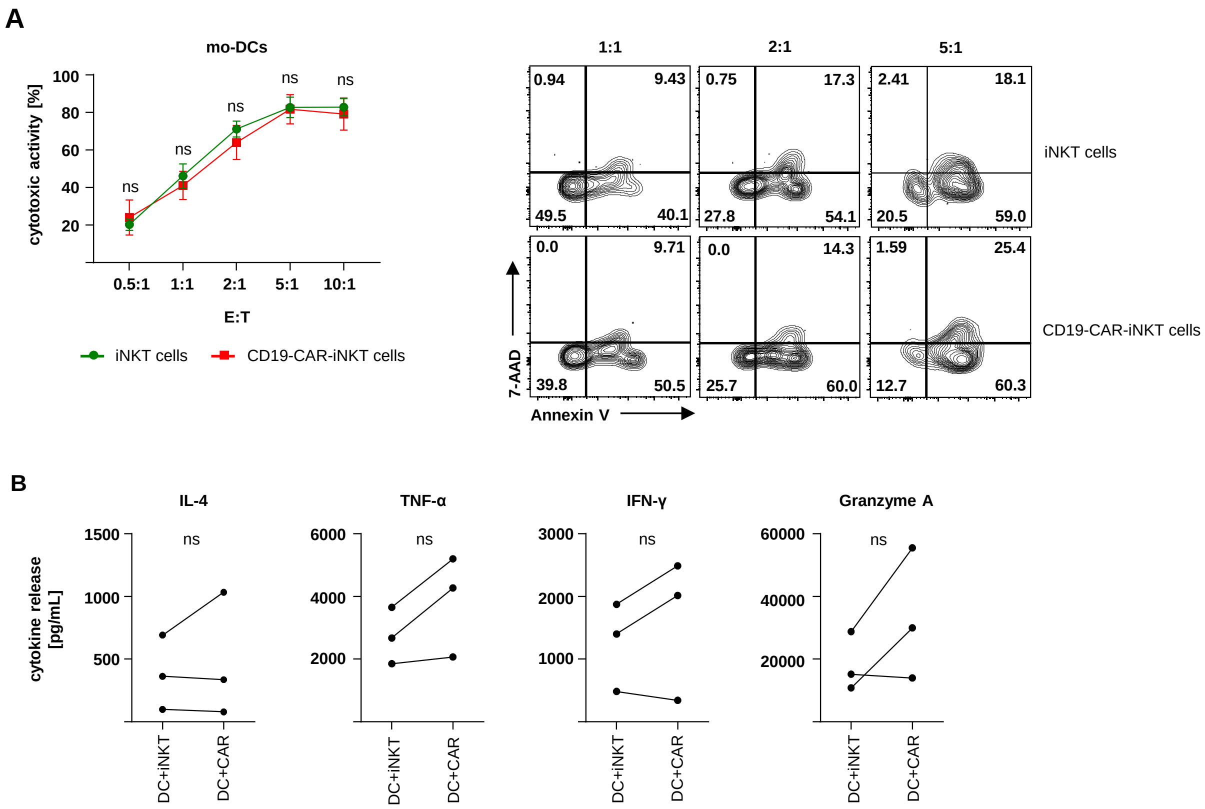

Figure 32: CD19-CAR-iNKT cells maintain the iNKT-cell ability to induce DC apoptosis

Mo-DCs were co-cultured with iNKT cells or CD19-CAR-iNKT cells at a 1:5 ratio (DC:iNKT cells). After 4h, the cells were stained with annexin V and 7-AAD and analyzed by flow cytometry. Supernatants of the apoptosis assays were collected for multiplex analysis. Pooled data (mean, left) and representative dot plots (right) showing blood DC apoptosis induction by iNKT cells (green) and CD19-CAR-iNKT cells (red) are depicted in **(A)**. CD3+ iNKT cells/CD19-CAR-iNKT cells were excluded from the analysis by gating on CD3- cells only. Pooled data show results for at least three different donors analyzed independently. Error bars show SEM. Data of the multiplex analysis in pg/mL for IL-4, TNF-α, IFN-γ and granzyme A are shown in **(B)**. DC+iNKT stands for DCs incubated with iNKT cells and DC+CAR stands for DCs co-cultured with CD19-CAR-iNKT cells. Two-way ANOVA **(A)** and paired t-test **(B)**. ns p>0.05.

As for untransduced iNKT cells, CD19-CAR-iNKT cells were also able to efficiently induce DC apoptosis in a dose-dependent manner. No significant difference could be observed between CD19-CAR-iNKT cells and untransduced iNKT cells (**Fig. 32A**). Further, multiplex analysis revealed a similar cytokine release pattern by both CD19-

CAR-iNKT cells. However, a higher effect in favor of CD19-CAR-iNKT cells could be observed (**Fig. 32B**).

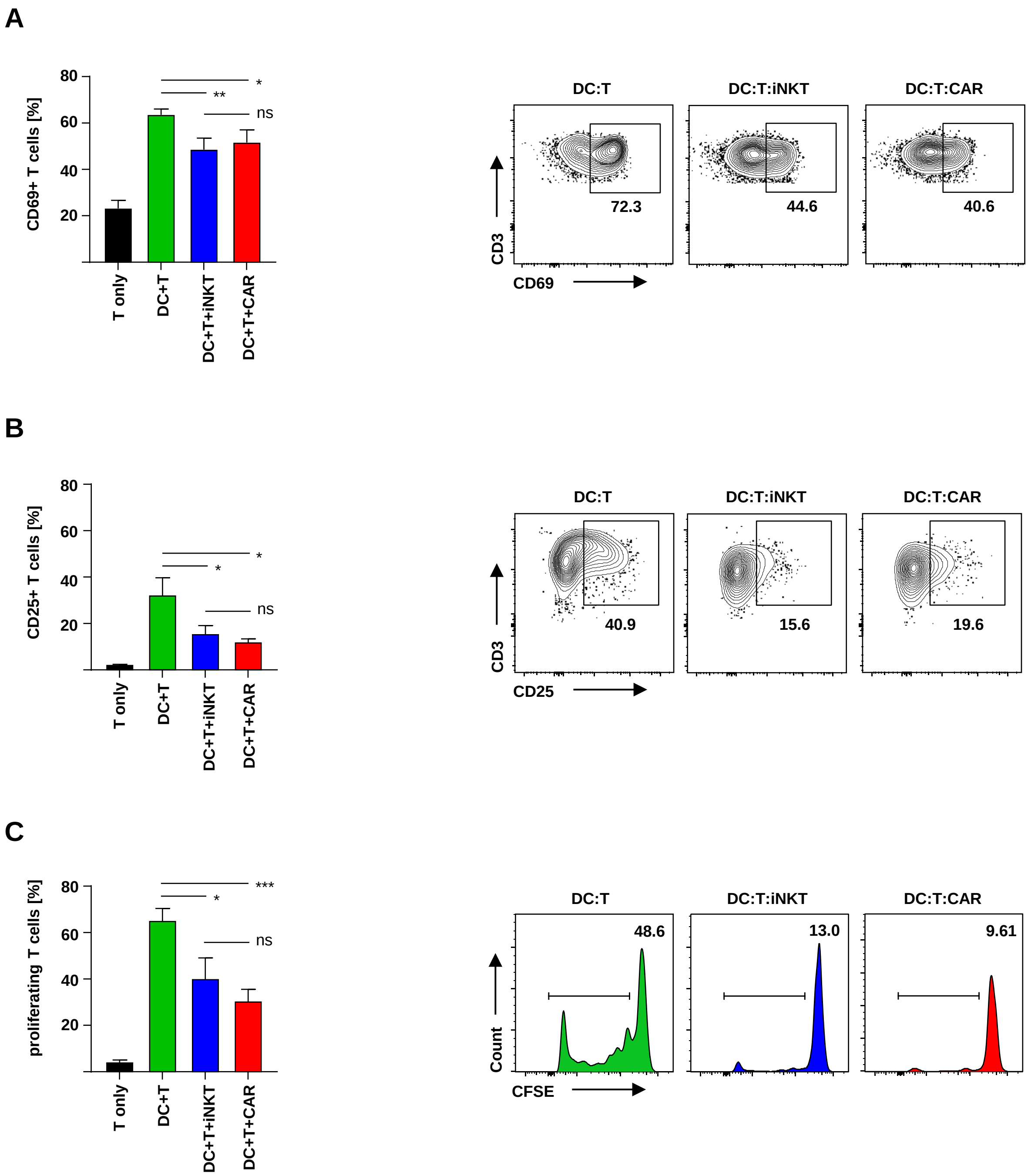

Figure 33: CD19-CAR-iNKT cells efficiently prevent T-cell activation and proliferation

T cells were co-cultured with mo-DCs and untransduced iNKT cells/CD19-CAR-iNKT cells at a 1:1:5 ratio (T cell:DC:iNKT/CD19-CAR-iNKT cells) and analyzed by flow cytometry for early and late T-cell activation (CD69 on day 1 and CD25 on day 3, respectively) and proliferation (CFSE dilution, on day 7). **(A)** shows histograms and representative dot plots of early activation of T cells after 24h co-culture. **(B)** depicts pooled data and representative dot plots demonstrating T-cell activation on day 3 and **(C)** demonstrates histograms and dot plots of proliferating T cells after co-incubation with mo-DCs for 7 days. Co-cultures without iNKT cells were used as a positive control and T cells cultured alone were used as the negative control. T cells only are shown in black, DCs plus T cells in green, DCs plus T cells plus iNKT cells in blue and DCs plus T cells plus CD19-CAR-iNKT cells in red. Exclusion of iNKT cells followed gating on CFSE positive populations on days 1 and 3 and PBS57-CD1d-tetramer negative populations on day 7. Only alive (VD-) T cells were analyzed. Histograms show pooled data (mean) of seven different donors, analyzed independently. Error bars show SEM. Two-way ANOVA. ns $p>0.05$, * $p\leq0.05$, ** $p\leq0.01$, *** $p\leq0.001$.

Analyses of MLR showed that CD69 (**Fig. 33A**) and CD25 expression (**Fig. 33B**) by T cells and T-cell proliferation (**Fig. 33C**) were significantly decreased upon CD19-CAR-iNKT-cell addition. No significant difference could be observed between CD19-CAR-iNKT cells and untransduced iNKT cells.

Altogether, these data demonstrate that CD19-CAR-iNKT cells are as efficient as untransduced iNKT cells in promoting DC apoptosis and consequently preventing T-cell allogeneic reactions.

4.2.7 CD19-CAR-iNKT cells can still prevent T-cell activation and proliferation, even upon checkpoint inhibition

Another point addressed in this work was the use of checkpoint inhibitors to improve the function of CD19-CAR-iNKT cells. As it has been shown that checkpoint inhibition provokes allo-reactions, this set of experiments aimed at assessing the safety of checkpoint inhibition and CD19-CAR-iNKT cells *in vitro* using our MLR model. Where stated, the PD-1 checkpoint inhibitor nivolumab or its IgG4 isotype control was added to the MLR. After a 7-day-co-culture with untransduced iNKT cells or CD19-CAR-iNKT cells and DCs, T cells were analyzed for their CD69 and CD25 expression and proliferation. The results are depicted in figure 34.

As observed in the previous assay, both untransduced iNKT cells and CD19-CAR-iNKT cells prevented T-cell activation and proliferation. A non-significant trend in favor of nivolumab-treated T cells in the positive control could be observed for the CD25 expression and T-cell proliferation. Despite that, untransduced iNKT cells and CD19-CAR-iNKT cells were significantly able to impair the function of isotype control and nivolumab-treated T cells with a slightly better effect observed for cells treated with nivolumab (**Fig.34A-C**).

In summary, these results demonstrate the ability of CD19-CAR-iNKT cells in inhibiting T-cell activation and proliferation even under checkpoint inhibition.

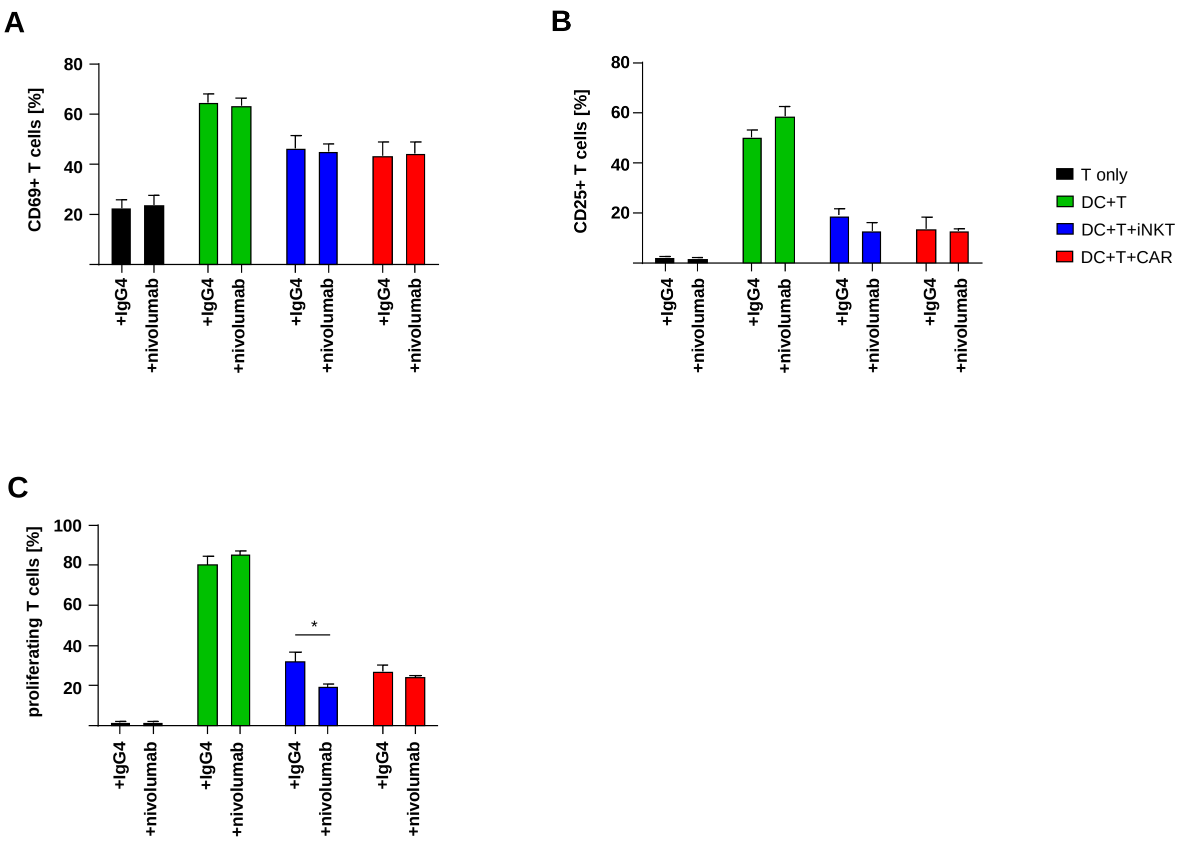

Figure 34: CD19-CAR-iNKT cells efficiently prevent T-cell activation and proliferation despite checkpoint inhibition

T cells were co-incubated with mo-DCs and iNKT cells/CD19-CAR-iNKT cells at a 1:1:5 ratio (T cell:DC:iNKT/CD19-CAR-iNKT cells). CD69 (day 1) and CD25 (day 3) expression and CFSE dilution (day 7) were analyzed by flow cytometry. Nivolumab or its isotype control (IgG4) was added to the assays at 10 µg/mL. **(A)** shows histograms of T-cell early activation (CD69). **(B)** depicts pooled data CD25 expression by T cells on day 3 and **(C)** shows histograms of proliferating T cells on day 7. Co-cultures without untransduced iNKT cells/CD19-CAR-iNKT cells were used as positive control and T cells cultured alone were used as a negative control. T cells only are depicted in black, DCs plus T cells are shown in green, DCs plus T cells plus iNKT cells are shown in blue and DCs plus T cells plus CD19-CAR-iNKT cells are shown in red. Exclusion of iNKT cells followed gating on CFSE positive populations on days 1 and 3 and PBS57-CD1d-tetramer negative populations on day 7. Only alive (VD-) T cells were analyzed. Histograms show pooled data (mean) of four different donors, analyzed independently. Error bars show SEM. Two-way ANOVA. * $p \leq 0.05$. Only the statistical data comparing IgG4 and nivolumab-treated groups is shown. Non-significant statistical analyses ($p > 0.05$) are not depicted.

5 Discussion

5.1 Analysis of the tolerogenic properties of iNKT cells in an allogeneic transplant setting

Allogeneic HCT is a well-established therapeutic strategy used for the treatment of several malignancies, especially for advanced and high-risk hematologic diseases. Through optimized donor selection, tailored preparative conditioning regimes and advanced supportive care, improved outcomes have been achieved, enabling long-term remission and survival, even for patients with a bad prognosis. Yet, GvHD and relapse are still important causes of morbidity and mortality after allogeneic HSCT [8, 11, 192].

Several approaches have been used for the prevention or treatment of GvHD such as immunosuppression and T-cell depletion. Nevertheless, immunosuppression also considerably affects the therapy outcomes, since it also inhibits immune reconstitution, infection control, and, importantly, GvL effects, leading to higher relapse rates [15, 193]. Thus, strategies to prevent GvHD while maintaining GvL effects are urgently needed.

Various studies have shown the potential of iNKT cells as an alternative tool for the prevention of GvHD in both murine and human models. A first murine study involving the adoptive reinfusion of sorted NK1.1+ T cells showed their tolerogenic properties for GvHD prevention [194]. Other studies in mice and rats showed the resistance of NKT cells against the usual conditioning regimen and higher numbers correlated with better GvHD suppression [110, 111]. Schneidawind et al. showed that CD4+ iNKT cells prevented GvHD in mice through the expansion of CD4+CD25+FoxP3+ Treg cells [65]. Third-party iNKT cells seem to have an equipotent effect on tolerance induction in mice, probably due to their highly conserved iTCR. In the present study, only third-party iNKT cells were analyzed since they are more readily accessible [115, 195].

The tolerogenic effect of iNKT cells has also been extensively studied in humans. Several studies have demonstrated a positive correlation between the frequency of iNKT cells and a lower incidence of GvHD [116-118, 196]. This observation was confirmed in another study with a cohort of 80 patients. Nevertheless, no correlation between iNKT-cell frequency and Treg expansion was observed [119]. Chen et al.

aimed at analyzing the effect of the Treg population for GvHD control by using an α-GalCer-analog in a phase II clinical study. However, in only 28% of the patients, a response toward Treg expansion could be noted, despite promising preclinical data [197]. Altogether, these data suggest that other mechanisms apart from Treg expansion might be involved in how iNKT cells exert their tolerogenic properties in humans.

GvHD is a well-characterized reaction against host tissues caused by the recognition of host antigens by donor T cells in the context of allogeneic HSCT [8, 198, 199]. The role of APCs as an important factor in the pathogenesis of GvHD has been emphasized in several studies and therefore, these cells represent interesting targets for GvHD prevention [200, 201]. In this context, iNKT cells have been shown to interact with DCs in different ways [202]. For instance, Schmid and Moraes-Ribeiro et al. observed that DCs “disappear” when co-cultured with iNKT cells [184]. Thus, this study first aimed at investigating factors involved in the interaction between *ex vivo* expanded human iNKT cells and DCs in the context of allo-reactions *in vitro*.

First, T-cell activation upon stimulation with Dynabeads® CD3/CD28 as artificial APCs (aAPCs) was investigated. Analyses of MLR revealed that the expression of CD69 and T-cell proliferation was also barely affected by iNKT cells in this setting, even at higher iNKT-cell ratios. Thus, these data suggest that iNKT cells need to interact with other cells rather than exerting a strong direct effect on alloreactive T cells.

Schmid and Moraes-Ribeiro et al. proposed that T-cell function can be impaired by iNKT cells when T cells are activated with DCs [184]. These results are in line with other studies: Coman et al. used a xenograft model of GvHD and could show *in vivo* that CD4- iNKT cells prevent T-cell activation through interaction with DCs. However, another study suggests that DN iNKT cells might be the subset associated with tolerogenic responses [203]. Nevertheless, both studies confirm the importance of the iNKT-cell-mediated DC apoptosis for the control of T-cell function. Importantly, an extension of the conditions tested in this work using transwell inserts confirmed the importance of direct cell contact for this effect. The present work adds significant knowledge to iNKT-cell biology by demonstrating that iNKT cells induce preferentially the apoptosis of cDCs, leading to a relative expansion of beneficial pDCs.

DCs arise from either myeloid or lymphoid hematopoietic stem cell progenitors in the bone marrow [204, 205]. The DC group is composed of heterogeneous subsets, which play distinct roles in modulating immune responses. These have been categorized into cDCs, pDCs and mo-DCs, depending on their lineage and expression of transcription factors as IFN regulatory factors 4 and 8 [206, 207]. Despite being considered interesting targets in the context of GvHD, unspecific DC-targeting might also have a negative effect since DCs also play a protective role after HSCT [206]. In humans, cDCs are robust IL-12 producers and exert an exceptional cross-priming function. However, cDCs are decisive T-cell stimulators in the context of allogeneic reactions. For instance, Markley et al. showed that cDCs play a critical role in antigen presentation after BM transplantation and could initiate GvHD [208]. cDCs have also been associated with the restoration of skin-associated DCs such as Langerhans DCs and this could contribute to the occurrence of skin GvHD [209, 210]. In contrast, pDCs are mostly associated with responses to viral antigen recognition through the robust release of type I and type III IFN [211, 212]. Interestingly, pDCs have been linked with better outcomes after allogeneic HCT through a decreased incidence of GvHD and enhanced GvL effects [213, 214]. Therefore, the modulation potential of iNKT cells on cDCs and pDCs could represent a useful approach to reducing the incidence of GvHD. The present work focused on the interaction of iNKT cells with human blood DCs. These are mainly cDCs and pDCs and can be easily isolated from PBMCs from healthy donors and GvHD patients. Through preferential apoptosis of cDCs, a decreased function of alloreactive T cells in both healthy donors and GvHD patients could be achieved. Moreover, this would lead to a bias in favor of pDCs, which might still perform important immune responses, such as pathogen control and GvL, while improving the outcomes of allogeneic HSCT.

Nevertheless, a direct impact of iNKT cells on T-cell function was only observed when higher numbers of iNKT cells were used, although in other studies low numbers are already associated with objective responses [65, 196]. Considering the plasticity and diversity of iNKT cells, it is plausible that other mechanisms, that are not mutually exclusive, might be responsible for the tolerogenic properties of these cells such as the expansion of Treg cells, the modulation of DC function and induction of a Th2 bias of T helper cells. Schneidawind et al. and Pillai et al. demonstrated *in vivo*, for instance, that the frequency of Treg cells need longer than seven days (as in the *in vitro* MLR model) to be noticed [65, 113]. Therefore, the optimization of the proposed *in vitro* model might be necessary to better understand these parameters. Further, distinct iNKT-cell subsets are associated with certain functional peculiarities which might explain different findings from other groups in humans and mice. Another factor to consider is the protocols used for iNKT-cell expansion, which might also influence the final fitness of these cells.

5.2 Analysis of the cytotoxic potential of iNKT cells in the context of CAR therapy

Preclinical studies have shown the efficacy and safety of iNKT cells both *in vitro* and *in vivo* in the context of tumor control [124, 125, 127-129]. Nevertheless, iNKT cells have produced only partial responses [136-138]. In contrast, CAR-T cells have delivered strikingly positive outcomes, particularly in the treatment of relapsed or refractory B-cell malignancies [155, 156]. However, CAR-T-cell therapy has been associated with high rates of adverse events such as cytokine release syndrome (CRS) and neurotoxicity [156]. Importantly, the application of CAR-T cells in an allogeneic setting is significantly limited since T cells could induce GvHD through their canonical TCR, especially in the case of off-the-shelf products [215].

In this context, iNKT cells represent an elegant alternative to T cells since they do not cause GvHD, but rather prevent it [65, 112, 115]. Besides, whereas the expression of the TCR by conventional CAR-T cells seems to be counterproductive, the engagement of the iTCR by iNKT cells may boost the function of CAR-iNKT cells. In this case, CAR-iNKT cells could not only induce cell death through CAR and CD1d pathways but also modulate the tumor microenvironment and other effector cells to enhance their cytotoxic potency [75, 108, 216].

In this work, a protocol for the generation of CD19-CAR-iNKT cells from third-party healthy donors was established. Since iNKT cells are rarely present in PBMCs, an expansion process was necessary for downstream applications. This step followed upfront isolation and transduction with retroviral supernatants, leading to high numbers of CD19-CAR-iNKT cells. These steps are in line with data obtained by Rotolo et al. [173]. Nevertheless, the present protocol was modified to use α-GalCer-loaded feeder cells and IL-2 for both activation and expansion steps instead of CD3/CD28 aAPCs, since the latter strategy was shown to have a deleterious effect on the iNKT-cell viability as soon as after the activation step, not allowing further processes. Indeed, iNKT-cell anergy caused by strong TCR stimulation through CD3/CD28 antibodies has been documented [217]. Despite overall good expansion rates, a significantly better expansion of non-transduced iNKT cells in contrast to CD19-CAR-iNKT cells was observed. This could be explained by the fact that a possible dysfunction of the normal cellular metabolism of CD19-CAR-iNKT cells upon integration in the genome after the stable retroviral cannot be excluded [218]. Further, minor cytotoxicity has also been observed through the use of Retronectin® as a transduction enhancer [219]. Nevertheless, this does not seem to affect their functionality and at last, both transduced and untransduced cells showed high expansion rates. Importantly, it could be demonstrated that this protocol also allows the efficient retroviral transduction of iNKT cells.

Phenotypical characterization of untransduced and transduced iNKT cells revealed a bias towards the CD4+ subset. CD4+ iNKT cells differentiate into Th1, Th2, Th17 and Treg cells, giving them the ability to express various cytokines such as IFN-γ, IL-2 (Th1), IL-4, IL-5 (Th2), IL-17, IL-21, IL-22 (Th17), IL-21 (Tfh) and IL-10 (Treg-like) [94-96, 220]. No consistent expansion pattern could be observed for the DN subset. The expanded cells showed low CD25 expression and a memory phenotype associated with iNKT cells through the CD44 expression [221]. Importantly, low levels of exhaustion were revealed with high levels of CD28 and low expression of important exhaustion markers such as PD-1, TIM-3 and TIGIT, despite the prolonged culture time and several stimulation rounds with α-GalCer [187, 222, 223].

The functionality of CD19-CAR-iNKT cells was first assessed by flow cytometric and ImageStream analyses against ALL, BL, CD1d+ cell lines and patient blasts. Strikingly, CD19-CAR-iNKT cells were shown to be highly efficient against various target cells. Comparing their cytotoxic potential, CAR-iNKT cells seem to be as efficient as CAR-T cells generated with the same 3rd generation construct (SFG.CD19-CD28/CD137ζ) against lymphoma cells [224]. Another study showed that 2nd generation CD19-CAR-iNKT cells were more efficient than CD19-CAR-T cells in eradicating brain lymphoma in a systemic xenograft tumor model [173].

Regarding their duality, CD19-CAR-iNKT cells were also analyzed against modified K562 cells that were retrovirally modified to express CD19 and/or CD1d. Overall, it could be observed that the addition of α-GalCer to these assays induced higher cytotoxicity against CD1d+ cells, whereas little effect could be observed against CD1d- target cells. Similar experiments performed by Rotolo et al. showed an approximately

15% increase in the cytotoxicity of 2nd generation CD19-CAR-iNKT cells against CD19+CD1d+ and around 5% against CD1d+ K562 cells upon treatment with α-GalCer. Conversely, in the present work, this effect was shown to be more pronounced against CD1d+ cells (around 20%) than against CD19+CD1d+ (around 10%) target cells. In both studies, cytotoxicity against WT and CD19+ does not seem to be affected by α-GalCer treatment [173].

iNKT cells recognize glycolipids presented by the MHC-I-like molecule CD1d, which is constitutionally expressed by APCs [72, 73]. This interaction induces a robust cytokine release by iNKT cells, which confers immunoregulatory properties and the ability to coordinate immune responses. The release of IFN-γ, TNF-α, IL-2, IL-4, IL-17 and IL-21 has been described previously [126, 225]. Apart from their immunoregulatory properties, iNKT cells promote direct cytotoxic responses. In this context, several pathways have been described such as the Fas/FasL, TRAIL and TNF-α pathways [128, 134, 135, 226]. Moreover, the perforin/granzyme B pathways have been shown to play a major role in the cytotoxicity of iNKT cells [74, 135, 227, 228]. Analyses of the cytokine profile revealed that CD19-CAR-iNKT cells do not seem to rely only on one single mechanism of cytotoxicity. Interestingly, the release of Th1 cytokines was shown to be enhanced upon engagement of the iTCR, which could contribute to direct and indirect cytotoxicity through their immunoregulatory properties [75]. For instance, iNKT cells promote the transactivation of NK cells [229]. Interestingly, iNKT cells have been also shown to alter the macrophage phenotype in the tumor microenvironment in a GM-CSF-dependent mechanism. Courtney et al. could demonstrate that iNKT cells reprogrammed M2- (anti-inflammatory) into M1-macrophages (pro-inflammatory), modulating the tumor microenvironment for tumor control [230]. Another study using a xenogeneic murine model demonstrated the importance of cross-presentation leading to better and long-term tumor control through modulation of other cytotoxic cells [108]. Aiming at the complete elimination of lymphoma cells by CD19-CAR-iNKT cells, the co-incubation time was increased to 24h. Nevertheless, no objective enhancement of the cytotoxicity of the effector cells was observed. However, PD-1 expression on CD19-CAR-iNKT cells was significantly increased upon CAR engagement. PD-1 has been extensively studied in the context of T-cell exhaustion and immunotherapies since its expression correlates with poor therapeutic responses. Nevertheless, this parameter should be used with parsimony. Although it correlates with certain phases of the exhaustion process, PD-1 expression is also increased shortly after T-cell activation and plays an important role in controlling exaggerated T-cell responses. [189, 190, 231]. Indeed, T-cell exhaustion is a much broader concept and cannot be solely characterized by the expression of a single marker. The evaluation of other parameters such as the expression of other checkpoint inhibitors (TIM-3, TIGIT, etc.) and transcription factors (TOX, Eomes, T-bet) is crucial to determine the exhaustion stage of a particular cell [190]. Importantly, other factors such as deficient cytokine expression and cytotoxicity may offer a better overview of the T-cell functionality [232]. Nevertheless, these preliminary data would still suggest that CD19-CAR-iNKT cells could be potentially following an exhaustion pathway. To date, very few studies have focused on the overall functionality of CD19-CAR-iNKT cells and no study at all focused on their fitness after CAR engagement. Thereby, this work presents the first data about the functionality of CD19-CAR-iNKT cells upon encounter with target cells expressing PD-1 ligands.

In this sense, the first goal of this experimental section was to study the influence of PD-1:PD-L1 interactions on CD19-CAR-iNKT-cell function. For that, Raji cells were genetically modified to overexpress the PD-1 ligands, PD-L1 and PD-L2. Challenging CD19-CAR-iNKT cells with these modified cells revealed that the PD-1:PD-L1/2 interaction seems to have a negative effect on the CD19-CAR-iNKT-cell cytotoxicity. In particular, PD-L1+ targets were less susceptible to CD19-CAR-iNKT cells. This effect was even more evident in multiplex assays, which revealed a significant decrease of several cytokines and granzyme B. These assays confirmed the trend observed in the cytotoxicity of CD19-CAR-iNKT cells after repetitive antigen encounters. The cytokine and effector molecule release were significantly impaired even after the first stimulation. Interestingly, these results are similar to those observed by Blaeschke et al. for CD19 and CD22-CAR-T cells and demonstrate that challenge with PD-L1+ target cells leads to impaired functionality which is not exclusive to iNKT cells [233]. Other studies on T cells also confirm these observations [234, 235].

Indeed, a convincing body of evidence has demonstrated the importance of the PD-1:PD-L1/2 axis for hematological malignancies. For instance, a study analyzed the BM aspirates of 107 patients with AML for the expression of usual exhaustion markers on AML blasts. Interestingly, PD-1+ CD8+ T cells were more present in BM samples of patients who had multiple relapses. Further, PD-L1 expression was found to be more frequent in TP53-mutated AML cells [236]. Another study analyzed the samples of 120 AML patients through RT-qPCR for PD-L1 expression. Similarly, higher PD-L1 expression on AML cells was shown to be associated with poorer response to treatment [237]. Also, murine CML was shown to express PD-L1. Additionally, PD-1 expression was increased on cytotoxic T lymphocytes in the same model, maintaining limited cytotoxicity and impaired cytokine release and expansion upon antigen encounter [238].

Altogether, these data suggest that the blockade of such interactions could be beneficial and improve the outcomes of the therapy. In this context, the use of antibodies such as nivolumab and pembrolizumab (both humanized anti-PD-1 IgG4 mAb) has achieved considerable clinical responses. Kadia et al. proposed the use of nivolumab as a maintenance agent against high-risk AML. Strikingly, the estimated OS at 12 and 18 months was 86% and 67% respectively. Importantly, the therapy was overall well-tolerated [239]. A multicenter phase II trial assessed the efficacy and safety of pembrolizumab after high-dose cytarabine in patients with relapsed and refractory AML. This approach was well-tolerated and an overall response rate of 46% and median OS of 11.1 months were observed [240]. Yet, this strategy must be considered with care in the case of allogeneic HSCT. Early data from a multicenter phase I study revealed that the use of ipilimumab after allogeneic HSCT was associated with severe immune-mediated adverse events and GvHD [241]. These effects were also observed in other clinical studies using nivolumab against hematological cancers [168, 169].

Considering these data and the influence of the PD-1:PD-L1/2 axis on CD19-CAR-iNKT cells, the next experiments focused on the effects of checkpoint inhibition on the function of CD19-CAR-iNKT cells. Checkpoint inhibitor application together with iNKT cells has already been described and showed promising results [187, 223]. However, the combination of CD19-CAR-iNKT cells and checkpoint inhibition has not been evaluated so far.

PD-1 checkpoint inhibition with nivolumab did not affect the short-term cytotoxicity of CD19-CAR-iNKT cells against modified Raji cells. However, the cytokine production of several cytokines and granzyme B was greatly enhanced upon checkpoint inhibition. No improvement of short-term cytolytic function but enhancement of cytokine release by CD19-CAR-T cells was also observed in another recent study: Here, the CAR was designed to co-express a PD-1/CD28 fusion protein, which converted the inhibitory effects of the PD-1 engagement into positive signals [233]. In the present analysis, only minor improvements could be observed in repetitive encounter assays. The same could be observed in the aforementioned study of Blaeschke et al. [233]. However, they also showed that cytotoxicity could be greatly improved by blockade of the PD-1 pathway after four restimulation rounds, suggesting that further improvements in the experimental setup may be necessary. Another study using CAR-T cells demonstrated that PD-1 checkpoint inhibition through PD-1 blocking antibodies results in increased cytotoxicity, cytokine production and proliferation of CAR-T cells directed against mesothelioma [163]. Likewise, proliferation assays revealed a significantly improved proliferation rate of effector cells treated with nivolumab.

CAR-bearing cells and conventional T cells share the same mechanisms for cell death induction [242]. In this context, both mediate their cytolytic function mostly through the perforin/granzyme pathway [242, 243]. Thereby, the effector cells release perforin into the immunological synapsis, which generates pores in the cell membranes and allows the entrance of granzymes into the cells. Once in the cytoplasm, granzymes induce cell apoptosis in a caspase-dependent process [244, 245]. In both short and long-term assays, no difference in perforin release was noted. This could explain, why no improved cytotoxicity was observed even upon a significant increase of granzyme B by cells treated with nivolumab. Interestingly, granzyme B quantification has been evaluated as an important marker to determine the efficacy of early T-cell responses after PD-1 checkpoint inhibition and correlates positively with clinical responses [246, 247]. This might be due to their ability of cleaving elements of the extracellular matrix and consequently improve the interaction between T and target cells [248, 249]. PD-1 checkpoint inhibition also enhanced the cytokine expression considerably. Mechanistically, cytokines have also been held responsible for the anti-tumoral properties of CAR-T cells through IFN-γ-mediated stromal targeting which may be extrapolated to CAR-iNKT cells [250]. As for untransduced iNKT cells, the increase in cytokine release could be associated with the recruitment of other effector cells and the promotion of further tumor control. This question could not be addressed within the scope of this work since purified effector cells were analyzed.

Finally, CD19-CAR-iNKT cells were tested for their ability to prevent alloreactive T-cell responses. Despite small changes in the protocol for the expansion of iNKT cells, these were still able to promote DC apoptosis and prevent T-cell activation and proliferation.

Importantly, checkpoint inhibition did not impair these immunoregulatory properties of iNKT cells or CD19-CAR-iNKT cells. In contrast to adoptively transferred (CAR)-T cells, CAR-iNKT cells may also prevent GvHD and decrease therapy-related mortality with lower relapse rates.

Altogether, this work shows the potential of CD19-CAR-iNKT cells against CD19+ malignancies as a promising alternative to CAR-T cells in the context of allogeneic HSCT, which could be used as an off-the-shelf immunotherapeutic approach.

.

6 Conclusions and perspectives

Adoptive transfer of iNKT cells and administration of iNKT-cell stimulators have shown efficacy and safety in clinical trials, demonstrating their potential as a therapeutic tool in the context of allogeneic HSCT and for tumor therapy [136, 137]. In contrast to data obtained in murine systems, only a faint correlation between the expansion of regulatory T cells and iNKT cells has been established in humans [119]. In this work, a novel mechanism by which *ex vivo* expanded human iNKT cells promote immune tolerance *in vitro* is proposed. iNKT cells promote selective apoptosis of cDC and thereby iNKT cells prevent activation and proliferation of allo-reactive T cells. Meanwhile, other DC subsets are spared and may further contribute to beneficial immune responses. These data contribute to the current knowledge of iNKT-cell biology and the feasibility of their use as an immunotherapeutic tool.

An important challenge in this context is the implementation of allogeneic iNKT-cell-based therapies in a GMP environment. Considering that iNKT cells are a rare cell type and that patients who underwent multiple treatments might not possess the most suitable cells for further cellular therapies, using third-party iNKT cells might be an attractive alternative. Nevertheless, GMP-grade reagents for their expansion and purification lack. However, it has been demonstrated that low doses of iNKT cells can already be beneficial against GvHD. Therefore, an alternative could be the administration of a product that is only partially composed of iNKT cells, which should be enough to prevent harmful alloreactive immune responses. Jahnke et al. showed that iNKT cells present in DLI could be expanded *ex vivo* and still promote responses in a CD1d-dependent manner [127]. Therefore, the tailored expansion of iNKT cells in common cell products could already lead to an improvement in the therapy.

The second part of this work focused on the generation and analysis of CAR-iNKT cells against CD19+ malignancies. 3rd generation CD19-CAR-iNKT cells bearing costimulatory domains derived from CD28 and 4-1BB sequences were tested for the first time. These cells showed potent cytotoxicity against ALL, BL and CD1d+ cell lines as well as patient blasts. PD-1 checkpoint inhibition in combination with CAR-iNKT cells was also assessed. Indeed, engagement of the CAR by PD-L1/2+ lymphoma cells decreased their cytotoxicity and diminished the release of cytokines and effector molecules. This could be partially reversed by PD-1 checkpoint inhibition.

Altogether, this work reinforces a novel mechanism of GvHD prevention through iNKT cells and highlights iNKT cells as an interesting alternative to T cells for CAR-based therapies. Bearing CAR receptors, allogeneic iNKT cells could be successfully applied as an off-the-shelf alternative to CAR-T cells without the drawback of having a receptor that might elicit allo-reactions but prevent GvHD. Given the current limitations of bringing CD19-CAR-iNKT cells into a clinical trial, the use of expanded but not purified CD19-CAR-iNKT cells would still be feasible due to their preserved CD1d restriction. This concept is presented in figure 35. Importantly, this work also suggests that even upon checkpoint inhibition, CD19-CAR-iNKT cells might still be able to control alloreactive T cells and prevent GvHD.

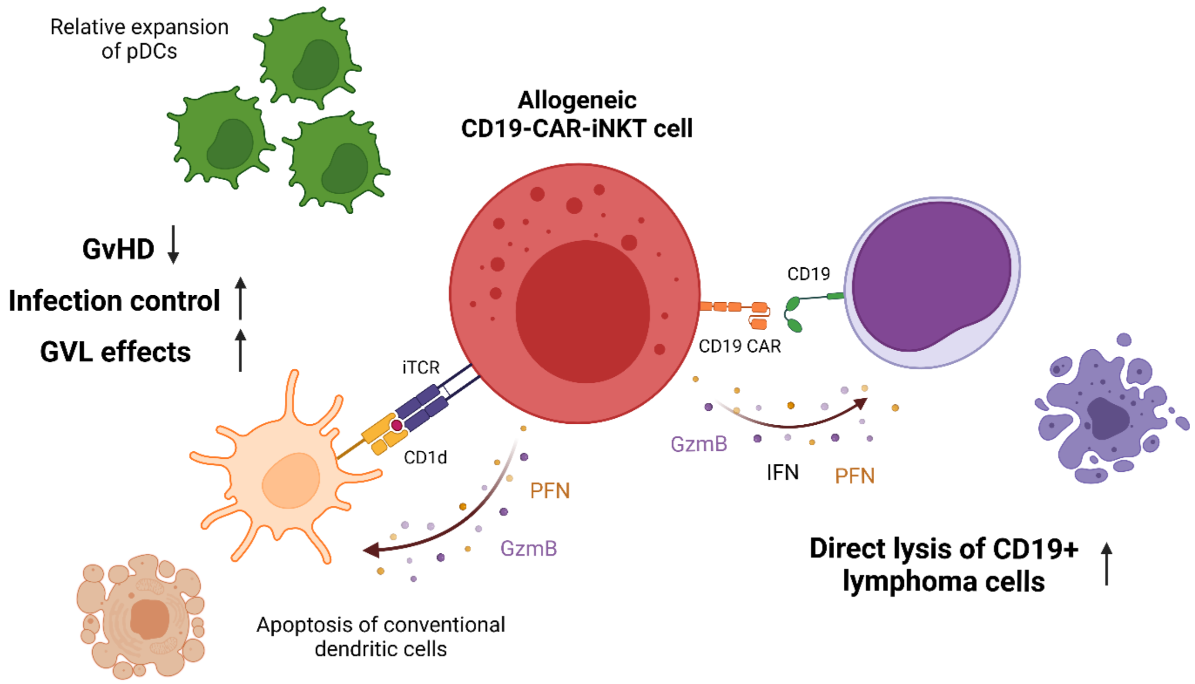

Figure 35: Schematic representation of the multifunctionality of iNKT cells for both immune tolerance and tumor control

CAR-iNKT cells (for example, against CD19) have a dual effect that could be of relevance in clinical settings. Besides exerting efficient direct tumor control by the fast release of cytolytic molecules, CAR-iNKT cells might also use their immunoregulatory properties for tolerance induction. In this context, CAR-iNKT cells still enable control of T-cell function through specific DC subsets. On the other side, they could further enhance tumor control by stimulating other effector cells (indirect activation, not shown). Figure generated with Biorender®.

7 References

[1]. Copelan EA. Hematopoietic stem-cell transplantation. N Engl J Med. 2006;354(17):1813-26.

[2]. Hatzimichael E, Tuthill M. Hematopoietic stem cell transplantation. Stem Cells Cloning. 2010;3:105-17.

[3]. Niederwieser D, Baldomero H, Atsuta Y, Aljurf M, Seber A, Greinix HT, et al. One and Half Million Hematopoietic Stem Cell Transplants (HSCT). Dissemination, Trends and Potential to Improve Activity By Telemedicine from the Worldwide Network for Blood and Marrow Transplantation (WBMT). Blood. 2019;134.

[4]. Kröger N, Fleischhauer, K., Hanke, F., Mannes, S., Neidlinger, H., Schuh, C., Flossdorf, S., Beier, R., Sykora, K.-L., Mischke, K., Türüchanow, I., Zimmermann, M. Jahresbericht 2021. DRST Deutsches Register für Stammzelltransplantationen e. V.; 2022.

[5]. Lennard AL, Jackson GH. Stem cell transplantation. BMJ. 2000;321(7258):433-7.

[6]. Klein J, Sato A. The HLA system. First of two parts. N Engl J Med. 2000;343(10):702-9.

[7]. Neefjes J, Jongsma ML, Paul P, Bakke O. Towards a systems understanding of MHC class I and MHC class II antigen presentation. Nat Rev Immunol. 2011;11(12):823-36.

[8]. Ferrara JLM, Levine JE, Reddy P, Holler E. Graft-versus-host disease. The Lancet. 2009;373(9674):1550-61.

[9]. Petersdorf EW, Longton GM, Anasetti C, Martin PJ, Mickelson EM, Smith AG, et al. The significance of HLA-DRB1 matching on clinical outcome after HLA-A, B, DR identical unrelated donor marrow transplantation. Blood. 1995;86(4):1606-13.

[10]. Granot N, Storb R. History of hematopoietic cell transplantation: challenges and progress. Haematologica. 2020;105(12):2716-29.

[11]. van den Brink MR, Porter DL, Giralt S, Lu SX, Jenq RR, Hanash A, et al. Relapse after allogeneic hematopoietic cell therapy. Biol Blood Marrow Transplant. 2010;16(1 Suppl):S138-45.

[12]. Luznik L, Jones RJ, Fuchs EJ. High-dose cyclophosphamide for graft-versus-host disease prevention. Curr Opin Hematol. 2010;17(6):493-9.

[13]. Sorror ML, Leisenring W, Deeg HJ, Martin PJ, Storb R. Twenty-year follow-up of a controlled trial comparing a combination of methotrexate plus cyclosporine with cyclosporine alone for prophylaxis of graft-versus-host disease in patients administered HLA-identical marrow grafts for leukemia. Biol Blood Marrow Transplant. 2005;11(10):814-5.

[14]. Storb R, Deeg HJ, Whitehead J, Appelbaum F, Beatty P, Bensinger W, et al. Methotrexate and cyclosporine compared with cyclosporine alone for prophylaxis of acute graft versus host disease after marrow transplantation for leukemia. N Engl J Med. 1986;314(12):729-35.

[15]. Horowitz MM, Gale RP, Sondel PM, Goldman JM, Kersey J, Kolb HJ, et al. Graft-versus-leukemia reactions after bone marrow transplantation. Blood. 1990;75(3):555-62.

[16]. Jamil MO, Mineishi S. State-of-the-art acute and chronic GVHD treatment. Int J Hematol. 2015;101(5):452-66.

[17]. Atkinson K, Horowitz MM, Gale RP, van Bekkum DW, Gluckman E, Good RA, et al. Risk factors for chronic graft-versus-host disease after HLA-identical sibling bone marrow transplantation. Blood. 1990;75(12):2459-64.

[18]. Shlomchik WD. Graft-versus-host disease. Nat Rev Immunol. 2007;7(5):340-52.

[19]. Xun CQ, Thompson JS, Jennings CD, Brown SA, Widmer MB. Effect of total body irradiation, busulfan-cyclophosphamide, or cyclophosphamide conditioning on inflammatory cytokine release and development of acute and chronic graft-versus-host disease in H-2-incompatible transplanted SCID mice. Blood. 1994;83(8):2360-7.

[20]. Hill GR, Crawford JM, Cooke KR, Brinson YS, Pan L, Ferrara JL. Total body irradiation and acute graft-versus-host disease: the role of gastrointestinal damage and inflammatory cytokines. Blood. 1997;90(8):3204-13.

[21]. Rus V, Svetic A, Nguyen P, Gause WC, Via CS. Kinetics of Th1 and Th2 cytokine production during the early course of acute and chronic murine graft-versus-host disease. Regulatory role of donor CD8+ T cells. J Immunol. 1995;155(5):2396-406.

[22]. Nikolic B, Lee S, Bronson RT, Grusby MJ, Sykes M. Th1 and Th2 mediate acute graft-versus-host disease, each with distinct end-organ targets. J Clin Invest. 2000;105(9):1289-98.

[23]. Hill GR, Ferrara JLM. The primacy of the gastrointestinal tract as a target organ of acute graft-versus-host disease: rationale for the use of cytokine shields in allogeneic bone marrow transplantation. Blood. 2000;95(9):2754-9.

[24]. Braun MY, Lowin B, French L, Acha-Orbea H, Tschopp J. Cytotoxic T cells deficient in both functional fas ligand and perforin show residual cytolytic activity yet lose their capacity to induce lethal acute graft-versus-host disease. J Exp Med. 1996;183(2):657-61.

[25]. Dzierzak-Mietla M, Markiewicz M, Siekiera U, Mizia S, Koclega A, Zielinska P, et al. Occurrence and Impact of Minor Histocompatibility Antigens' Disparities on Outcomes of Hematopoietic Stem Cell Transplantation from HLA-Matched Sibling Donors. Bone Marrow Res. 2012;2012:257086.

[26]. Falkenburg JHF, van de Corput L, Marijt EWA, Willemze R. Minor histocompatibility antigens in human stem cell transplantation. Experimental Hematology. 2003;31(9):743-51.

[27]. Koyama M, Hill GR. Alloantigen presentation and graft-versus-host disease: fuel for the fire. Blood. 2016;127(24):2963-70.

[28]. Cooke KR, Luznik L, Sarantopoulos S, Hakim FT, Jagasia M, Fowler DH, et al. The Biology of Chronic Graft-versus-Host Disease: A Task Force Report from the National Institutes of Health Consensus Development Project on Criteria for Clinical Trials in Chronic Graft-versus-Host Disease. Biol Blood Marrow Transplant. 2017;23(2):211-34.

[29]. She K, Gilman AL, Aslanian S, Shimizu H, Krailo M, Chen Z, et al. Altered Toll-like receptor 9 responses in circulating B cells at the onset of extensive chronic graft-versus-host disease. Biol Blood Marrow Transplant. 2007;13(4):386-97.

[30]. Amarnath S, Flomerfelt FA, Costanzo CM, Foley JE, Mariotti J, Konecki DM, et al. Rapamycin generates anti-apoptotic human Th1/Tc1 cells via autophagy for induction of xenogeneic GVHD. Autophagy. 2010;6(4):523-41.

[31]. Bouazzaoui A, Spacenko E, Mueller G, Miklos S, Huber E, Holler E, et al. Chemokine and chemokine receptor expression analysis in target organs of acute graft-versus-host disease. Genes Immun. 2009;10(8):687-701.

[32]. Acosta-Rodriguez EV, Napolitani G, Lanzavecchia A, Sallusto F. Interleukins 1beta and 6 but not transforming growth factor-beta are essential for the differentiation of interleukin 17-producing human T helper cells. Nat Immunol. 2007;8(9):942-9.

[33]. Bettelli E, Carrier Y, Gao W, Korn T, Strom TB, Oukka M, et al. Reciprocal developmental pathways for the generation of pathogenic effector TH17 and regulatory T cells. Nature. 2006;441(7090):235-8.

[34]. Krenger W, Hollander GA. The thymus in GVHD pathophysiology. Best Pract Res Clin Haematol. 2008;21(2):119-28.

[35]. Fukushi N, Arase H, Wang B, Ogasawara K, Gotohda T, Good RA, et al. Thymus: a direct target tissue in graft-versus-host reaction after allogeneic bone marrow transplantation that results in abrogation of induction of self-tolerance. Proc Natl Acad Sci U S A. 1990;87(16):6301-5.

[36]. Weinberg K, Blazar BR, Wagner JE, Agura E, Hill BJ, Smogorzewska M, et al. Factors affecting thymic function after allogeneic hematopoietic stem cell transplantation. Blood. 2001;97(5):1458-66.

[37]. Wu T, Young JS, Johnston H, Ni X, Deng R, Racine J, et al. Thymic damage, impaired negative selection, and development of chronic graft-versus-host disease caused by donor CD4+ and CD8+ T cells. J Immunol. 2013;191(1):488-99.

[38]. Zhang Y, Hexner E, Frank D, Emerson SG. CD4+ T cells generated de novo from donor hemopoietic stem cells mediate the evolution from acute to chronic graft-versus-host disease. J Immunol. 2007;179(5):3305-14.

[39]. Fujii H, Cuvelier G, She K, Aslanian S, Shimizu H, Kariminia A, et al. Biomarkers in newly diagnosed pediatric-extensive chronic graft-versus-host disease: a report from the Children's Oncology Group. Blood. 2008;111(6):3276-85.

[40]. Miklos DB, Kim HT, Miller KH, Guo L, Zorn E, Lee SJ, et al. Antibody responses to H-Y minor histocompatibility antigens correlate with chronic graft-versus-host disease and disease remission. Blood. 2005;105(7):2973-8.

[41]. Nakasone H, Tian L, Sahaf B, Kawase T, Schoenrock K, Perloff S, et al. Allogeneic HY antibodies detected 3 months after female-to-male HCT predict chronic GVHD and nonrelapse mortality in humans. Blood. 2015;125(20):3193-201.

[42]. Srinivasan M, Flynn R, Price A, Ranger A, Browning JL, Taylor PA, et al. Donor B-cell alloantibody deposition and germinal center formation are required for the development of murine chronic GVHD and bronchiolitis obliterans. Blood. 2012;119(6):1570-80.

[43]. Wynn TA, Ramalingam TR. Mechanisms of fibrosis: therapeutic translation for fibrotic disease. Nat Med. 2012;18(7):1028-40.

[44]. Filipovich AH, Weisdorf D, Pavletic S, Socie G, Wingard JR, Lee SJ, et al. National Institutes of Health consensus development project on criteria for clinical trials in chronic graft-versus-host disease: I. Diagnosis and staging working group report. Biol Blood Marrow Transplant. 2005;11(12):945-56.

[45]. Martin PJ, Schoch G, Fisher L, Byers V, Anasetti C, Appelbaum FR, et al. A retrospective analysis of therapy for acute graft-versus-host disease: initial treatment. Blood. 1990;76(8):1464-72.

[46]. Gratwohl A, Hermans J, Apperley J, Arcese W, Bacigalupo A, Bandini G, et al. Acute graft-versus-host disease: grade and outcome in patients with chronic myelogenous leukemia. Working Party Chronic Leukemia of the European Group for Blood and Marrow Transplantation. Blood. 1995;86(2):813-8.

[47]. Greinix HT, Eikema DJ, Koster L, Penack O, Yakoub-Agha I, Montoto S, et al. Incidence of Acute Graft-Versus-Host Disease and Survival after Allogeneic Hematopoietic Cell Transplantation over Time: A Study from the Transplant Complications and Chronic Malignancies Working Party of the EBMT. Blood. 2018;132.

[48]. MacMillan ML, Weisdorf DJ, Wagner JE, DeFor TE, Burns LJ, Ramsay NK, et al. Response of 443 patients to steroids as primary therapy for acute graft-versus-host disease: comparison of grading systems. Biol Blood Marrow Transplant. 2002;8(7):387-94.

[49]. Cragg L, Blazar BR, Defor T, Kolatker N, Miller W, Kersey J, et al. A randomized trial comparing prednisone with antithymocyte globulin/prednisone as an initial systemic therapy for moderately severe acute graft-versus-host disease. Biology of Blood and Marrow Transplantation. 2000;6(4):441-7.

[50]. Arai S, Margolis J, Zahurak M, Anders V, Vogelsang GB. Poor outcome in steroid-refractory graft-versus-host disease with antithymocyte globulin treatment. Biol Blood Marrow Transplant. 2002;8(3):155-60.

[51]. MacMillan ML, Weisdorf DJ, Davies SM, DeFor TE, Burns LJ, Ramsay NK, et al. Early antithymocyte globulin therapy improves survival in patients with steroid-resistant acute graft-versus-host disease. Biol Blood Marrow Transplant. 2002;8(1):40-6.

[52]. Barr ML, Meiser BM, Eisen HJ, Roberts RF, Livi U, Dall'Amico R, et al. Photopheresis for the prevention of rejection in cardiac transplantation. Photopheresis Transplantation Study Group. N Engl J Med. 1998;339(24):1744-51.

[53]. Greinix HT, Knobler RM, Worel N, Schneider B, Schneeberger A, Hoecker P, et al. The effect of intensified extracorporeal photochemotherapy on long-term survival in patients with severe acute graft-versus-host disease. Haematologica. 2006;91(3):405-8.

[54]. Busca A, Locatelli F, Marmont F, Ceretto C, Falda M. Recombinant human soluble tumor necrosis factor receptor fusion protein as treatment for steroid refractory graft-versus-host disease following allogeneic hematopoietic stem cell transplantation. Am J Hematol. 2007;82(1):45-52.

[55]. Zeiser R, von Bubnoff N, Butler J, Mohty M, Niederwieser D, Or R, et al. Ruxolitinib for Glucocorticoid-Refractory Acute Graft-versus-Host Disease. N Engl J Med. 2020;382(19):1800-10.

[56]. Gomez-Almaguer D, Ruiz-Arguelles GJ, del Carmen Tarin-Arzaga L, Gonzalez-Llano O, Gutierrez-Aguirre H, Cantu-Rodriguez O, et al. Alemtuzumab for the treatment of steroid-refractory acute graft-versus-host disease. Biol Blood Marrow Transplant. 2008;14(1):10-5.

[57]. Bordigoni P, Dimicoli S, Clement L, Baumann C, Salmon A, Witz F, et al. Daclizumab, an efficient treatment for steroid-refractory acute graft-versus-host disease. Br J Haematol. 2006;135(3):382-5.

[58]. Wolff D, Ayuk F, Elmaagacli A, Bertz H, Lawitschka A, Schleuning M, et al. Current practice in diagnosis and treatment of acute graft-versus-host disease: results from a survey among German-Austrian-Swiss hematopoietic stem cell transplant centers. Biol Blood Marrow Transplant. 2013;19(5):767-76.

[59]. Zeiser R, Wolff, D., Scheid, C., Luft, T., Greinix, H., Dreger, P., Finke, J., Holler, E., Halter, J. Graft-versus-Host Erkrankung, akut. In: e.V. DDGfHuMO, editor. https://www.onkopedia.com/de2022.

[60]. Lee SJ, Klein JP, Barrett AJ, Ringden O, Antin JH, Cahn JY, et al. Severity of chronic graft-versus-host disease: association with treatment-related mortality and relapse. Blood. 2002;100(2):406-14.

[61]. Wolff D, Gerbitz A, Ayuk F, Kiani A, Hildebrandt GC, Vogelsang GB, et al. Consensus conference on clinical practice in chronic graft-versus-host disease (GVHD): first-line and topical treatment of chronic GVHD. Biol Blood Marrow Transplant. 2010;16(12):1611-28.

[62]. Johnston HF, Xu Y, Racine JJ, Cassady K, Ni X, Wu T, et al. Administration of anti-CD20 mAb is highly effective in preventing but ineffective in treating chronic graft-versus-host disease while preserving strong graft-versus-leukemia effects. Biol Blood Marrow Transplant. 2014;20(8):1089-103.

[63]. Allen JL, Tata PV, Fore MS, Wooten J, Rudra S, Deal AM, et al. Increased BCR responsiveness in B cells from patients with chronic GVHD. Blood. 2014;123(13):2108-15.

[64]. Cutler C, Miklos D, Kim HT, Treister N, Woo SB, Bienfang D, et al. Rituximab for steroid-refractory chronic graft-versus-host disease. Blood. 2006;108(2):756-62.

[65]. Schneidawind D, Pierini A, Alvarez M, Pan Y, Baker J, Buechele C, et al. CD4+ invariant natural killer T cells protect from murine GVHD lethality through expansion of donor CD4+CD25+FoxP3+ regulatory T cells. Blood. 2014;124(22):3320-8.

[66]. Schneidawind D, Pierini A, Negrin RS. Regulatory T cells and natural killer T cells for modulation of GVHD following allogeneic hematopoietic cell transplantation. Blood. 2013;122(18):3116-21.

[67]. Rezvani K, Mielke S, Ahmadzadeh M, Kilical Y, Savani BN, Zeilah J, et al. High donor FOXP3-positive regulatory T-cell (Treg) content is associated with a low risk of GVHD following HLA-matched allogeneic SCT. Blood. 2006;108(4):1291-7.

[68]. Zeiser R, Wolff, D., Scheid, C., Luft, T., Greinix, H., Dreger, P., Finke, J., Holler, E., Halter, J. Graft-versus-Host Erkrankung, chronisch. In: e.V. DDGfHuMO, editor. https://www.onkopedia.com/de2022.

[69]. Finke J, Bethge WA, Schmoor C, Ottinger HD, Stelljes M, Zander AR, et al. Standard graft-versus-host disease prophylaxis with or without anti-T-cell

globulin in haematopoietic cell transplantation from matched unrelated donors: a randomised, open-label, multicentre phase 3 trial. The Lancet Oncology. 2009;10(9):855-64.

[70]. Lantz OB, Albert An Invariant T Cell Receptor α Chain Is Used by a Unique Subset of Major Histocompatibility Complex Class I-specific CD4 + and CD4-8- T Cells in Mice and Humans. The Journal of Experimental Medicine. 1994;180.

[71]. Bendelac A. Positive Selection of Mouse NK1+ T Cells by C131-expressing Cortical Thymocytes. J Exp Med. 1995.

[72]. Exley M, Garcia J, Balk SP, Porcelli S. Requirements for CD1d recognition by human invariant Valpha24+ CD4-CD8- T cells. J Exp Med. 1997;186(1):109-20.

[73]. Bendelac A, Lantz O, Quimby ME, Yewdell JW, Bennink JR, Brutkiewicz RR. CD1 recognition by mouse NK1+ T lymphocytes. Science. 1995;268(5212):863-5.

[74]. Nicol A, Nieda M, Koezuka Y, Porcelli S, Suzuki K, Tadokoro K, et al. Human invariant valpha24+ natural killer T cells activated by alpha-galactosylceramide (KRN7000) have cytotoxic anti-tumour activity through mechanisms distinct from T cells and natural killer cells. Immunology. 2000;99(2):229-34.

[75]. Metelitsa LS, Naidenko OV, Kant A, Wu HW, Loza MJ, Perussia B, et al. Human NKT cells mediate antitumor cytotoxicity directly by recognizing target cell CD1d with bound ligand or indirectly by producing IL-2 to activate NK cells. J Immunol. 2001;167(6):3114-22.

[76]. Matsuda JL, Naidenko OV, Gapin L, Nakayama T, Taniguchi M, Wang CR, et al. Tracking the response of natural killer T cells to a glycolipid antigen using CD1d tetramers. J Exp Med. 2000;192(5):741-54.

[77]. Coquet JM, Kyparissoudis K, Pellicci DG, Besra G, Berzins SP, Smyth MJ, et al. IL-21 is produced by NKT cells and modulates NKT cell activation and cytokine production. J Immunol. 2007;178(5):2827-34.

[78]. Krijgsman D, Hokland M, Kuppen PJK. The Role of Natural Killer T Cells in Cancer-A Phenotypical and Functional Approach. Front Immunol. 2018;9:367.

[79]. Benlagha K, Wei DG, Veiga J, Teyton L, Bendelac A. Characterization of the early stages of thymic NKT cell development. J Exp Med. 2005;202(4):485-92.

[80]. Egawa T, Eberl G, Taniuchi I, Benlagha K, Geissmann F, Hennighausen L, et al. Genetic evidence supporting selection of the Valpha14i NKT cell lineage from double-positive thymocyte precursors. Immunity. 2005;22(6):705-16.

[81]. Koseki H, Imai K, Nakayama F, Sado T, Moriwaki K, Taniguchi M. Homogenous junctional sequence of the V14+ T-cell antigen receptor alpha chain expanded in unprimed mice. Proc Natl Acad Sci U S A. 1990;87(14):5248-52.

[82]. Porcelli S, Gerdes D, Fertig AM, Balk SP. Human T cells expressing an invariant V alpha 24-J alpha Q TCR alpha are CD4- and heterogeneous with respect to TCR beta expression. Hum Immunol. 1996;48(1-2):63-7.

[83]. Bezbradica JS, Hill T, Stanic AK, Van Kaer L, Joyce S. Commitment toward the natural T (iNKT) cell lineage occurs at the CD4+8+ stage of thymic ontogeny. Proc Natl Acad Sci U S A. 2005;102(14):5114-9.

[84]. Schumann J, Mycko MP, Dellabona P, Casorati G, MacDonald HR. Cutting edge: influence of the TCR Vbeta domain on the selection of semi-invariant NKT cells by endogenous ligands. J Immunol. 2006;176(4):2064-8.

[85]. Skold M, Faizunnessa NN, Wang CR, Cardell S. CD1d-specific NK1.1+ T cells with a transgenic variant TCR. J Immunol. 2000;165(1):168-74.

[86]. Wei DG, Lee H, Park SH, Beaudoin L, Teyton L, Lehuen A, et al. Expansion and long-range differentiation of the NKT cell lineage in mice expressing CD1d exclusively on cortical thymocytes. J Exp Med. 2005;202(2):239-48.

[87]. Gumperz JE, Miyake S, Yamamura T, Brenner MB. Functionally distinct subsets of CD1d-restricted natural killer T cells revealed by CD1d tetramer staining. J Exp Med. 2002;195(5):625-36.

[88]. Benlagha K, Kyin T, Beavis A, Teyton L, Bendelac A. A thymic precursor to the NK T cell lineage. Science. 2002;296(5567):553-5.

[89]. Godfrey DI, MacDonald HR, Kronenberg M, Smyth MJ, Van Kaer L. NKT cells: what's in a name? Nat Rev Immunol. 2004;4(3):231-7.

[90]. Kawano T, Cui J, Koezuka Y, Toura I, Kaneko Y, Motoki K, et al. CD1d-restricted and TCR-mediated activation of valpha14 NKT cells by glycosylceramides. Science. 1997;278(5343):1626-9.

[91]. Arrenberg P, Halder R, Dai Y, Maricic I, Kumar V. Oligoclonality and innate-like features in the TCR repertoire of type II NKT cells reactive to a beta-linked self-glycolipid. Proc Natl Acad Sci U S A. 2010;107(24):10984-9.

[92]. Blomqvist M, Rhost S, Teneberg S, Löfbom L, Østerbye T, Brigl M, et al. Multiple tissue-specific isoforms of sulfatide activate CD1d-restricted type II NKT cells. Eur J Immunol. 2009;39(7):1726-35.

[93]. Lee PT, Benlagha K, Teyton L, Bendelac A. Distinct functional lineages of human V(alpha)24 natural killer T cells. J Exp Med. 2002;195(5):637-41.

[94]. Moreira-Teixeira L, Resende M, Coffre M, Devergne O, Herbeuval JP, Hermine O, et al. Proinflammatory environment dictates the IL-17-producing capacity of human invariant NKT cells. J Immunol. 2011;186(10):5758-65.

[95]. Moreira-Teixeira L, Resende M, Devergne O, Herbeuval JP, Hermine O, Schneider E, et al. Rapamycin combined with TGF-beta converts human invariant NKT cells into suppressive Foxp3+ regulatory cells. J Immunol. 2012;188(2):624-31.

[96]. Chang PP, Barral P, Fitch J, Pratama A, Ma CS, Kallies A, et al. Identification of Bcl-6-dependent follicular helper NKT cells that provide cognate help for B cell responses. Nat Immunol. 2011;13(1):35-43.

[97]. Jahng A, Maricic I, Aguilera C, Cardell S, Halder RC, Kumar V. Prevention of autoimmunity by targeting a distinct, noninvariant CD1d-reactive T cell population reactive to sulfatide. J Exp Med. 2004;199(7):947-57.

[98]. Zhao J, Weng X, Bagchi S, Wang CR. Polyclonal type II natural killer T cells require PLZF and SAP for their development and contribute to CpG-mediated antitumor response. Proc Natl Acad Sci U S A. 2014;111(7):2674-9.

[99]. Brigl M, Tatituri RV, Watts GF, Bhowruth V, Leadbetter EA, Barton N, et al. Innate and cytokine-driven signals, rather than microbial antigens, dominate in natural killer T cell activation during microbial infection. J Exp Med. 2011;208(6):1163-77.

[100]. De Santo C, Salio M, Masri SH, Lee LY, Dong T, Speak AO, et al. Invariant NKT cells reduce the immunosuppressive activity of influenza A virus-induced myeloid-derived suppressor cells in mice and humans. J Clin Invest. 2008;118(12):4036-48.

[101]. Mallevaey T, Zanetta JP, Faveeuw C, Fontaine J, Maes E, Platt F, et al. Activation of invariant NKT cells by the helminth parasite schistosoma mansoni. J Immunol. 2006;176(4):2476-85.

[102]. Paget C, Mallevaey T, Speak AO, Torres D, Fontaine J, Sheehan KC, et al. Activation of invariant NKT cells by toll-like receptor 9-stimulated dendritic cells requires type I interferon and charged glycosphingolipids. Immunity. 2007;27(4):597-609.

[103]. Brennan PJ, Brigl M, Brenner MB. Invariant natural killer T cells: an innate activation scheme linked to diverse effector functions. Nat Rev Immunol. 2013;13(2):101-17.

[104]. Terabe M, Matsui S, Noben-Trauth N, Chen H, Watson C, Donaldson DD, et al. NKT cell-mediated repression of tumor immunosurveillance by IL-13 and the IL-4R-STAT6 pathway. Nat Immunol. 2000;1(6):515-20.

[105]. Terabe M, Matsui S, Park J-M, Mamura M, Noben-Trauth N, Donaldson DD, et al. Transforming Growth Factor-β Production and Myeloid Cells Are an Effector Mechanism through Which CD1d-restricted T Cells Block Cytotoxic T Lymphocyte–mediated Tumor Immunosurveillance. Journal of Experimental Medicine. 2003;198(11):1741-52.

[106]. King IL, Fortier A, Tighe M, Dibble J, Watts GF, Veerapen N, et al. Invariant natural killer T cells direct B cell responses to cognate lipid antigen in an IL-21-dependent manner. Nat Immunol. 2011;13(1):44-50.

[107]. Unutmaz D, Bricard G, Venkataswamy MM, Yu KOA, Im JS, Ndonye RM, et al. α-Galactosylceramide Analogs with Weak Agonist Activity for Human iNKT Cells Define New Candidate Anti-Inflammatory Agents. PLoS ONE. 2010;5(12).

[108]. Simonetta F, Lohmeyer JK, Hirai T, Maas-Bauer K, Alvarez M, Wenokur AS, et al. Allogeneic CAR Invariant Natural Killer T Cells Exert Potent Antitumor Effects through Host CD8 T-Cell Cross-Priming. Clin Cancer Res. 2021;27(21):6054-64.

[109]. Chang YJ, Huang JR, Tsai YC, Hung JT, Wu D, Fujio M, et al. Potent immune-modulating and anticancer effects of NKT cell stimulatory glycolipids. Proc Natl Acad Sci U S A. 2007;104(25):10299-304.

[110]. Lan F, Zeng D, Higuchi M, Huie P, Higgins JP, Strober S. Predominance of NK1.1+TCR alpha beta+ or DX5+TCR alpha beta+ T cells in mice conditioned with fractionated lymphoid irradiation protects against graft-versus-host disease: "natural suppressor" cells. J Immunol. 2001;167(4):2087-96.

[111]. Lan F, Zeng D, Higuchi M, Higgins JP, Strober S. Host conditioning with total lymphoid irradiation and antithymocyte globulin prevents graft-versus-host disease: the role of CD1-reactive natural killer T cells. Biol Blood Marrow Transplant. 2003;9(6):355-63.

[112]. Pillai AB, George TI, Dutt S, Teo P, Strober S. Host NKT cells can prevent graft-versus-host disease and permit graft antitumor activity after bone marrow transplantation. J Immunol. 2007;178(10):6242-51.

[113]. Pillai AB, George TI, Dutt S, Strober S. Host natural killer T cells induce an interleukin-4-dependent expansion of donor CD4+CD25+Foxp3+ T regulatory cells that protects against graft-versus-host disease. Blood. 2009;113(18):4458-67.

[114]. Duramad O, Laysang A, Li J, Ishii Y, Namikawa R. Pharmacologic expansion of donor-derived, naturally occurring CD4(+)Foxp3(+) regulatory T cells reduces acute graft-versus-host disease lethality without abrogating the graft-versus-leukemia effect in murine models. Biol Blood Marrow Transplant. 2011;17(8):1154-68.

[115]. Schneidawind D, Baker J, Pierini A, Buechele C, Luong RH, Meyer EH, et al. Third-party CD4+ invariant natural killer T cells protect from murine GVHD lethality. Blood. 2015;125(22):3491-500.

[116]. Haraguchi K, Takahashi T, Hiruma K, Kanda Y, Tanaka Y, Ogawa S, et al. Recovery of Valpha24+ NKT cells after hematopoietic stem cell transplantation. Bone Marrow Transplant. 2004;34(7):595-602.

[117]. Chaidos A, Patterson S, Szydlo R, Chaudhry MS, Dazzi F, Kanfer E, et al. Graft invariant natural killer T-cell dose predicts risk of acute graft-versus-host disease in allogeneic hematopoietic stem cell transplantation. Blood. 2012;119(21):5030-6.

[118]. Rubio MT, Bouillie M, Bouazza N, Coman T, Trebeden-Negre H, Gomez A, et al. Pre-transplant donor CD4(-) invariant NKT cell expansion capacity predicts the occurrence of acute graft-versus-host disease. Leukemia. 2017;31(4):903-12.

[119]. Malard F, Labopin M, Chevallier P, Guillaume T, Duquesne A, Rialland F, et al. Larger number of invariant natural killer T cells in PBSC allografts correlates

with improved GVHD-free and progression-free survival. Blood. 2016;127(14):1828-35.

[120]. Kobayashi E, Motoki K, Uchida T, Fukushima H, Koezuka Y. KRN7000, a novel immunomodulator, and its antitumor activities. Oncol Res. 1995;7(10-11):529-34.

[121]. Morita M, Motoki K, Akimoto K, Natori T, Sakai T, Sawa E, et al. Structure-activity relationship of alpha-galactosylceramides against B16-bearing mice. J Med Chem. 1995;38(12):2176-87.

[122]. Motoki K, Morita M, Kobayashi E, Uchida T, Akimoto K, Fukushima H, et al. Immunostimulatory and antitumor activities of monoglycosylceramides having various sugar moieties. Biol Pharm Bull. 1995;18(11):1487-91.

[123]. Hayakawa Y, Rovero S, Forni G, Smyth MJ. Alpha-galactosylceramide (KRN7000) suppression of chemical- and oncogene-dependent carcinogenesis. Proc Natl Acad Sci U S A. 2003;100(16):9464-9.

[124]. Toura I, Kawano T, Akutsu Y, Nakayama T, Ochiai T, Taniguchi M. Cutting Edge: Inhibition of Experimental Tumor Metastasis by Dendritic Cells Pulsed with α-Galactosylceramide1. The Journal of Immunology. 1999;163(5):2387-91.

[125]. Gebremeskel S, Clattenburg DR, Slauenwhite D, Lobert L, Johnston B. Natural killer T cell activation overcomes immunosuppression to enhance clearance of postsurgical breast cancer metastasis in mice. Oncoimmunology. 2015;4(3):e995562.

[126]. Schmid H, Schneidawind C, Jahnke S, Kettemann F, Secker KA, Duerr-Stoerzer S, et al. Culture-Expanded Human Invariant Natural Killer T Cells Suppress T-Cell Alloreactivity and Eradicate Leukemia. Front Immunol. 2018;9:1817.

[127]. Jahnke S, Schmid H, Secker KA, Einhaus J, Duerr-Stoerzer S, Keppeler H, et al. Invariant NKT Cells From Donor Lymphocyte Infusions (DLI-iNKTs) Promote ex vivo Lysis of Leukemic Blasts in a CD1d-Dependent Manner. Front Immunol. 2019;10:1542.

[128]. Metelitsa LS, Weinberg KI, Emanuel PD, Seeger RC. Expression of CD1d by myelomonocytic leukemias provides a target for cytotoxic NKT cells. Leukemia. 2003;17(6):1068-77.

[129]. Takahashi T, Haraguchi K, Chiba S, Yasukawa M, Shibata Y, Hirai H. Valpha24+ natural killer T-cell responses against T-acute lymphoblastic leukaemia cells: implications for immunotherapy. Br J Haematol. 2003;122(2):231-9.

[130]. Wu DY, Segal NH, Sidobre S, Kronenberg M, Chapman PB. Cross-presentation of disialoganglioside GD3 to natural killer T cells. J Exp Med. 2003;198(1):173-81.

[131]. Song L, Asgharzadeh S, Salo J, Engell K, Wu HW, Sposto R, et al. Valpha24-invariant NKT cells mediate antitumor activity via killing of tumor-associated macrophages. J Clin Invest. 2009;119(6):1524-36.

[132]. Kuylenstierna C, Bjorkstrom NK, Andersson SK, Sahlstrom P, Bosnjak L, Paquin-Proulx D, et al. NKG2D performs two functions in invariant NKT cells: direct TCR-independent activation of NK-like cytolysis and co-stimulation of activation by CD1d. Eur J Immunol. 2011;41(7):1913-23.

[133]. Nishimura T, Kitamura H, Iwakabe K, Yahata T, Ohta A, Sato M, et al. The interface between innate and acquired immunity: glycolipid antigen presentation by CD1d-expressing dendritic cells to NKT cells induces the differentiation of antigen-specific cytotoxic T lymphocytes. Int Immunol. 2000;12(7):987-94.

[134]. Gansuvd B, Hagihara M, Yu Y, Inoue H, Ueda Y, Tsuchiya T, et al. Human umbilical cord blood NK T cells kill tumors by multiple cytotoxic mechanisms. Hum Immunol. 2002;63(3):164-75.

[135]. Wingender G, Krebs P, Beutler B, Kronenberg M. Antigen-specific cytotoxicity by invariant NKT cells in vivo is CD95/CD178-dependent and is correlated with antigenic potency. J Immunol. 2010;185(5):2721-9.

[136]. Giaccone G, Punt CJ, Ando Y, Ruijter R, Nishi N, Peters M, et al. A phase I study of the natural killer T-cell ligand alpha-galactosylceramide (KRN7000) in patients with solid tumors. Clin Cancer Res. 2002;8(12):3702-9.

[137]. Nieda M, Okai M, Tazbirkova A, Lin H, Yamaura A, Ide K, et al. Therapeutic activation of Valpha24+Vbeta11+ NKT cells in human subjects results in highly coordinated secondary activation of acquired and innate immunity. Blood. 2004;103(2):383-9.

[138]. Yamasaki K, Horiguchi S, Kurosaki M, Kunii N, Nagato K, Hanaoka H, et al. Induction of NKT cell-specific immune responses in cancer tissues after NKT cell-targeted adoptive immunotherapy. Clin Immunol. 2011;138(3):255-65.

[139]. Guedan S, Calderon H, Posey AD, Jr., Maus MV. Engineering and Design of Chimeric Antigen Receptors. Mol Ther Methods Clin Dev. 2019;12:145-56.

[140]. Xie YJ, Dougan M, Jailkhani N, Ingram J, Fang T, Kummer L, et al. Nanobody-based CAR T cells that target the tumor microenvironment inhibit the growth of solid tumors in immunocompetent mice. Proc Natl Acad Sci U S A. 2019;116(16):7624-31.

[141]. Brown CE, Alizadeh D, Starr R, Weng L, Wagner JR, Naranjo A, et al. Regression of Glioblastoma after Chimeric Antigen Receptor T-Cell Therapy. N Engl J Med. 2016;375(26):2561-9.

[142]. Rafiq S, Hackett CS, Brentjens RJ. Engineering strategies to overcome the current roadblocks in CAR T cell therapy. Nature Reviews Clinical Oncology. 2020;17(3):147-67.

[143]. Bridgeman JS, Hawkins RE, Bagley S, Blaylock M, Holland M, Gilham DE. The optimal antigen response of chimeric antigen receptors harboring the CD3zeta transmembrane domain is dependent upon incorporation of the receptor into the endogenous TCR/CD3 complex. J Immunol. 2010;184(12):6938-49.

[144]. Alabanza L, Pegues M, Geldres C, Shi V, Wiltzius JJW, Sievers SA, et al. Function of Novel Anti-CD19 Chimeric Antigen Receptors with Human Variable Regions Is Affected by Hinge and Transmembrane Domains. Mol Ther. 2017;25(11):2452-65.

[145]. Makita S, Yoshimura K, Tobinai K. Clinical development of anti-CD19 chimeric antigen receptor T-cell therapy for B-cell non-Hodgkin lymphoma. Cancer Sci. 2017;108(6):1109-18.

[146]. Brocker T, Karjalainen K. Signals through T cell receptor-zeta chain alone are insufficient to prime resting T lymphocytes. J Exp Med. 1995;181(5):1653-9.

[147]. Maher J, Brentjens RJ, Gunset G, Riviere I, Sadelain M. Human T-lymphocyte cytotoxicity and proliferation directed by a single chimeric TCRzeta /CD28 receptor. Nat Biotechnol. 2002;20(1):70-5.

[148]. Krause A, Guo HF, Latouche JB, Tan C, Cheung NK, Sadelain M. Antigen-dependent CD28 signaling selectively enhances survival and proliferation in

genetically modified activated human primary T lymphocytes. J Exp Med. 1998;188(4):619-26.

[149]. Kawalekar OU, O'Connor RS, Fraietta JA, Guo L, McGettigan SE, Posey AD, Jr., et al. Distinct Signaling of Coreceptors Regulates Specific Metabolism Pathways and Impacts Memory Development in CAR T Cells. Immunity. 2016;44(2):380-90.

[150]. Tokarew N, Ogonek J, Endres S, von Bergwelt-Baildon M, Kobold S. Teaching an old dog new tricks: next-generation CAR T cells. Br J Cancer. 2019;120(1):26-37.

[151]. Chmielewski M, Abken H. TRUCKs: the fourth generation of CARs. Expert Opin Biol Ther. 2015;15(8):1145-54.

[152]. Kochenderfer JN, Wilson WH, Janik JE, Dudley ME, Stetler-Stevenson M, Feldman SA, et al. Eradication of B-lineage cells and regression of lymphoma in a patient treated with autologous T cells genetically engineered to recognize CD19. Blood. 2010;116(20):4099-102.

[153]. Kalos M, Levine BL, Porter DL, Katz S, Grupp SA, Bagg A, et al. T cells with chimeric antigen receptors have potent antitumor effects and can establish memory in patients with advanced leukemia. Sci Transl Med. 2011;3(95):95ra73.

[154]. Grupp SA, Kalos M, Barrett D, Aplenc R, Porter DL, Rheingold SR, et al. Chimeric antigen receptor-modified T cells for acute lymphoid leukemia. N Engl J Med. 2013;368(16):1509-18.

[155]. Maude SL, Laetsch TW, Buechner J, Rives S, Boyer M, Bittencourt H, et al. Tisagenlecleucel in Children and Young Adults with B-Cell Lymphoblastic Leukemia. N Engl J Med. 2018;378(5):439-48.

[156]. Neelapu SS, Locke FL, Bartlett NL, Lekakis LJ, Miklos DB, Jacobson CA, et al. Axicabtagene Ciloleucel CAR T-Cell Therapy in Refractory Large B-Cell Lymphoma. N Engl J Med. 2017;377(26):2531-44.

[157]. Sotillo E, Barrett DM, Black KL, Bagashev A, Oldridge D, Wu G, et al. Convergence of Acquired Mutations and Alternative Splicing of CD19 Enables Resistance to CART-19 Immunotherapy. Cancer Discov. 2015;5(12):1282-95.

[158]. Gardner R, Wu D, Cherian S, Fang M, Hanafi LA, Finney O, et al. Acquisition of a CD19-negative myeloid phenotype allows immune escape of MLL-rearranged B-ALL from CD19 CAR-T-cell therapy. Blood. 2016;127(20):2406-10.

[159]. Byrne M, Oluwole OO, Savani B, Majhail NS, Hill BT, Locke FL. Understanding and Managing Large B Cell Lymphoma Relapses after Chimeric Antigen Receptor T Cell Therapy. Biol Blood Marrow Transplant. 2019;25(11):e344-e51.

[160]. McGray AJ, Hallett R, Bernard D, Swift SL, Zhu Z, Teoderascu F, et al. Immunotherapy-induced CD8+ T cells instigate immune suppression in the tumor. Mol Ther. 2014;22(1):206-18.

[161]. Spranger S, Spaapen RM, Zha Y, Williams J, Meng Y, Ha TT, et al. Up-regulation of PD-L1, IDO, and T(regs) in the melanoma tumor microenvironment is driven by CD8(+) T cells. Sci Transl Med. 2013;5(200):200ra116.

[162]. Beatty GL, Moon EK. Chimeric antigen receptor T cells are vulnerable to immunosuppressive mechanisms present within the tumor microenvironment. Oncoimmunology. 2014;3(11):e970027.

[163]. Cherkassky L, Morello A, Villena-Vargas J, Feng Y, Dimitrov DS, Jones DR, et al. Human CAR T cells with cell-intrinsic PD-1 checkpoint blockade resist tumor-mediated inhibition. J Clin Invest. 2016;126(8):3130-44.

[164]. Gargett T, Yu W, Dotti G, Yvon ES, Christo SN, Hayball JD, et al. GD2-specific CAR T Cells Undergo Potent Activation and Deletion Following Antigen Encounter but can be Protected From Activation-induced Cell Death by PD-1 Blockade. Mol Ther. 2016;24(6):1135-49.

[165]. Burga RA, Thorn M, Point GR, Guha P, Nguyen CT, Licata LA, et al. Liver myeloid-derived suppressor cells expand in response to liver metastases in mice and inhibit the anti-tumor efficacy of anti-CEA CAR-T. Cancer Immunol Immunother. 2015;64(7):817-29.

[166]. Ping Y, Li F, Nan S, Zhang D, Shi X, Shan J, et al. Augmenting the Effectiveness of CAR-T Cells by Enhanced Self-Delivery of PD-1-Neutralizing scFv. Front Cell Dev Biol. 2020;8:803.

[167]. Heczey A, Louis CU, Savoldo B, Dakhova O, Durett A, Grilley B, et al. CAR T Cells Administered in Combination with Lymphodepletion and PD-1 Inhibition to Patients with Neuroblastoma. Mol Ther. 2017;25(9):2214-24.

[168]. Wong E, Dawson E, Davis J, Koldej R, Ludford-Menting M, Lansdown M, et al. Nivolumab for Relapsed or Residual Haematological Malignancies after Allogeneic Haematopoietic Stem Cell Transplantation (NIVALLO). Blood. 2018;132(Supplement 1):4633-.

[169]. Davids MS, Kim HT, Costello CL, Herrera AF, Locke FL, Maegawa RO, et al. A Phase I/Ib Study of Nivolumab for Relapsed Hematologic Malignancies after Allogeneic Hematopoietic Cell Transplantation (alloHCT). Blood. 2018;132(Supplement 1):705-.

[170]. Rossi J, Paczkowski P, Shen YW, Morse K, Flynn B, Kaiser A, et al. Preinfusion polyfunctional anti-CD19 chimeric antigen receptor T cells are associated with clinical outcomes in NHL. Blood. 2018;132(8):804-14.

[171]. Long AH, Haso WM, Shern JF, Wanhainen KM, Murgai M, Ingaramo M, et al. 4-1BB costimulation ameliorates T cell exhaustion induced by tonic signaling of chimeric antigen receptors. Nat Med. 2015;21(6):581-90.

[172]. Yang Y, Kohler ME, Chien CD, Sauter CT, Jacoby E, Yan C, et al. TCR engagement negatively affects CD8 but not CD4 CAR T cell expansion and leukemic clearance. Sci Transl Med. 2017;9(417).

[173]. Rotolo A, Caputo VS, Holubova M, Baxan N, Dubois O, Chaudhry MS, et al. Enhanced Anti-lymphoma Activity of CAR19-iNKT Cells Underpinned by Dual CD19 and CD1d Targeting. Cancer Cell. 2018;34(4):596-610 e11.

[174]. Heczey A, Liu D, Tian G, Courtney AN, Wei J, Marinova E, et al. Invariant NKT cells with chimeric antigen receptor provide a novel platform for safe and effective cancer immunotherapy. Blood. 2014;124(18):2824-33.

[175]. Tian G, Courtney AN, Jena B, Heczey A, Liu D, Marinova E, et al. CD62L+ NKT cells have prolonged persistence and antitumor activity in vivo. J Clin Invest. 2016;126(6):2341-55.

[176]. Poels R, Drent E, Lameris R, Katsarou A, Themeli M, van der Vliet HJ, et al. Preclinical Evaluation of Invariant Natural Killer T Cells Modified with CD38 or BCMA Chimeric Antigen Receptors for Multiple Myeloma. Int J Mol Sci. 2021;22(3).

[177]. Heczey A, Courtney AN, Montalbano A, Robinson S, Liu K, Li M, et al. Anti-GD2 CAR-NKT cells in patients with relapsed or refractory neuroblastoma: an interim analysis. Nat Med. 2020;26(11):1686-90.

[178]. Delfanti G, Dellabona P, Casorati G, Fedeli M. Adoptive Immunotherapy With Engineered iNKT Cells to Target Cancer Cells and the Suppressive Microenvironment. Front Med (Lausanne). 2022;9:897750.

[179]. Godfrey DI, Hammond KJL, Poulton LD, Smyth MJ, Baxter AG. NKT cells: facts, functions and fallacies. Immunology Today. 2000;21(11):573-83.

[180]. Schmid H. Humane invariante natürliche Killer-T-Zellen unterdrücken die Alloreaktivität von T-Zellen und kontrollieren das Tumorwachstum in vitro: Eberhard-Karls Universität Tübingen; 2020.

[181]. van Engeland M, Nieland LJW, Ramaekers FCS, Schutte B, Reutelingsperger CPM. Annexin V-Affinity assay: A review on an apoptosis detection system based on phosphatidylserine exposure. Cytometry. 1998;31(1):1-9.

[182]. Kasakovski D, Xu L, Li Y. T cell senescence and CAR-T cell exhaustion in hematological malignancies. J Hematol Oncol. 2018;11(1):91.

[183]. Schmid H. Humane invariante natürliche Killer-T-Zellen unterdrücken die Alloreaktivität von T-Zellen und kontrollieren das Tumorwachstum in vitro: Eberhard-Karls Universität Tübingen; 2020.

[184]. Schmid H, Ribeiro EM, Secker KA, Duerr-Stoerzer S, Keppeler H, Dong R, et al. Human invariant natural killer T cells promote tolerance by preferential apoptosis induction of conventional dendritic cells. Haematologica. 2022;107(2):427-36.

[185]. Becher B, Greter M. Acquitting an APC: DCs found "not guilty" after trial by ablation. Eur J Immunol. 2012;42(10):2551-4.

[186]. Mellman I, Steinman RM. Dendritic cells: specialized and regulated antigen processing machines. Cell. 2001;106(3):255-8.

[187]. Parekh VV, Lalani S, Kim S, Halder R, Azuma M, Yagita H, et al. PD-1/PD-L blockade prevents anergy induction and enhances the anti-tumor activities of glycolipid-activated invariant NKT cells. J Immunol. 2009;182(5):2816-26.

[188]. Parekh VV, Wilson MT, Olivares-Villagomez D, Singh AK, Wu L, Wang CR, et al. Glycolipid antigen induces long-term natural killer T cell anergy in mice. J Clin Invest. 2005;115(9):2572-83.

[189]. Agata Y, Kawasaki A, Nishimura H, Ishida Y, Tsubata T, Yagita H, et al. Expression of the PD-1 antigen on the surface of stimulated mouse T and B lymphocytes. Int Immunol. 1996;8(5):765-72.

[190]. Gumber D, Wang LD. Improving CAR-T immunotherapy: Overcoming the challenges of T cell exhaustion. EBioMedicine. 2022;77:103941.

[191]. Wherry EJ, Kurachi M. Molecular and cellular insights into T cell exhaustion. Nat Rev Immunol. 2015;15(8):486-99.

[192]. Anasetti C, Logan BR, Lee SJ, Waller EK, Weisdorf DJ, Wingard JR, et al. Peripheral-blood stem cells versus bone marrow from unrelated donors. N Engl J Med. 2012;367(16):1487-96.

[193]. Martinez C, Urbano-Ispizua A. Graft-versus-host disease therapy: something else beyond glucocorticoids? Haematologica. 2011;96(9):1249-51.

[194]. Zeng D, Lewis D, Dejbakhsh-Jones S, Lan F, Garcia-Ojeda M, Sibley R, et al. Bone marrow NK1.1(-) and NK1.1(+) T cells reciprocally regulate acute graft versus host disease. J Exp Med. 1999;189(7):1073-81.

[195]. Brossay L, Kronenberg M. Highly conserved antigen-presenting function of CD1d molecules. Immunogenetics. 1999;50(3-4):146-51.

[196]. Rubio MT, Moreira-Teixeira L, Bachy E, Bouillie M, Milpied P, Coman T, et al. Early posttransplantation donor-derived invariant natural killer T-cell recovery predicts the occurrence of acute graft-versus-host disease and overall survival. Blood. 2012;120(10):2144-54.

[197]. Chen YB, Efebera YA, Johnston L, Ball ED, Avigan D, Lekakis LJ, et al. Increased Foxp3(+)Helios(+) Regulatory T Cells and Decreased Acute Graft-versus-Host Disease after Allogeneic Bone Marrow Transplantation in Patients Receiving Sirolimus and RGI-2001, an Activator of Invariant Natural Killer T Cells. Biol Blood Marrow Transplant. 2017;23(4):625-34.

[198]. Ferrara JLM, Levy R, Chao NJ. Pathophysiologic mechanisms of acute graft-vs.-host disease. Biology of Blood and Marrow Transplantation. 1999;5(6):347-56.

[199]. Reddy P. Pathophysiology of acute graft-versus-host disease. Hematol Oncol. 2003;21(4):149-61.

[200]. Duffner UA, Maeda Y, Cooke KR, Reddy P, Ordemann R, Liu C, et al. Host dendritic cells alone are sufficient to initiate acute graft-versus-host disease. J Immunol. 2004;172(12):7393-8.

[201]. Zhang Y, Louboutin JP, Zhu J, Rivera AJ, Emerson SG. Preterminal host dendritic cells in irradiated mice prime CD8+ T cell-mediated acute graft-versus-host disease. J Clin Invest. 2002;109(10):1335-44.

[202]. Caielli S, Conforti-Andreoni C, Di Pietro C, Usuelli V, Badami E, Malosio ML, et al. On/off TLR signaling decides proinflammatory or tolerogenic dendritic cell maturation upon CD1d-mediated interaction with invariant NKT cells. J Immunol. 2010;185(12):7317-29.

[203]. Liu TY, Uemura Y, Suzuki M, Narita Y, Hirata S, Ohyama H, et al. Distinct subsets of human invariant NKT cells differentially regulate T helper responses via dendritic cells. Eur J Immunol. 2008;38(4):1012-23.

[204]. Watowich SS, Liu YJ. Mechanisms regulating dendritic cell specification and development. Immunol Rev. 2010;238(1):76-92.

[205]. Manz MG, Traver D, Miyamoto T, Weissman IL, Akashi K. Dendritic cell potentials of early lymphoid and myeloid progenitors. Blood. 2001;97(11):3333-41.

[206]. Yu H, Tian Y, Wang Y, Mineishi S, Zhang Y. Dendritic Cell Regulation of Graft-Vs.-Host Disease: Immunostimulation and Tolerance. Front Immunol. 2019;10:93.

[207]. Collin M, Bigley V. Human dendritic cell subsets: an update. Immunology. 2018;154(1):3-20.

[208]. Markey KA, Banovic T, Kuns RD, Olver SD, Don AL, Raffelt NC, et al. Conventional dendritic cells are the critical donor APC presenting alloantigen after experimental bone marrow transplantation. Blood. 2009;113(22):5644-9.

[209]. Martinez-Cingolani C, Grandclaudon M, Jeanmougin M, Jouve M, Zollinger R, Soumelis V. Human blood BDCA-1 dendritic cells differentiate into Langerhans-like cells with thymic stromal lymphopoietin and TGF-beta. Blood. 2014;124(15):2411-20.

[210]. Ito T, Inaba M, Inaba K, Toki J, Sogo S, Iguchi T, et al. A CD1a+/CD11c+ subset of human blood dendritic cells is a direct precursor of Langerhans cells. J Immunol. 1999;163(3):1409-19.

[211]. Siegal FP, Kadowaki N, Shodell M, Fitzgerald-Bocarsly PA, Shah K, Ho S, et al. The nature of the principal type 1 interferon-producing cells in human blood. Science. 1999;284(5421):1835-7.

[212]. Cella M, Jarrossay D, Facchetti F, Alebardi O, Nakajima H, Lanzavecchia A, et al. Plasmacytoid monocytes migrate to inflamed lymph nodes and produce large amounts of type I interferon. Nat Med. 1999;5(8):919-23.

[213]. Lu Y, Giver CR, Sharma A, Li JM, Darlak KA, Owens LM, et al. IFN-gamma and indoleamine 2,3-dioxygenase signaling between donor dendritic cells and T cells regulates graft versus host and graft versus leukemia activity. Blood. 2012;119(4):1075-85.

[214]. Hassan M, Ulezko Antonova A, Li JM, Hosoba S, Rupji M, Kowalski J, et al. Flt3L Treatment of Bone Marrow Donors Increases Graft Plasmacytoid Dendritic Cell Content and Improves Allogeneic Transplantation Outcomes. Biol Blood Marrow Transplant. 2019;25(6):1075-84.

[215]. Bedoya F, Frigault MJ, Maus MV. The Flipside of the Power of Engineered T Cells: Observed and Potential Toxicities of Genetically Modified T Cells as Therapy. Molecular Therapy. 2017;25(2):314-20.

[216]. Ko HJ, Lee JM, Kim YJ, Kim YS, Lee KA, Kang CY. Immunosuppressive myeloid-derived suppressor cells can be converted into immunogenic APCs with the help of activated NKT cells: an alternative cell-based antitumor vaccine. J Immunol. 2009;182(4):1818-28.

[217]. Iyoda T, Ushida M, Kimura Y, Minamino K, Hayuka A, Yokohata S, et al. Invariant NKT cell anergy is induced by a strong TCR-mediated signal plus co-stimulation. Int Immunol. 2010;22(11):905-13.

[218]. Eekels JJ, Pasternak AO, Schut AM, Geerts D, Jeeninga RE, Berkhout B. A competitive cell growth assay for the detection of subtle effects of gene transduction on cell proliferation. Gene Ther. 2012;19(11):1058-64.

[219]. Rajabzadeh A, Hamidieh AA, Rahbarizadeh F. Spinoculation and retronectin highly enhance the gene transduction efficiency of Mucin-1-specific chimeric antigen receptor (CAR) in human primary T cells. BMC Mol Cell Biol. 2021;22(1):57.

[220]. Cherwinski HM, Schumacher JH, Brown KD, Mosmann TR. Two types of mouse helper T cell clone. III. Further differences in lymphokine synthesis between Th1 and Th2 clones revealed by RNA hybridization, functionally monospecific bioassays, and monoclonal antibodies. J Exp Med. 1987;166(5):1229-44.

[221]. van der Vliet HJJ, Nishi N, de Gruijl TD, von Blomberg BME, van den Eertwegh AJM, Pinedo HM, et al. Human natural killer T cells acquire a memory-activated phenotype before birth. Blood. 2000;95(7):2440-2.

[222]. Wang Y, Bhave MS, Yagita H, Cardell SL. Natural Killer T-Cell Agonist alpha-Galactosylceramide and PD-1 Blockade Synergize to Reduce Tumor Development in a Preclinical Model of Colon Cancer. Front Immunol. 2020;11:581301.

[223]. Chang WS, Kim JY, Kim YJ, Kim YS, Lee JM, Azuma M, et al. Cutting edge: Programmed death-1/programmed death ligand 1 interaction regulates the induction and maintenance of invariant NKT cell anergy. J Immunol. 2008;181(10):6707-10.

[224]. Yoo HJ, Liu Y, Wang L, Schubert ML, Hoffmann JM, Wang S, et al. Tumor-Specific Reactive Oxygen Species Accelerators Improve Chimeric Antigen Receptor T Cell Therapy in B Cell Malignancies. Int J Mol Sci. 2019;20(10).

[225]. Coquet JM, Chakravarti S, Kyparissoudis K, McNab FW, Pitt LA, McKenzie BS, et al. Diverse cytokine production by NKT cell subsets and identification of an IL-17-producing CD4-NK1.1- NKT cell population. Proc Natl Acad Sci U S A. 2008;105(32):11287-92.

[226]. Nieda M, Nicol A, Koezuka Y, Kikuchi A, Lapteva N, Tanaka Y, et al. TRAIL expression by activated human CD4(+)V alpha 24NKT cells induces in vitro and in vivo apoptosis of human acute myeloid leukemia cells. Blood. 2001;97(7):2067-74.

[227]. Kawano T, Cui J, Koezuka Y, Toura I, Kaneko Y, Sato H, et al. Natural killer-like nonspecific tumor cell lysis mediated by specific ligand-activated Valpha14 NKT cells. Proc Natl Acad Sci U S A. 1998;95(10):5690-3.

[228]. Beilke JN, Kuhl NR, Van Kaer L, Gill RG. NK cells promote islet allograft tolerance via a perforin-dependent mechanism. Nat Med. 2005;11(10):1059-65.

[229]. Carnaud C, Lee D, Donnars O, Park S-H, Beavis A, Koezuka Y, et al. Cutting Edge: Cross-Talk Between Cells of the Innate Immune System: NKT Cells Rapidly Activate NK Cells. The Journal of Immunology. 1999;163(9):4647-50.

[230]. Courtney AN, Tian G, Liu D, Marinova E, Heczey A, Xu X, et al. Cross-talk between NKT cells and tumor associated macrophages in the tumor

microenvironment. The Journal of Immunology. 2016;196(1_Supplement):142.7-.7.

[231]. Kinter AL, Godbout EJ, McNally JP, Sereti I, Roby GA, O'Shea MA, et al. The common gamma-chain cytokines IL-2, IL-7, IL-15, and IL-21 induce the expression of programmed death-1 and its ligands. J Immunol. 2008;181(10):6738-46.

[232]. Blank CU, Haining WN, Held W, Hogan PG, Kallies A, Lugli E, et al. Defining 'T cell exhaustion'. Nat Rev Immunol. 2019;19(11):665-74.

[233]. Blaeschke F, Stenger D, Apfelbeck A, Cadilha BL, Benmebarek MR, Mahdawi J, et al. Augmenting anti-CD19 and anti-CD22 CAR T-cell function using PD-1-CD28 checkpoint fusion proteins. Blood Cancer J. 2021;11(6):108.

[234]. Latchman Y, Wood CR, Chernova T, Chaudhary D, Borde M, Chernova I, et al. PD-L2 is a second ligand for PD-1 and inhibits T cell activation. Nat Immunol. 2001;2(3):261-8.

[235]. Rodig N, Ryan T, Allen JA, Pang H, Grabie N, Chernova T, et al. Endothelial expression of PD-L1 and PD-L2 down-regulates CD8+ T cell activation and cytolysis. Eur J Immunol. 2003;33(11):3117-26.

[236]. Williams P, Basu S, Garcia-Manero G, Hourigan CS, Oetjen KA, Cortes JE, et al. The distribution of T-cell subsets and the expression of immune checkpoint receptors and ligands in patients with newly diagnosed and relapsed acute myeloid leukemia. Cancer. 2019;125(9):1470-81.

[237]. Yang S, Huang XJ. the Poorer-Risk AML, the Weaker Immunologic Surveillance? --Higher PD-L1 Expression on Non-APL AML Cells Is Associated with Poorer Risk Status According to Cytogenetics and Molecular Abnormailties. Blood. 2016;128(22):1619-.

[238]. Mumprecht S, Schurch C, Schwaller J, Solenthaler M, Ochsenbein AF. Programmed death 1 signaling on chronic myeloid leukemia-specific T cells results in T-cell exhaustion and disease progression. Blood. 2009;114(8):1528-36.

[239]. Kadia TM, Cortes JE, Ghorab A, Ravandi F, Jabbour E, Daver NG, et al. Nivolumab (Nivo) maintenance (maint) in high-risk (HR) acute myeloid leukemia (AML) patients. Journal of Clinical Oncology. 2018;36(15_suppl):7014-.

[240]. Zeidner JF, Vincent BG, Ivanova A, Moore D, McKinnon KP, Wilkinson AD, et al. Phase II Trial of Pembrolizumab after High-Dose Cytarabine in Relapsed/Refractory Acute Myeloid Leukemia. Blood Cancer Discov. 2021;2(6):616-29.

[241]. Davids MS, Kim HT, Bachireddy P, Costello C, Liguori R, Savell A, et al. Ipilimumab for Patients with Relapse after Allogeneic Transplantation. N Engl J Med. 2016;375(2):143-53.

[242]. Davenport AJ, Jenkins MR, Cross RS, Yong CS, Prince HM, Ritchie DS, et al. CAR-T Cells Inflict Sequential Killing of Multiple Tumor Target Cells. Cancer Immunol Res. 2015;3(5):483-94.

[243]. Hombach A, Wieczarkowiecz A, Marquardt T, Heuser C, Usai L, Pohl C, et al. Tumor-specific T cell activation by recombinant immunoreceptors: CD3 zeta signaling and CD28 costimulation are simultaneously required for efficient IL-2 secretion and can be integrated into one combined CD28/CD3 zeta signaling receptor molecule. J Immunol. 2001;167(11):6123-31.

[244]. Cullen SP, Martin SJ. Mechanisms of granule-dependent killing. Cell Death Differ. 2008;15(2):251-62.

[245]. de Saint Basile G, Menasche G, Fischer A. Molecular mechanisms of biogenesis and exocytosis of cytotoxic granules. Nat Rev Immunol. 2010;10(8):568-79.

[246]. Nguyen A, Ramesh A, Kumar S, Nandi D, Brouillard A, Wells A, et al. Granzyme B nanoreporter for early monitoring of tumor response to immunotherapy. Sci Adv. 2020;6(40).

[247]. Larimer BM, Bloch E, Nesti S, Austin EE, Wehrenberg-Klee E, Boland G, et al. The Effectiveness of Checkpoint Inhibitor Combinations and Administration Timing Can Be Measured by Granzyme B PET Imaging. Clin Cancer Res. 2019;25(4):1196-205.

[248]. Prakash MD, Munoz MA, Jain R, Tong PL, Koskinen A, Regner M, et al. Granzyme B promotes cytotoxic lymphocyte transmigration via basement membrane remodeling. Immunity. 2014;41(6):960-72.

[249]. Kuczek DE, Larsen AMH, Thorseth ML, Carretta M, Kalvisa A, Siersbaek MS, et al. Collagen density regulates the activity of tumor-infiltrating T cells. J Immunother Cancer. 2019;7(1):68.

[250]. Textor A, Listopad JJ, Wuhrmann LL, Perez C, Kruschinski A, Chmielewski M, et al. Efficacy of CAR T-cell therapy in large tumors relies upon stromal targeting by IFNgamma. Cancer Res. 2014;74(23):6796-805.

8 Appendix

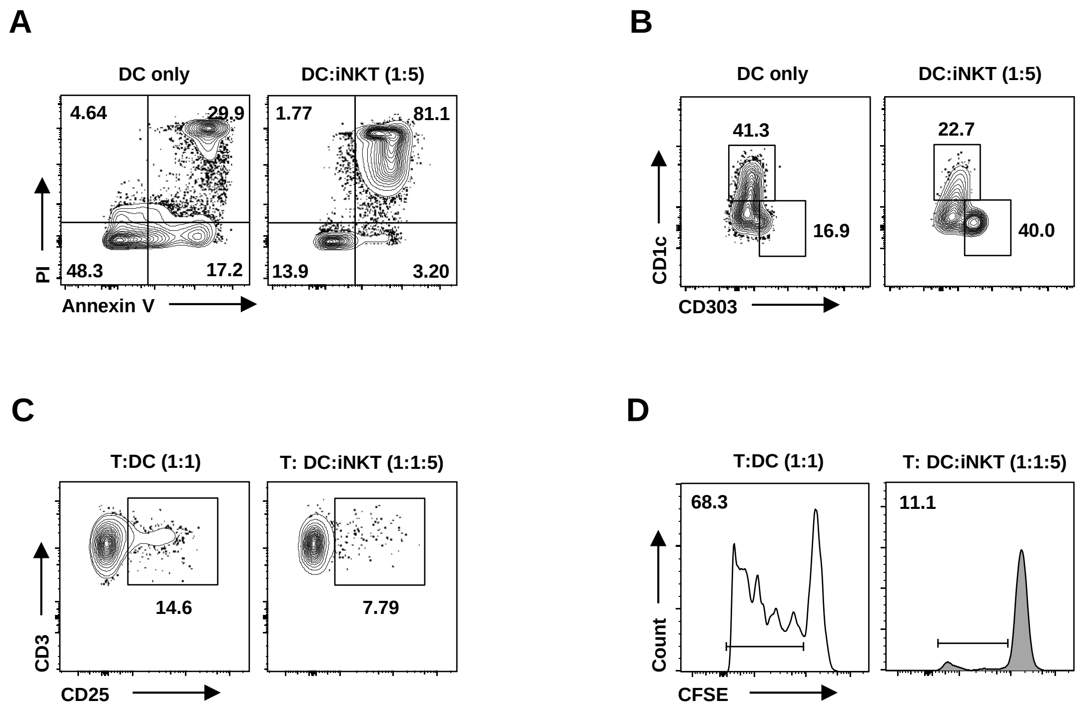

Appendix data 1: Third-party iNKT cells induce DC apoptosis and impair T-cell function in a patient-based system (Patient 2).

DC apoptosis induction of patient samples by iNKT cells was analyzed after 4h co-incubation and flow cytometric analysis for annexin V surface expression. Moreover, T-cell activation and proliferation were analyzed in a MLR. Patient T cells were co-incubated with blood DCs at a 1:1 ratio (T cell:DC) for 7 days. The cells were analyzed by flow cytometry on day 1 and 3 for activation (CD69 and CD25, respectively) and on day 7 for proliferation (CFSE dilution). Where stated, 5-fold iNKT cells were added to the cultures. DC apoptosis induction is shown in **(A)**. Discrimination of the remaining alive DCs (annexin V-VD-) with anti-CD1c and anti-CD303 antibodies is depicted in **(B)**. **(C)** and **(D)** shows plots with CD25 expression and proliferation of patient T cells on day 3 and 7, respectively, in presence or absence of third-party iNKT cells. For **(A)** and **(B)**, gates were set on CD3- singlets**.** For **(C)** and **(D),** iNKT-cell exclusion followed gating on CFSE positive populations on day 3 and on PBS57-CD1d-tetramer negative populations on day 7.

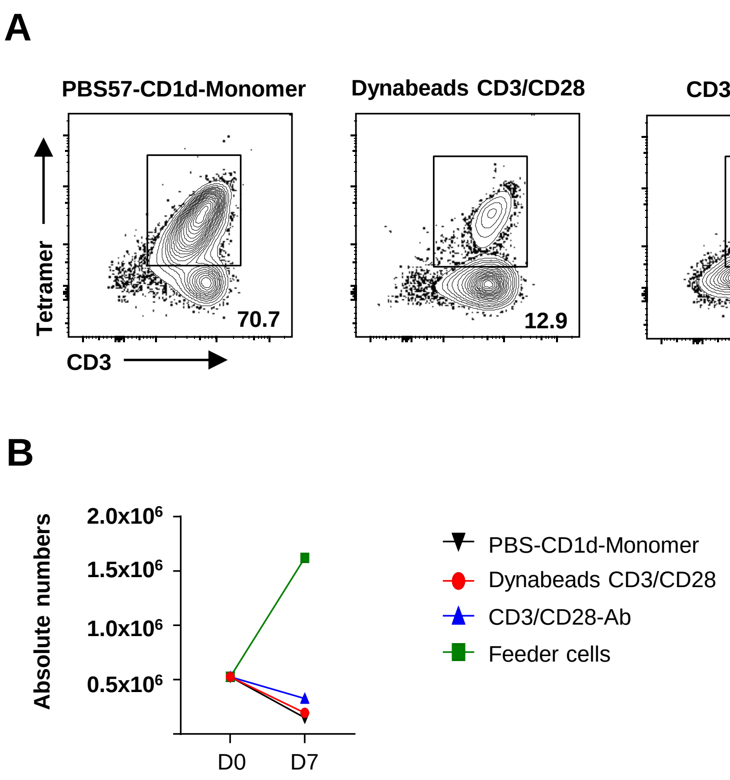

Appendix data 2: Different strategies to promote cell activation before transduction.
Freshly isolated iNKT cells were incubated with PBS57-loaded CD1d monomer, Dynabeads CD3/CD28, CD3/CD28 antibodies (CD3/CD28-Ab) and α-GalCer-loaded feeder cells for 7 days. After this time, the cells were harvested and analyzed by flow cytometry. **(A)** and **(B)** show representative FACS data and absolute numbers (n=1). Dot plots depict the percentage of iNKT cells (Tetramer+) amongst CD3+ living cells (VD-). Only singlets were analyzed.

Appendix data 3: Statistic analysis of the data in figure 27B.

Condition	Significance
K562-WT	
iNKT+DMSO vs. iNKT+α-GalCer	ns
iNKT+DMSO vs. CD19-CAR-iNKT+DMSO	*
iNKT+DMSO vs. CD19-CAR-iNKT+α-GalCer	**
iNKT+α-GalCer vs. CD19-CAR-iNKT+DMSO	*
iNKT+α-GalCer vs. CD19-CAR-iNKT+α-GalCer	*
CD19-CAR-iNKT+DMSO vs. CD19-CAR-iNKT+α-GalCer	ns
K562-CD19	
iNKT+DMSO vs. iNKT+α-GalCer	ns
iNKT+DMSO vs. CD19-CAR-iNKT+DMSO	****
iNKT+DMSO vs. CD19-CAR-iNKT+α-GalCer	****
iNKT+α-GalCer vs. CD19-CAR-iNKT+DMSO	****
iNKT+α-GalCer vs. CD19-CAR-iNKT+α-GalCer	****
CD19-CAR-iNKT+DMSO vs. CD19-CAR-iNKT+α-GalCer	ns
K562-CD1d	
iNKT+DMSO vs. iNKT+α-GalCer	**
iNKT+DMSO vs. CD19-CAR-iNKT+DMSO	ns
iNKT+DMSO vs. CD19-CAR-iNKT+α-GalCer	****
iNKT+α-GalCer vs. CD19-CAR-iNKT+DMSO	ns
iNKT+α-GalCer vs. CD19-CAR-iNKT+α-GalCer	**
CD19-CAR-iNKT+DMSO vs. CD19-CAR-iNKT+α-GalCer	****
K562-DP	
iNKT+DMSO vs. iNKT+α-GalCer	****
iNKT+DMSO vs. CD19-CAR-iNKT+DMSO	****
iNKT+DMSO vs. CD19-CAR-iNKT+α-GalCer	****
iNKT+α-GalCer vs. CD19-CAR-iNKT+DMSO	ns
iNKT+α-GalCer vs. CD19-CAR-iNKT+α-GalCer	***
CD19-CAR-iNKT+DMSO vs. CD19-CAR-iNKT+α-GalCer	**

*ns p>0.05, * p≤0.05 ** p≤0.01, *** p≤0.001, **** p≤0.0001.*

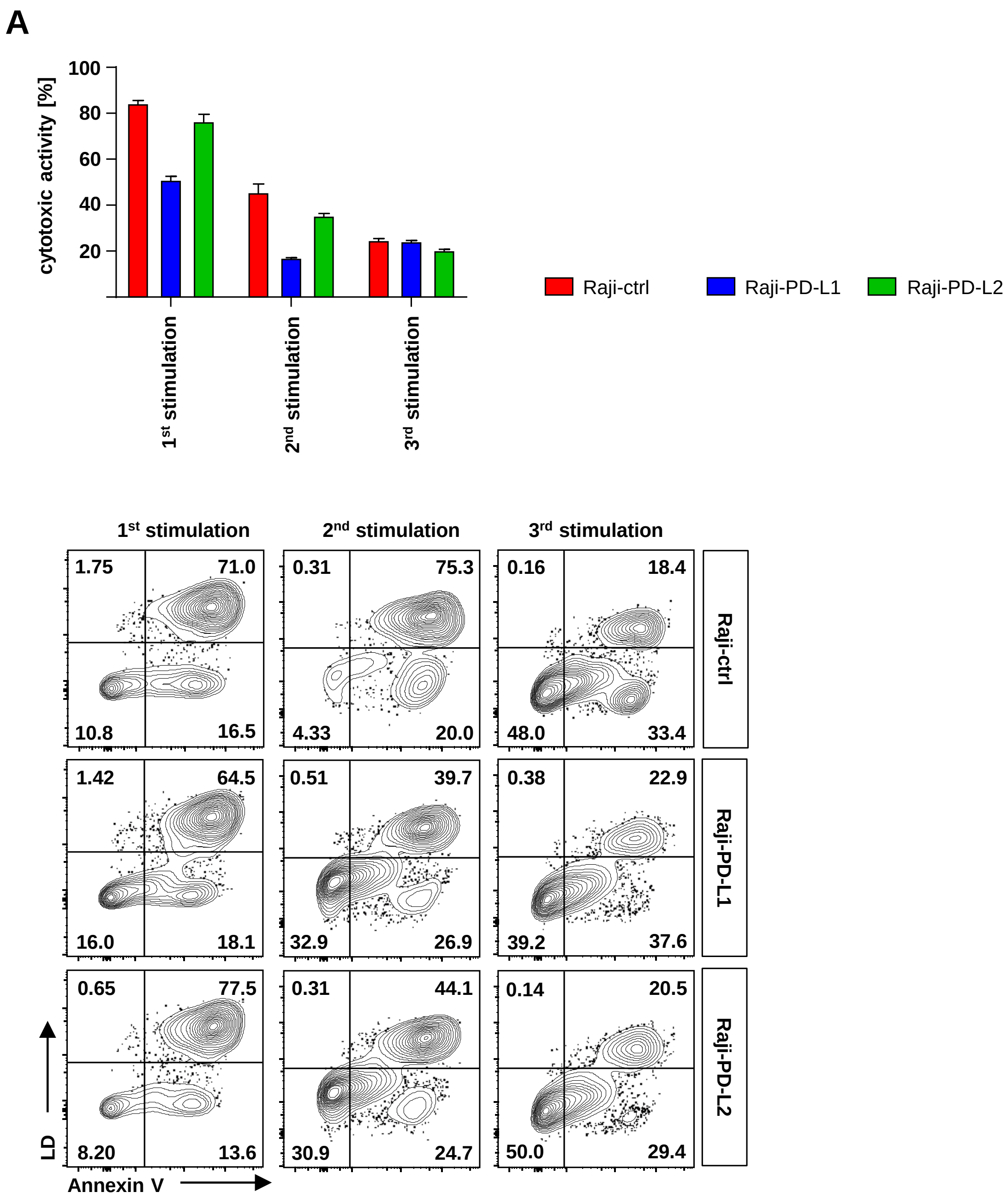

Appendix data 4: Functionality of CD19-CAR-iNKT cells is impaired upon repetitive antigen contact (healthy donor 2)

CD19-CAR-iNKT cells were challenged with irradiated target cells every week throughout three stimulation rounds. CD19-CAR-iNKT cells were analyzed for their cytotoxicity against PD-L1/2+ Raji cells. After 24h co-incubation, the cells were harvested and analyzed by flow cytometry. The supernatants were collected for multiplex analysis. **(A)** shows the cytotoxicity course of CD19-CAR-iNKT cells for one donor throughout three stimulations with Raji-Ctrl (red), Raji-PD-L1 (blue) and Raji-PD-L2 (green) (above) and representative dot plots (below). Target cells were discriminated of CD19-CAR-iNKT cells through the FSC-A vs SSC-A gate and CTV+ staining. Only singlets were analyzed. Error bars show SD.

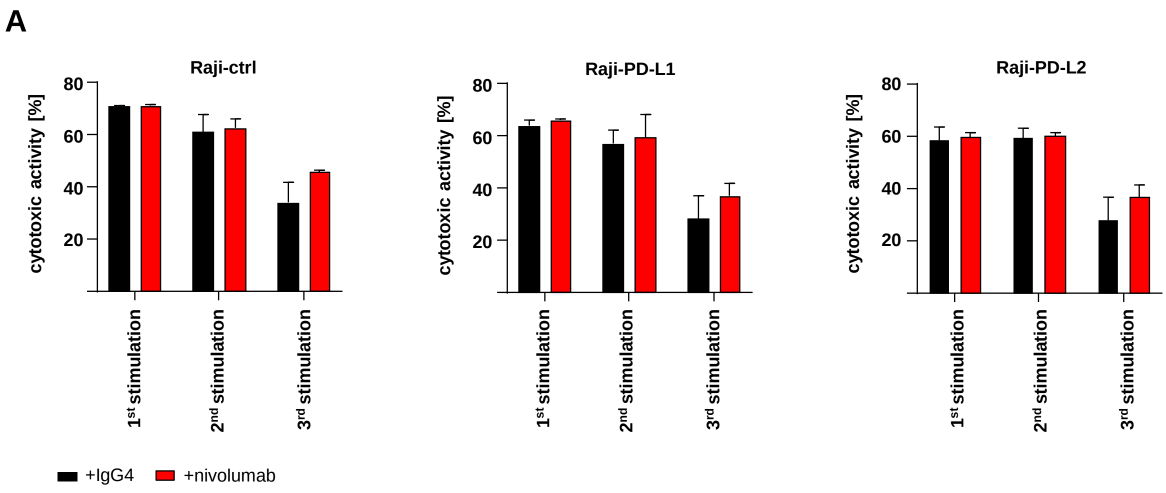

Appendix data 5: Checkpoint inhibition partially improves cytotoxicity and the release of cytokines from CD19-CAR-iNKT cells after repetitive antigen encounter (healthy donor 2). CD19-CAR-iNKT cells were challenged with irradiated target cells every 7 days three times. Every week, CD19-CAR-iNKT cells were further analyzed for their cytotoxicity against PD-L1/2+ Raji cells. Where stated, nivolumab or its IgG4 isotype control were added to the assay. After 24h co-incubation, the cells were harvested and analyzed by flow cytometry. The supernatants were collected for multiplex analysis. **(A)** shows the cytotoxicity of CD19-CAR-iNKT cells for one donor in the course of three stimulations with Raji-Ctrl (left), Raji-PD-L1 (middle) and Raji-PD-L2 (right) (above) and representative dot plots (below). Data in black shows results for IgG4-treated cells, while red shows data with nivolumab-treatment. Target cells were discriminated of CD19-CAR-iNKT cells through the FSC-A vs SSC-A gate and CTV+ staining. Only singlets were analyzed. Error bars show SD.